

603650

EFFECT OF JP-5 PROPERTIES ON HOT GAS CORROSION AND FLAME RADIATION

SUMMARY REPORT

NAVY BUWEPS CONTRACT NOW 63-0406-d

JUNE, 1964

35



#10012
#10011

DDC
AUG 17 1964
DDC-IRA D

BEST AVAILABLE COPY

Released to Defense Documentation Center
without limitations by permission
of the
Chief, Bureau of Naval Weapons

PHILLIPS PETROLEUM COMPANY

CLEARINGHOUSE FOR FEDERAL SCIENTIFIC AND TECHNICAL INFORMATION, CFSTI
DOCUMENT MANAGEMENT BRANCH 410.11

LIMITATIONS IN REPRODUCTION QUALITY

Accession #

63150



1. We regret that legibility of this document is in part unsatisfactory. Reproduction has been made from best available copy.



2. A portion of the original document contains fine detail which may make reading of photocopy difficult.



3. The original document contains color, but distribution copies are available in black-and-white reproduction only.



4. The original distribution copies contain color which will be shown in black-and-white when it is necessary to reprint.



5. The processing copy is available on loan at CFSTI.



6.

PHILLIPS PETROLEUM COMPANY
RESEARCH DIVISION
BARTLESVILLE, OKLAHOMA

SUMMARY REPORT

FOK

NAVY BUWEPS CONTRACT NOW 63-0406-d

EFFECT OF JP-5 PROPERTIES ON

HOT GAS CORROSION AND

FLAME RADIATION

by

R. M. Schirmer

E. W. Aldrich

Released to Defense Documentation Center
without limitation by permission
of the
Chief, Bureau of Naval Weapons

Summary Report

Navy BuWeps Contract NOw 63-0406-d

EFFECT OF JP-5 PROPERTIES ON HOT GAS CORROSION AND FLAME RADIATION

by

R. M. Schirmer and F. W. Aldrich

S U M M A R Y

This report summarizes results of hydrocarbon fuel performance studies carried out by Phillips Petroleum Company for the Bureau of Naval Weapons under Contract NOw 63-0406-d during the one year period from April 1, 1963 through March 31, 1964. The primary effort was an experimental investigation to determine whether the maximum sulfur content of 0.4 weight per cent, currently allowed in grade JP-5 aviation turbine fuel, is a safe level for protection of the superalloys used in high performance engines when operated in a marine environment. A second phase dealt with the effect of fuel molecular structure and volatility on the total radiant energy from combustor flames, which by contributing to the operating temperature of hot section components limits aircraft turbine engine power and durability.

In preliminary tests, five superalloys, typical of those used for turbine blades and guide vanes, were exposed to temperature-velocity-pressure conditions simulating take-off operation. It was shown, in a twelve hour duration test using a fuel containing one weight per cent sulfur, that the presence of "sea salt", at a level of 15 parts per million in the combustor air, greatly increased hot corrosion.

In the major program, specimens of Inconel 713C and Sierra Metal 200 were exposed to vitiated air from the Phillips 2-inch combustor at 2000 F, a pressure of 15 atmospheres and a velocity of 500 ft/sec during five hour cyclic tests. A statistically designed program was used to evaluate the effects on metal losses and changes in tensile properties of three sulfur concentration levels in fuel (0.0002, 0.040 and 0.40 weight per cent) at three "sea salt" concentrations in the air (zero, 1.50 and 15.0 parts per million) and also any sulfur x "sea salt" interaction.

Both superalloys showed good resistance to oxidation and erosion in the absence of sulfur and "sea salt". There was little or no evidence of sulfur corrosion in the absence of "sea salt". Catastrophic "sea salt" corrosion was encountered by both superalloys in some instances. A significant sulfur x "sea salt" interaction was shown for both superalloys; but, while hot corrosion of Inconel 713C was accelerated, hot corrosion of Sierra Metal 200 was inhibited.

(Continued)

S U M M A R Y (Continued)

Decreasing sulfur concentration in fuel, from the current JP-5 specification of 0.40 to 0.040 weight per cent, did not reduce "sea salt" corrosion significantly. However, the complex interaction found with ingested "sea water" does not allow for a recommendation as to the maximum sulfur limit in JP-5, without additional data. It is recommended that this study be extended to include additional superalloys, evaluated over a range in exhaust gas temperatures.

In supplementary tests, characteristic sulfidation attack on Inconel 713C was identified only at temperatures below the freezing point of sodium sulfate (1623 F). At higher temperatures, where test specimens were no longer covered by a heavy sodium sulfate scale, the mechanism of attack appeared to be more one of gross oxidation. Catastrophic rates of "sea salt" corrosion at 2000 F were not reduced by the substitution of sodium chloride to obtain an essentially sulfur-free environment.

In the second phase of these performance studies, measurements were made of total radiant energy from flames of a series of pure hydrocarbons, varying widely in molecular structure and boiling point. The hydrocarbons were burned in the Phillips Microburner which simulates the high intensity, turbulent diffusion type combustion process of an aircraft turbine engine. Operation was over a broad range of fuel-air mixtures at atmospheric pressure.

The Microburner tests did not differentiate among hydrocarbons (including all of the normal- and iso-paraffins, the mono- and bi-cycloparaffins and the straight and branch chain olefins) having hydrogen contents above about 13 weight per cent, heats of combustion above about 18,200, Luminometer Numbers above about 40 and ASTM Smoke Points above about 20 mm. At lower values, the total radiant energy increased rapidly with decrease in these properties. The hydrocarbons, other than those listed above, were rated in the following order of increasing flame radiation: the cycloolefins, tetracyclododecane, tetralin and the alkylbenzenes, benzene and styrene, and methylnaphthalene.

The results also show that fuel volatility was not a significant factor under the test conditions.

The correlations of fuel properties with flame radiation in the Microburner are compared with available information on flame radiation in the Phillips 2-inch combustor, and the J-57 and J-79 aviation turbine engine combustors, operated at 5 atmospheres pressures. In contrast to the lack of differentiation by the Microburner among fuels having hydrogen contents above about 13 weight per cent, flame radiation in the 2-inch, J-57 and J-79 combustors is a linear function of hydrogen content over the entire range investigated.

It is concluded that the effect of hydrocarbon structure on flame radiation changes with combustor operating pressure. Therefore, measurements of the relative burning quality of aviation turbine fuels should be made at the pressure levels of interest, rather than at atmospheric pressure. Continuation of these studies, using Phillips 2-inch combustor operated at pressures up to 15 atmospheres, is recommended.

Summary Report

Navy BuWeps Contract NOW 63-0406-d

EFFECT OF JP-5 PROPERTIES ON HOT GAS CORROSION AND FLAME RADIATION

TABLE OF CONTENTS

	<u>Page</u>
<u>SUMMARY</u>	1-11
I. <u>INTRODUCTION</u>	1
A. <u>HOT CORROSION</u>	1
1. Gas Turbine Operation in Marine Environment.	1
2. Hot Corrosion of Superalloys.	2
3. Review of Previous Work by Phillips Petroleum Company.	2
4. Contract NOW 63-0406-d	3
B. <u>FLAME RADIATION</u>	4
1. Gas Turbine Durability	4
2. Control of Soot Formation.	5
3. Review of Previous Work by Phillips Petroleum Company.	6
4. Contract NOW 63-0406-d.	8
II. <u>HOT CORROSION OF SUPERALLOYS</u>	8
A. <u>TEST EQUIPMENT</u>	8
1. Phillips 2-Inch Combustor.	8
2. Specimen Holder.	10
3. Specimen Electrocleaning	15
4. Specimen Modification for Tensile.	15
B. <u>TEST MATERIALS</u>	19
1. Fuel.	19
a. Sulfur in Petroleum	19
b. Sulfur in JP-5.	19
c. Base Fuel.	21

(Continued)

TABLE OF CONTENTS (CONTINUED)

	<u>Page</u>
2. Sea Water	24
a. Composition	24
b. Ingestion Rate.	24
3. Superalloys	27
C. <u>PRELIMINARY TESTS</u>	31
1. Procedure	31
2. Test Results.	31
D. <u>MAJOR PROGRAM</u>	33
1. Procedure	33
2. Test Results.	35
3. Discussion.	35
a. Oxidation and Erosion	35
b. Sulfur Corrosion.	35
c. "Sea Salt" Corrosion.	35
d. Combined Sulfur-"Sea Salt" Corrosion.	48
e. Metallography	48
4. Conclusions	51
E. <u>SUPPLEMENTARY TESTS</u>	54
1. Effect of Temperature on Hot Corrosion.	54
2. X-ray Diffraction Analysis.	56
3. Sodium Corrosion.	58
F. <u>RECOMMENDATIONS</u>	59
III. <u>FLAME RADIATION</u>	60
A. TEST EQUIPMENT.	60
1. Phillips Microburner.	60
2. Equipment for Measuring Flame Radiation	66

(Continued)

TABLE OF CONTENTS (CONTINUED)

	<u>Page</u>
B. <u>TEST HYDROCARBONS</u>	68
C. <u>TEST PROCEDURE</u>	68
D. <u>TEST RESULTS</u>	73
E. <u>DISCUSSION</u>	79
1. Effect of Hydrocarbon Type	79
2. Effect of Hydrocarbon Properties	79
3. Correlation with Full-Scale Combustors	89
F. <u>CONCLUSIONS</u>	95
G. <u>RECOMMENDATIONS</u>	95
IV. <u>ACKNOWLEDGMENT</u>	96
V. <u>REFERENCES</u>	97

TABULATIONS

TABLE I - DESIGN DETAILS OF MODIFIED 2-INCH COMBUSTOR	11
TABLE II - SULFUR CONTENT OF REPRESENTATIVE U.S. PRODUCTION SAMPLES OF JP-5	20
TABLE III - TYPICAL PROPERTIES OF BASE FUEL USED IN PRELIMINARY TESTS.	21
TABLE IV - PHYSICAL AND CHEMICAL PROPERTIES OF BASE FUEL USED IN MAJOR PROGRAM	23
TABLE V - COMPOSITION OF ASTM D 665 SYNTHETIC "SEA WATER".	25
TABLE VI - COMPOSITION OF SEA WATER	26
TABLE VII - COMPOSITION OF SUPERALLOY TEST SPECIMENS USED IN PRELIMINARY TESTS.	28
TABLE VIII- COMPOSITION OF SUPERALLOY TEST SPECIMENS USED IN MAJOR PROGRAM	29
TABLE IX - INSPECTION STANDARDS FOR SUPERALLOY TEST SPECIMENS USED IN MAJOR PROGRAM.	30

(Continued)

TABLE OF CONTENTS (CONTINUED)

	<u>Page</u>
TABLE X - RESULTS OF PRELIMINARY HOT CORROSION TESTS.	31
TABLE XI - OPERATING CONDITIONS OF PHILLIPS 2-INCH COMBUSTOR	34
TABLE XII - SUMMARY OF WEIGHT LOSS AND TENSILE PROPERTY DATA ON INCONEL 713C TEST SPECIMENS (2000 F TEST CONDITIONS) . . .	36
TABLE XIII- SUMMARY OF WEIGHT LOSS AND TENSILE PROPERTY DATA ON SIERRA METAL 200 TEST SPECIMENS (2000 F TEST CONDITIONS). . .	38
TABLE XIV - EFFECT OF EXHAUST GAS TEMPERATURE ON HOT CORROSION OF INCONEL 713C.	54
TABLE XV - X-RAY DIFFRACTION OF SIERRA METAL 200 CORROSION PRODUCTS	56
TABLE XVI - EFFECT OF VARIOUS SODIUM CONTAINING COMPOUNDS ON HOT CORROSION.	58
TABLE XVII- PHYSICAL AND CHEMICAL PROPERTIES OF TEST HYDROCARBONS. . .	70
TABLE XVIII-AXIAL FLAME RADIATION AT VARIOUS FUEL-AIR MIXTURE RATIOS .	80
TABLE XIX - TRANSVERSE FLAME RADIATION AT VARIOUS FUEL-AIR MIXTURE RATIOS	81
TABLE XX - COMPARISON OF CURVES OF FLAME RADIATION AGAINST HYDROCARBON PROPERTIES	84
TABLE XXI - CONDITIONS OF OPERATION OF THE PHILLIPS 2-INCH COMBUSTOR AND THE J-57 AND J-79 AIRCRAFT ENGINE COMBUSTORS	94

ILLUSTRATIONS

Figure 1. - PHILLIPS LABORATORY SCALE COMBUSTOR	9
Figure 2. - PHILLIPS 2-INCH COMBUSTOR INSTALLATION FOR HOT GAS CORROSION STUDIES.	12
Figure 3. - NORTHWEST VIEW OF PHILLIPS RESEARCH FACILITY FOR JET FUELS	13
Figure 4. - VIEW OF CONTROL PANEL FOR LABORATORY SCALE COMBUSTOR STUDIES OF JET FUELS - PHILLIPS RESEARCH TEST FACILITY . .	14
Figure 5. - TEST SPECIMEN HOLDER FOR PHILLIPS 2-INCH COMBUSTOR	16
Figure 6. - CATHODIC DESCALING APPARATUS FOR CLEANING TEST SPECIMENS FOLLOWING EXPOSURE TO HOT GAS CORROSION.	17
Figure 7. - MODIFICATION OF TEST SPECIMEN FOR TENSILE EVALUATION FOLLOWING EXPOSURE TO HOT GAS CORROSION.	18

(Continued)

TABLE OF CONTENTS (CONTINUED)

	<u>Page</u>
Figure 8. - TURBINE GUIDE VANE METAL LOSS AS A FUNCTION OF TEST DURATION FOR EXPOSURE TO SULFUR AND/OR SEA SALT LADEN ATMOSPHERES	32
Figure 9. - PHOTOGRAPH OF INCONEL 713C TEST SPECIMENS AFTER EXPOSURE TO HOT GAS CORROSION IN PHILLIPS 2-INCH COMBUSTOR AT 2000 F TEST CONDITIONS	40
Figure 10. - EFFECT OF SULFUR AND SEA SALT ON INCONEL 713C TEST SPECIMEN WEIGHT LOSS AS A RESULT OF EXPOSURE TO HOT GAS CORROSION IN PHILLIPS 2-INCH COMBUSTOR AT 2000 F TEST CONDITION.	41
Figure 11. - EFFECT OF SULFUR AND SEA SALT ON INCONEL 713C TEST SPECIMEN MEAN WEIGHT LOSS AS A RESULT OF EXPOSURE TO HOT GAS CORROSION IN PHILLIPS 2-INCH COMBUSTOR AT 2000 F TEST CONDITION	42
Figure 12. - EFFECT OF SULFUR AND SEA SALT ON INCONEL 713C TEST SPECIMEN TENSILE PROPERTIES AFTER EXPOSURE TO HOT GAS CORROSION IN PHILLIPS 2-INCH COMBUSTOR AT 2000 F TEST CONDITION.	43
Figure 13. - PHOTOGRAPHS OF SIERRA METAL 200 TEST SPECIMENS AFTER EXPOSURE TO HOT GAS CORROSION IN PHILLIPS 2-INCH COMBUSTOR AT 2000 F TEST CONDITION.	44
Figure 14. - EFFECT OF SULFUR AND SEA SALT ON SIERRA METAL 200 TEST SPECIMEN WEIGHT LOSS AS A RESULT OF EXPOSURE TO HOT GAS CORROSION IN PHILLIPS 2-INCH COMBUSTOR AT 2000 F TEST CONDITION.	45
Figure 15. - EFFECT OF SULFUR AND SEA SALT ON SIERRA METAL 200 TEST SPECIMEN MEAN WEIGHT LOSS AS A RESULT OF EXPOSURE TO HOT GAS CORROSION IN PHILLIPS 2-INCH COMBUSTOR AT 2000 F TEST CONDITION...	46
Figure 16. - EFFECT OF SULFUR AND SEA SALT ON SIERRA METAL 200 TEST SPECIMEN TENSILE PROPERTIES AFTER EXPOSURE TO HOT GAS CORROSION IN PHILLIPS 2-INCH COMBUSTOR AT 2000 F TEST CONDITION.	47
Figure 17. - PHOTOMICROGRAPHS AT 100X OF INCONEL 713C TEST SPECIMENS AFTER EXPOSURE TO HOT GAS CORROSION IN PHILLIPS 2-INCH COMBUSTOR AT 2000 F TEST CONDITION	49
Figure 18. - PHOTOMICROGRAPHS AT 600X OF INCONEL 713C TEST SPECIMENS AFTER EXPOSURE TO HOT GAS CORROSION IN PHILLIPS 2-INCH COMBUSTOR AT 2000 F TEST CONDITION	50
Figure 19. - PHOTOMICROGRAPHS AT 100X OF SIERRA METAL 200 TEST SPECIMENS AFTER EXPOSURE TO HOT GAS CORROSION IN PHILLIPS 2-INCH COMBUSTOR AT 2000 F TEST CONDITION.	52

TABLE OF CONTENTS (CONTINUED)

	<u>Page</u>
Figure 20. - PHOTOMICROGRAPHS AT 600X OF SIERRA METAL 200 TEST SPECIMENS AFTER EXPOSURE TO HOT GAS CORROSION IN PHILLIPS 2-INCH COMBUSTOR AT 2000 F TEST CONDITION	53
Figure 21. - PHOTOGRAPHS OF INCONEL 713C TEST SPECIMENS AFTER EXPOSURE TO HOT GAS CORROSION IN PHILLIPS 2-INCH COMBUSTOR AT VARIOUS TEMPERATURES	55
Figure 22. - PHOTOMICROGRAPHS OF INCONEL 713C TEST SPECIMENS AFTER EXPOSURE TO HOT GAS CORROSION IN PHILLIPS 2-INCH COMBUSTOR AT VARIOUS TEMPERATURES	57
Figure 23. - PHILLIPS MICROBURNER AND AUXILIARY EQUIPMENT FOR STUDY OF FLAME RADIATION.	61
Figure 24. - PHILLIPS MICROBURNER SET UP FOR MEASUREMENT OF FLAME RADIATION.	62
Figure 25. - EXPLODED VIEW OF MODEL 5 PHILLIPS MICROBURNER	63
Figure 26. - SCHEMATIC FLOW DIAGRAM OF PHILLIPS MICROBURNER TEST FACILITY	64
Figure 27. - PHILLIPS MICROBURNER AND CONTROL PANEL.	65
Figure 28. - FLOW PATTERN THROUGH COMBUSTION CHAMBER - PHILLIPS MICROBURNER.	67
Figure 29. - APPARATUS FOR CALIBRATION OF L & N RAYOTUBES.	69
Figure 30. - SPREAD IN LUMINOMETER NUMBER OVER BOILING RANGE OF HYDROCARBONS USED IN MICROBURNER STUDIES OF FLAME RADIATION.	71
Figure 31. - SPREAD IN HYDROGEN CONTENT OVER BOILING RANGE OF HYDROCARBONS USED IN MICROBURNER STUDIES OF FLAME RADIATION . .	72
Figure 32. - PHILLIPS MICROBURNER FLAME WITH ISOCTANE AT LEAN LIMIT. .	74
Figure 33. - PHILLIPS MICROBURNER FLAME WITH TOLUENE AT LEAN LIMIT. . .	75
Figure 34. - PHILLIPS MICROBURNER FLAME WITH TOLUENE AT STOICHIOMETRIC AIR-FUEL MIXTURE	76
Figure 35. - EXAMPLES OF THE CHANGE IN TRANSVERSE FLAME RADIATION WITH FUEL-AIR MIXTURE RATIO	77
Figure 36. - EXAMPLES OF THE CHANGE IN AXIAL FLAME RADIATION WITH FUEL-AIR MIXTURE RATIO	78

(Continued)

TABLE OF CONTENTS (CONTINUED)

	<u>Page</u>
Figure 37. - EFFECT OF HYDROCARBON TYPE ON TRANSVERSE FLAME RADIATION IN PHILLIPS MICROBURNER.	82
Figure 38. - EFFECT OF HYDROCARBON TYPE ON AXIAL FLAME RADIATION IN PHILLIPS MICROBURNER	83
Figure 39. - EFFECT OF HYDROGEN CONTENT ON FLAME RADIATION OF STOICHIOMETRIC MIXTURES IN THE PHILLIPS MICROBURNER .	85
Figure 40. - EFFECT OF HEAT OF COMBUSTION ON FLAME RADIATION OF STOICHIOMETRIC MIXTURES IN THE PHILLIPS MICROBURNER .	86
Figure 41. - EFFECT OF LUMINOMETER NUMBER ON FLAME RADIATION OF STOICHIOMETRIC MIXTURES IN THE PHILLIPS MICROBURNER.	87
Figure 42. - EFFECT OF ASTM SMOKE POINT ON FLAME RADIATION OF STOICHIOMETRIC MIXTURES IN THE PHILLIPS MICROBURNER. .	88
Figure 43. - ILLUSTRATION OF THE LACK OF EFFECT OF VOLATILITY ON TRANSVERSE RADIANT ENERGY OF STOICHIOMETRIC MIXTURES IN THE PHILLIPS MICROBURNER.	90
Figure 44. - ILLUSTRATION OF THE LACK OF EFFECT OF VOLATILITY ON AXIAL RADIANT ENERGY OF STOICHIOMETRIC MIXTURES IN THE PHILLIPS MICROBURNER	91
Figure 45. - CORRELATION OF HYDROGEN CONTENT WITH FLAME RADIATION IN THE PHILLIPS 2-INCH COMBUSTOR AND THE J-57 and J-79 COMBUSTORS AT 5 ATMOSPHERES PRESSURE	92
Figure 46. - CORRELATION OF LUMINOMETER NUMBER WITH FLAME RADIATION IN THE PHILLIPS 2-INCH COMBUSTOR AND THE J-57 AND J-79 COMBUSTORS AT 5 ATMOSPHERES PRESSURE	93

PHILLIPS PETROLEUM COMPANY

BARTLESVILLE, OKLAHOMA

SUMMARY REPORT

FOR

NAVY BUWEPS CONTRACT NOW 63-0406-d

EFFECT OF JP-5 PROPERTIES ON HOT GAS CORROSION AND FLAME RADIATION

I. INTRODUCTION

A. HOT CORROSION

1. Gas Turbine Engine Operation in Marine Environment

In the past, the 0.4 weight per cent of sulfur allowed in grade JP-5 aviation turbine fuel has not accelerated the corrosion of engine hot section parts significantly. The concentration of sulfurous gases in the combustor exhaust stream has not been high enough, under the oxidizing conditions and at the temperatures prevailing, to result in sulfidation of turbine blades. The chromium content of the nickel-base alloys involved, which aids the superalloy in resisting attack by oxygen and sulfur, has been near 20 per cent and operating temperatures have not exceeded 1700 F.

Continued development of the aircraft turbine engine, to decrease specific fuel consumption and increase specific power, has required the development of new alloys to permit higher cycle temperatures. Engines of advanced design are operating now with turbine inlet gas temperatures of 2100 F. These new alloys are characterized by a reduction of chromium content to near 10 per cent in order to increase the concentration of high temperature strengthening elements. While their resistance to oxidation appears satisfactory, reports of accelerated corrosion by sulfidation must be evaluated carefully by the Navy.

Catastrophic corrosion of nickel-base alloys having low chromium content has been encountered where operation has been over or near the sea (1, 2). Traces of sodium sulfate, a major constituent of sea salt, has been detected on corroded turbine blades. It has been possible to reproduce the essential features of the attack on the new type superalloys in laboratory tests by exposure to "sea salt".

Required aircraft operational patterns exclude control over sea water and sea salt ingestion by the engine. However, other approaches to limiting sulfidation of hot section components are being investigated by the Navy. The use of transpiration air cooled turbine blades has been suggested as a design approach to lower metal operating temperatures (3). Another approach might be the use of fuel of low sulfur content to reduce the concentration of sulfurous gases (4).

Changes in metallurgy to improve corrosion resistance do not appear promising, since they would lose the physical properties which made a desirable structural material in the first place. However, the application of suitable protective coatings to resist attack by corrosive materials is being vigorously pursued, with much promise (5). Perhaps suitable coatings of a self-healing nature might be made by the use of proper fuel additives, as has been the practice with industrial gas turbine engines operating on residual fuels. Such a feature would be of great value, for even under the best circumstances coatings are susceptible to random defect failures and reliability remains as the major problem confronting the user. The perfection of a self-healing coating system might allow the use of refractory-metal-base alloys operable at temperatures near 3000 F.

2. Hot Corrosion of Superalloys

Superalloys (nickel-chromium-cobalt base with smaller amounts of aluminum, titanium, columbium, molybdenum, etc.) have been developed for service in oxidizing atmospheres at temperatures near 2000 F. Their superior physical properties are required by aircraft turbine engines for hot section components, such as rotating turbine blades, where mechanical and thermal stresses are at a maximum. Their resistance to oxidation damage results from the growth of stable adherent metal oxide scales; therefore, these parts do suffer from oxidation damage, but it is usually not significant until after hundreds, or even thousands, of hours of operation.

Under the oxidizing conditions existing in the hot section of an aircraft turbine engine, sulfur attack is normally no more severe than oxygen attack, due to the formation of a surface oxide film on the alloy (6). However, the deposition of ash from the air or fuel opens the way for catastrophic rates of sulfidation, associated with the fluxing action of molten phases formed on the surface of the metal structure (7, 8, 9, 10). A common source of such deposits is sea salt, which is rich in sodium sulfate. The deposits may serve to collect and concentrate sulfur, which is normally present in harmless concentrations in the exhaust gas, and convey it to the metal surface beneath the deposit.

There is no generally satisfactory solution to this problem short of removal of the molten phase from contact with the metal. With operation in a marine environment, it is not usually feasible to prevent the ingestion of sea water and sea salt. The alternate has been to keep the temperature below the fusion temperature of the predominantly sodium sulfate deposit, or to use an alkaline earth additive to raise fusion temperature above the temperature of operation.

3. Review of Previous Work by Phillips Petroleum Company

Limited investigations of the effect of fuel sulfur on "hot section" durability of aircraft turbine engines have been conducted by Phillips Petroleum Company working under U. S. Navy Bureau of Naval Weapons Contracts NOas 58-310-d, NOas 60-6009-c, NOW 61-0590-d and N600(19)-58219 (11, 12, 13, 14). Much of this work has been summarized in a paper presented to the Institute of Petroleum (15). In addition, a small amount of exploratory work was conducted during the first quarterly period of the present Contract NOW 63-0406-d (16). These investigations have shown that:

1. The form in which sulfur exists in the fuel (i.e., organic sulfur compound type) is unimportant to hot corrosion as compared to the gross sulfur content of the fuel. (11, 12)
2. The extent of sulfidation is a linear function with time, indicating that its mechanism is not diffusion controlled by a coherent barrier layer of scale. (11, 12, 13, 14, 15, 16)
3. The aromatic content of the fuel (0 to 25 per cent) had no measurable effect on hot corrosion rates indicating that variations in exhaust gas soot content and flame radiant heating at high pressure were not significant. (16)
4. The relative rates of hot corrosion for a group of superalloys at atmospheric pressure did not correlate with rates obtained at high pressure, indicating that sulfidation reactions are pressure dependent and vary with alloy composition. (14)
5. Sulfur had little, or no, effect on hot corrosion - in the absence of "sea salt". (15)
6. "Sea salt" accelerated hot corrosion at high temperatures 1600 to 2000 F, but had no effect at 1350 F. (13, 16).

4. Contract NOW 63-0406-d

An experimental investigation of the corrosion by hot gases of modern superalloys used in aircraft turbine engines of advanced design was conducted by Phillips Petroleum Company during the third quarterly period, October through December 1963, of U. S. Navy Bureau of Naval Weapons Contract NOW 63-0406-d. Coupons of aluminum-titanium-hardened nickel-chromium-base alloys were exposed to high velocity gases, at high temperature and high pressure, to evaluate the effect of the latter's sulfur and "sea salt" content.

This study was made to determine whether the maximum sulfur limit of 0.4 weight per cent, currently allowed in grade JP-5 aviation turbine fuel, is a safe level for the protection from hot corrosion of turbine blade alloys used in advanced engines when operating in a marine environment. If not, information was sought to show whether a reduction in the sulfur limit for JP-5 would alleviate hot corrosion significantly.

The use of oversimplified test methods, such as furnace exposure to high temperature or torch exposure to high temperature and high velocity, does not provide exposure to the full range of variables encountered in actual service. While a limited amount of such data are available from the literature (4, 6, 7, 8, 9, 10), they cannot be accepted with confidence.

A more restrictive limitation on the amount of sulfur allowed in JP-5 carries with it the certainty of decreased availability, and the potential of increased cost. The former can be very important in the event of a national emergency, while even a small increment in the latter can amount to a substantial sum because of the large volumes involved.

Therefore, this investigation (17) was carefully designed, using a high-pressure burner rig to obtain exposure of superalloy test specimens to conditions closely simulating those prevailing in service.

For maximum severity of test conditions, a high compression ratio aviation turbine engine operating at sea-level take-off conditions was simulated. The superalloy test specimens were exposed to the exhaust gas from a combustor operated at the following conditions:

1. Combustor inlet temperature of 1000 F.
2. Combustor pressure of 15 atmospheres.
3. Combustor exhaust gas temperature of 2000 F.
4. Combustor reference velocity of 200 ft/sec.
5. Cyclic operation each hour, with 55 minutes at temperature.

A statistically designed test program (18) was conducted to show whether the concentration of sulfur in the fuel accelerated "sea salt" corrosion significantly. The extent of hot corrosion was based on evaluation of:

1. Test specimen weight loss.
2. Deterioration in test specimen tensile properties.

B. FLAME RADIATION

1. Gas Turbine Durability

An inherent conflict exists in the combustion chamber of all gas turbine engines, between their maximum structural temperature and the flame which they must contain. If chemical equilibrium were attained during the constant pressure combustion process, and hydrocarbon-air mixtures were in the neighborhood of stoichiometric, the thermal environment would be near 4000 F. Somewhat lower temperatures, 3000 - 3500 F, are usually indicated in actual practice. However, the materials presently available for fabrication of combustion chambers must operate at much lower temperatures if rapid failure is to be avoided. Clarke and Jackson (19) indicate that metal operating temperatures of 900 - 1300 F, with peaks up to 1700 F, are commensurate with the usual desired combustor life. Droege Mueller (4) cites, as a typical example, a 50 per cent reduction in the fatigue life of a combustor by a metal temperature increase of 25 F. Therefore, provision must be made for the cooling of combustion chamber parts and control must be exercised over the heat transfer variables of the flame.

For consideration of the heat transfer processes, we may regard the combustion chamber simply as two concentric containers. Compressed air enters the annular space between the outer case and the inner flame tube. The latter has suitably spaced holes through which the air is fed to the flame contained therein. The hot combustion products are diluted with excess air to reduce their temperature. Thus, the flame tube receives heat from the hot gases inside it by convection and radiation, and loses heat by radiation to the outer case and by convection to the

surrounding annulus air. However, the flame tube is largely protected from the searing heat of the combustion gases by direction of a film of cooling air over its inner surface. This limits convective heating, but leaves radiant heating from the flame as a major contributor to the equilibrium temperature attained by the flame tube.

Aircraft turbine engine development has involved a steady increase in combustor inlet air temperature. Engines of advanced design are operating now with combustor inlet air temperatures of 900-1300°. It is pertinent to point out that this represents the "sink" temperature for cooling of combustor parts, and that it equals the maximum metal temperature commensurate with the usual desired combustor life. Thus, it is clearly no longer feasible to maintain flame tube temperatures at desired levels. This situation requires that flame radiation be minimized to obtain acceptable gas turbine durability.

2. Control of Soot Formation

The total radiant energy (W) from a flame is a function of its temperature (T), area (A) and emissivity (ϵ); and in accordance with the Stefan-Boltzmann Law, $W = \sigma \epsilon AT^4$, where σ is the Stefan-Boltzmann Constant. While all of these variables are affected by the design of the combustion chamber, they also are affected by the molecular structure of the hydrocarbon fuel. There appears to be no reason to expect significant improvements in combustor design which will reduce flame radiation. Rather, the increasing severity of operating conditions, resulting from higher pressures and temperatures, will increase flame temperature and emissivity. Therefore, the possibilities for relief by fuel selection must be carefully evaluated.

Generally, the heat transfer variables of flame temperature, area and emissivity tend to decrease in value with the increasing hydrogen content of the fuel. However, much of the literature concerning the effect of fuel composition appears to be unsatisfactory because of careless and superficial use of concepts connected with the measurement of flame radiation (20). Of principal concern has been the formation of soot particles in flames, which superimposes a continuum upon the molecular spectrum to produce the familiar yellow luminosity.

The mechanism of soot formation in hydrocarbon-air flame is not fully understood. However, the importance of the molecular structure of the fuel is well known. This can be illustrated by considering the significant reactions as competitive oxidation and dehydrogenation processes. The hydrocarbon molecule can either (a) fragment to oxides of carbon, or (b) polymerize to large polybenzenoid structures (soot). The greater the hydrogen content of the fuel molecule, the greater the alteration in structure that is required before condensation can take place, and the more likely that oxidation will prevent soot formation. Admittedly this is an oversimplified picture of soot formation, but the indications are clear that lower flame emissivities will be obtained with higher hydrogen content fuels (21).

A critical analysis has been made of current test methods, Smoke Point and Luminometer Number, used for evaluation of the burning quality of hydrocarbon fuels for aircraft turbine engines (21). Both are performance tests in which a sample of fuel is burned in a wick lamp to determine its relative soot forming tendency. Unfortunately, the laminar flow diffusion flame of the wick lamp differs appreciably from the highly turbulent combustion process in an aircraft turbine engine. Differences in the mechanism of soot

formation, as evidenced by the effect of hydrocarbon structure, are significant. This could result in undue emphasis being placed upon the attainment of a fuel property, such as very high Luminometer Number, from which no improvement in gas turbine durability would accrue.

It is well known that pressure favors the formation of soot, which usually escapes from the flame as exhaust smoke during take-off operation where pressure is at a maximum. The resultant high flame emissivities occur under already adverse conditions, for high pressure operation is associated with high combustor chamber inlet air temperatures and high flame tube collapse loads. Therefore, to be relevant, ratings of the sooting tendency of aviation turbine fuels must apply to the critical high pressure operating conditions.

Studies of total radiant energy from combustor flames at pressures of 1 - 15 atmospheres by Streets (22) have indicated that atmospheric pressure devices do not adequately describe the flame radiation, and hence flame tube durability, performance of fuels at high combustor pressures. This may be explained in part by studies of the sooting tendency of premixed flames at pressures of 1 - 20 atmospheres reported by Macfarlane and Holderness (23). Their data indicate that soot formation in general has approximately a pressure cubed dependence, but that it can vary from about P^1 to P^6 with differences in hydrocarbon structure.

Thus, it seems that there are (a) fundamental differences in the mechanism of soot formation in the diffusion flame of the wick lamp used in present specification test methods and in the turbulent diffusion combustion process of gas turbine engines, which are (b) further complicated by differences between hydrocarbon structures in the pressure dependence of their soot forming reactions. Further work to establish the relationship between the molecular structure of hydrocarbon fuels and flame radiation in turbulent diffusion combustion systems is required.

3. Review of Previous Work by Phillips Petroleum Company

Investigations of various aspects of flame radiation from aviation turbine fuels have been conducted during the past ten years by Phillips Petroleum Company working under U. S. Navy Contracts NOas 52-132-c, NOas 58-310-d, NOW 61-0590-d and M600(19)-58219. Most of this work has been summarized in the following papers and special reports:

- (a) Early work to establish the spectral characteristics of radiant energy from gas turbine combustor flames at pressures from 1 - 15 atmospheres for paraffinic and aromatic hydrocarbons was detailed in a special report, which later was presented as a paper to the American Chemical Society (24).
- (b) Subsequent studies of the effect of flame radiation on combustor durability at high operating pressures were summarized in a special report (25).
- (c) An investigation of the effect of aromatic type and aromatic content in grade JP-5 aviation turbine fuel on flame radiation was discussed in a paper presented to the Society of Automotive Engineers (26).
- (d) Experience accumulated during these studies and pertinent to the measurement of total radiant energy from gas turbine combustor flames was reviewed in a paper presented to the Society of Automotive Engineers (20).

In addition, an effort has been made to correlate and interpret available measurements of flame radiation from gas turbine combustors to indicate the effect of fuel composition (27), and a critical analysis has been made of current test methods used for evaluation of the burning quality of aviation turbine fuels (21).

Some of the more pertinent findings of these investigations are

- (a) The spectral distribution of the radiant energy from gas turbine combustor flames varies with operating conditions and fuels. Black body radiation is approached with increasing pressure and decreasing fuel hydrogen content. (24, 20, 27)
- (b) There is no significant correlation between measurements of total radiant energy from gas turbine combustor flames and their luminosity; i.e., visible radiation. (26, 27)
- (c) Measurements of total radiant energy from gas turbine combustor flames should include the infrared spectral region through 5 microns to obtain reliable data. This can be accomplished by the use of sapphire optical materials and a suitably calibrated total radiation pyrometer. (24, 20)
- (d) Emissivities of gas turbine combustor flames can vary from 0.03 for non-luminous flames to nearly one for luminous flames. (24, 20, 27)
- (e) The energy transferred by radiation from the flame to the exposed hot section parts in a gas turbine can represent as much as 10 per cent of the total energy released in the combustion process. (24)
- (f) Calculated estimates indicate that flame radiation may contribute 30-80 per cent of the total heat flux at the exposed surface of the flame tube in a gas turbine combustor. (22, 26)
- (g) There is a linear correlation between flame radiation and liner temperature in gas turbine combustors. Changes in flame tube operating temperature of about 400 F can result from variations in fuel burning quality. (26, 27)
- (h) Radiant heating of hot section parts in a gas turbine engine may vary with location because quenched combustion products can effectively absorb flame radiation. This may reverse expected benefits at down-stream locations from higher burning quality fuels. (20, 25, 26, 27)
- (i) Differences in flame radiation between fuels may be small at low combustor operating pressure, increase with pressure until flame emissivities of one are approached, and decrease at higher pressure. (24, 27)
- (j) Polycyclic aromatic fuel blends burn with higher flame emissivities in gas turbine combustors than monocyclic aromatic fuel blends of comparable ASTM Smoke Point. (26)
- (k) No significant reduction in flame radiation or flame tube temperature in gas turbine combustors resulted from the use of fuels having Luminometer Numbers above 100. (26, 27)
- (l) There is a linear correlation between measurements of total radiant energy from gas turbine combustor flames and the hydrogen content of hydrocarbon fuels. (21)

4. Contract NOW 63-0406-d

As a result of the critical analysis of current test methods used for evaluation of the burning quality of aviation turbine fuels made under Contract N600(19)-58219, it was recommended that the relationship between molecular structure of hydrocarbon fuels and flame radiation be investigated in a turbulent diffusion combustion system. (21) This study was outlined in Progress Report No. 2 (17), and the results of an experimental investigation using the Phillips Microburner and a group of 44 pure hydrocarbons were detailed in Progress Report No. 4 (28) by Phillips Petroleum Company working under U. S. Navy Bureau of Naval Weapons Contract NOW 63-0406-d.

The group of pure hydrocarbons were selected to include normal paraffins, isoparaffins, cycloparaffins (mono- and polycyclic), olefins (straight and branched chain and cyclic) and aromatics (mono- and bicyclic) over a wide range of boiling point for each hydrocarbon type. This insured also a large variation in such properties as hydrogen content, heat of combustion, Luminometer Number and Smoke Point.

The Phillips Microburner was selected for simplicity of operation and small fuel appetite. The latter is always important when working with pure hydrocarbons. Construction of the Phillips Microburner provides for air atomization of the fuel, which at low fuel flow rates approaches a premixed system. By operation over a broad range of over-all fuel-air mixture ratios, this feature allowed for the approach to a premixed turbulent flame at "lean" mixtures and a diffusion turbulent flame at "rich" mixtures. Unfortunately, the Phillips Microburner is an atmospheric pressure device, and so prohibited investigation of this most important operating variable.

Measurements were made of total radiant energy using a Leeds and Northrup Rayotube modified with sapphire optics for inclusion of the infrared spectral region out to 5 microns. Initially, it was planned to make these measurements with a dual-channel Barnes Research Radiometer for more accurate measurement of total radiant energy and simultaneous determination of flame temperature by measurement of radiant energy at the 4.4 micron carbon dioxide peak. Knowing total radiant energy and flame temperature, flame emissivity can be calculated. However, it was not available for this investigation, and so the Rayotube was used.

II. HOT CORROSION OF SUPERALLOYS

A. TEST EQUIPMENT

1. Phillips 2-Inch Combustor

The Phillips 2-inch combustor shown in Figure 1 was used in preliminary tests (16) without modification except for mounting of the test specimens (Section II, A-2) six inches downstream from the combustor section. When attempts were made to operate under very severe conditions (1000 F combustor inlet air temperature at 15 atmospheres pressure and 2000 F combustor outlet gas temperature), simulating a high compression ratio aviation turbine engine operating at sea-level take-off conditions, combustor liners failed rapidly as the result of melting. This necessitated the development of a modified 2-inch combustor. In this development (17), sixteen different designs were evaluated before a fully satisfactory combustor configuration could be selected.

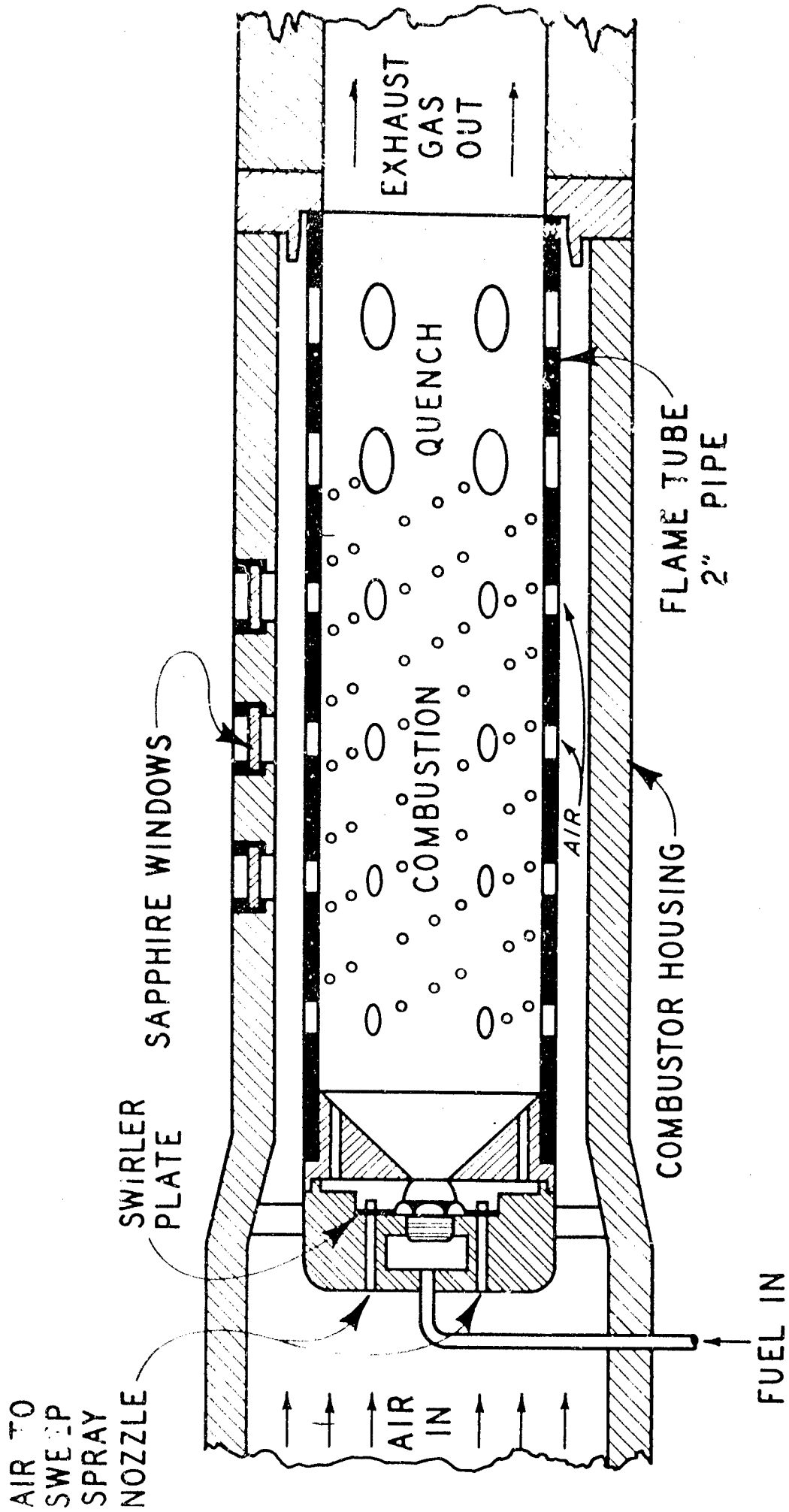


FIGURE 1

PHILLIPS LABORATORY SCALE TEST COMBUSTOR

Details of the design of the modified combustor are given in Table I and a schematic diagram of it is shown in Figure 2. Basically, both the original and modified Phillips 2-inch combustors embody the principal features of a modern aircraft turbine engine combustor. They are straight-through, can-type combustors with fuel atomization by a single, simplex-type nozzle. The flame tube is fabricated from 2-inch, Schedule 40, Inconel pipe. The modified combustor contains added internal deflector skirts for film cooling surfaces exposed to the flame.

The supporting test facility, pictured in part in Figure 3, has been described previously in detail (29). Briefly, air is supplied by rotary Fuller compressors, filtered by a Selas Vape-Sorber, and preheated by a Thermal Research heat-exchanger. Fuel is supplied by nitrogen pressurization of its supply tank. A view of the control panel is shown in Figure 4.

The design of the combustor installation provides for easy access to the fuel nozzle, flame tube and test specimens. The combustor installation was disassembled, inspected, and reconditioned after each test.

During preliminary testing synthetic "sea water" was injected into the primary zone of the combustor, near the fuel nozzle. The injection probe was water cooled to prevent vaporization of "sea water", and plugging of the orifice. After modification of the combustor to permit testing under very severe conditions, it became evident immediately that flame tube life would be limited to a single 5-hour test with "sea water" because of severe corrosion of the internal deflector skirts. Therefore, the "sea water" injection point was moved downstream to the quench zone of the combustor, as shown in Figure 2.

During preliminary testing an air-cooled, 310 stainless steel exhaust section was used. It soon became evident that this would not stand extended periods of operation with 2000 F exhaust gas temperature. Therefore, it was cooled by water jacketing, with excellent results.

The modifications increased combustor durability to such an extent that no failures of the flame tube or exhaust section occurred during the subsequent test program.

Data obtained (18) before and after relocation of the "sea water" injection probe and addition of water cooling to the exhaust section indicated that these changes had a negligible effect on hot gas corrosion of the super-alloy Inconel 713C. Good test repeatability was also indicated and an excellent spread in weight loss was obtained between tests with essentially sulfur-free base fuel and with the base fuel with added sulfur plus ingested "sea water".

2. Specimen Holder

The test specimen holder was of the same design employed in earlier work (16). Its general location with respect to the 2-inch combustor has already been indicated in Figure 2. It is separated from the 2-inch combustor by a six inch long water-cooled spool and is followed by another water-cooled spool one foot in length. It is mounted in a suitable cavity in a flange located between these two water-cooled spools.

TABLE IDESIGN DETAILS OF MODIFIED PHILLIPS 2-INCH COMBUSTORSplash Cooling Air

Hole Diameter, in.	0.0125
Holes/Station	16
No. of Stations	7
Total No. of Holes	112
Total Hole Area, in. ²	1.38
% Total Hole Area	42

Primary Combustion Air

Hole Diameter, in.	0.250
Total No. of Holes	4
Total Hole Area, in. ²	0.20
% Total Hole Area	6

Secondary Combustion Air

Hole Diameter, in.	0.375
Total No. of Holes	4
Total Hole Area, in. ²	0.44
% Total Hole Area	14

Quench Air

Hole Diameter, in.	0.625
Total No. of Holes	4
Total Hole Area, in. ²	1.22
% Total Hole Area	38

Total Combustor Area, in.²

3.24

% Cross Section Area

122

Fuel Nozzle and Combustor Dome

Spray Angle, degrees	45
Shield Hole Diameter, in.	0.625
Air Atomizer Swirl Plate	Yes

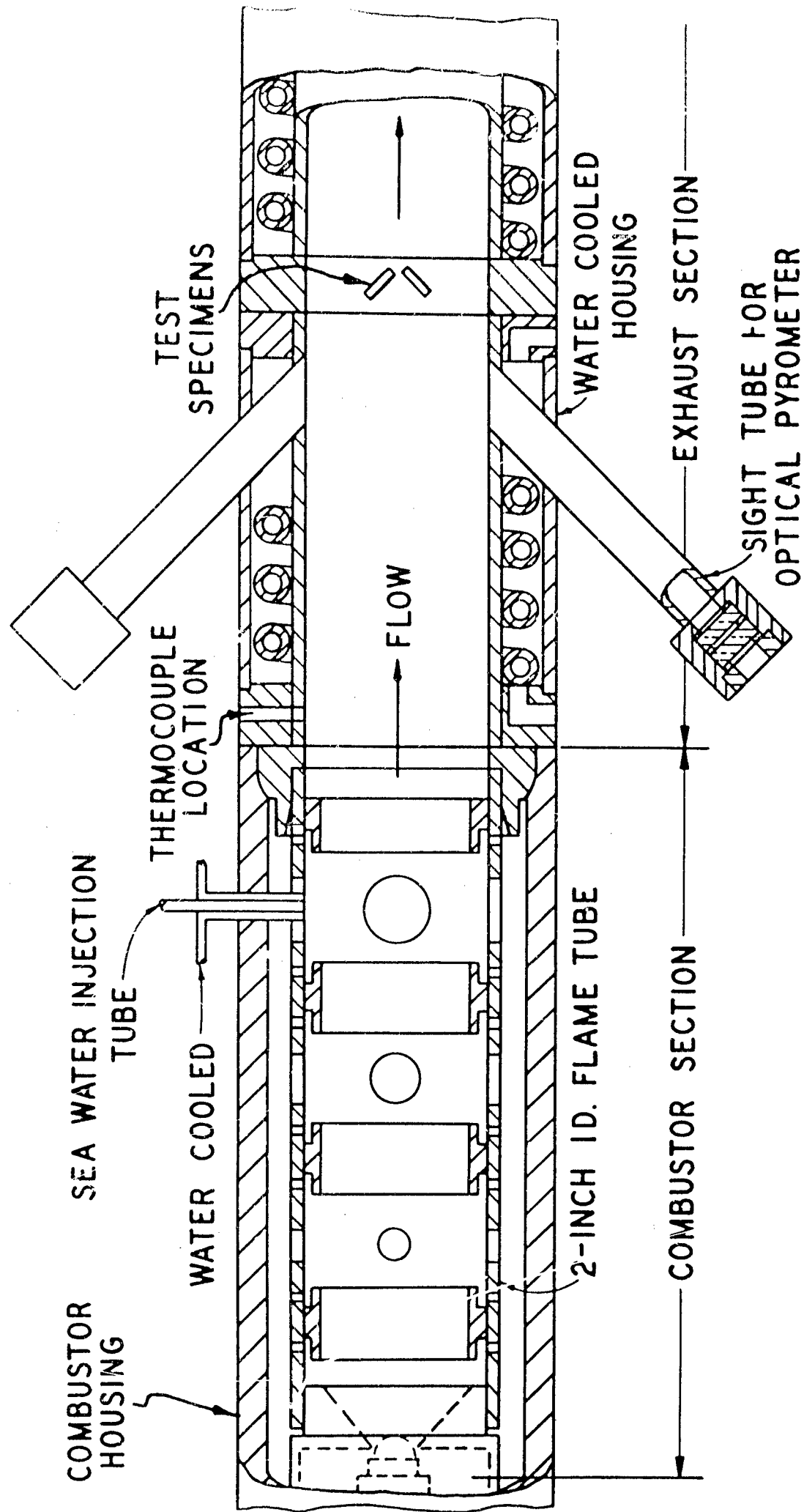


FIGURE 2
 PHILLIPS 2 - INCH COMBUSTOR INSTALLATION FOR HOT GAS CORROSION STUDIES

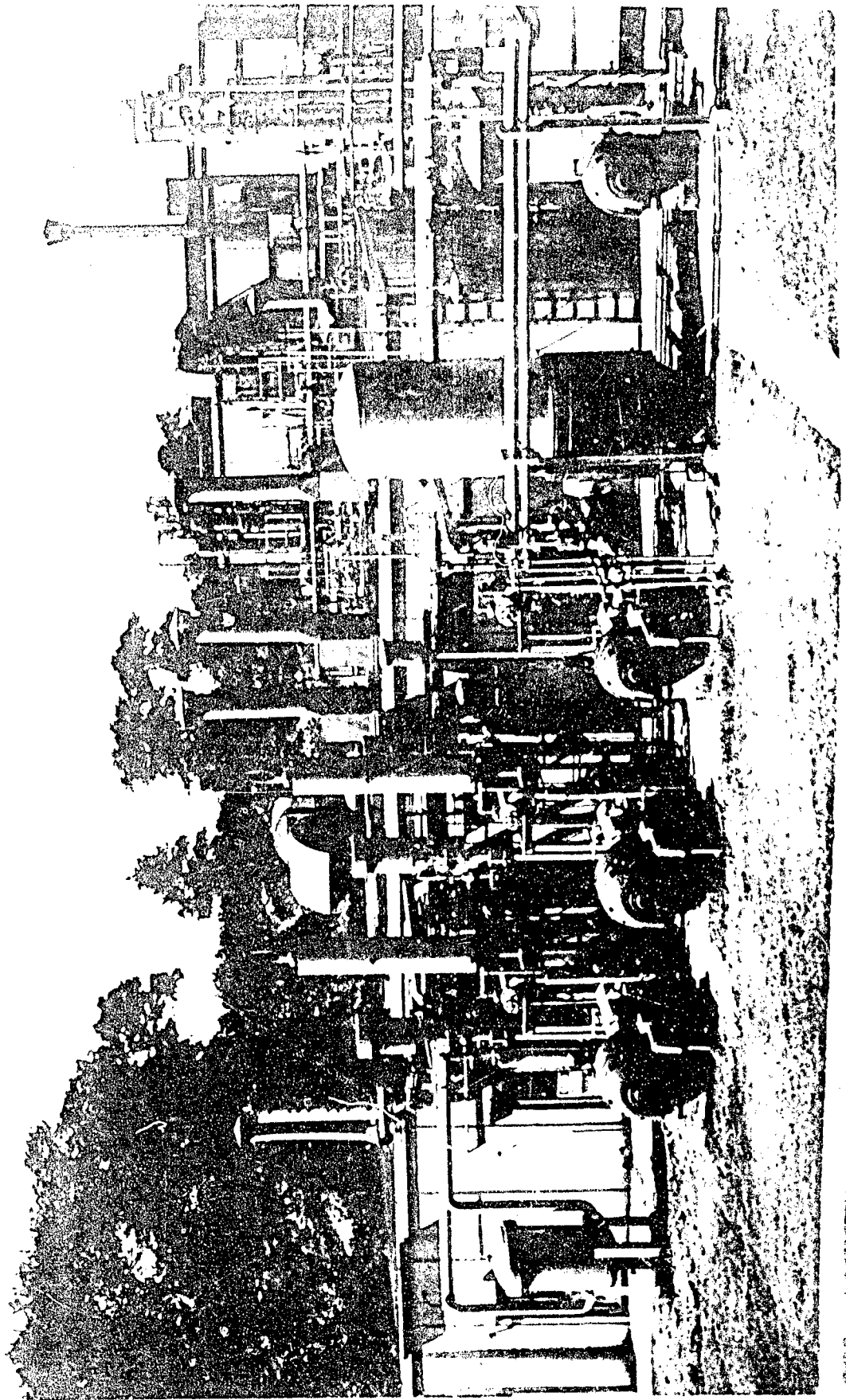


FIGURE 3
NORTHWEST VIEW OF PHILLIPS RESEARCH FACILITY FOR JET FUELS

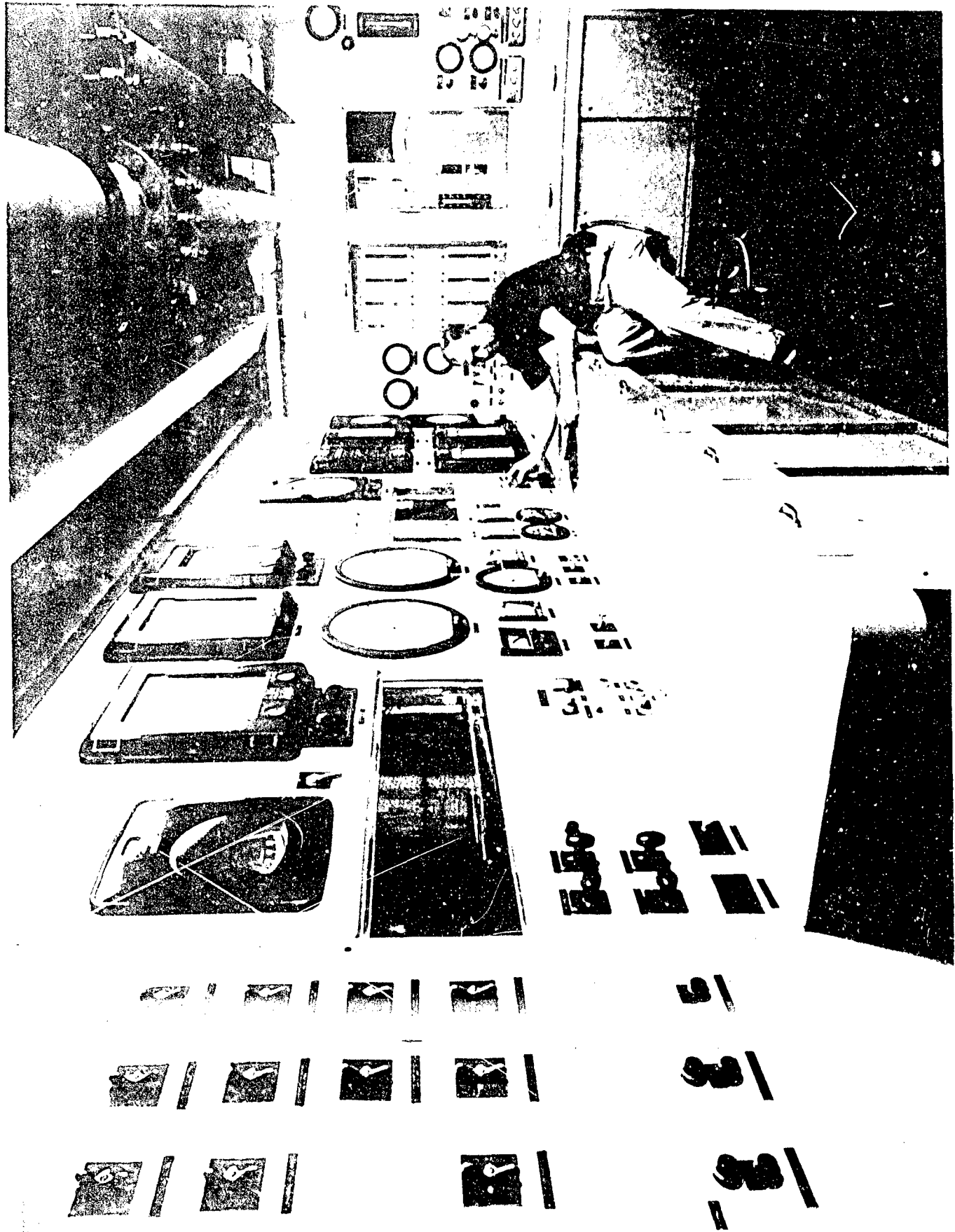


FIGURE 4
VIEW OF CONTROL PANEL FOR LABORATORY SCALE COMBUSTOR
STUDIES OF JET FUELS - PHILLIPS RESEARCH TEST FACILITY

The cross sectional area of the 2-inch pipe in which the test specimen holder is located is 3.36 in.²; however, the unblocked area in the test specimen holder is only 1.80 in.². The holder maintains the test specimens at an angle of 45 degrees to the direction of flow of the exhaust gas as shown in Figure 5. This provides for acceleration of the gas flow over the surface of the test specimens, much as over the turbine blading in an actual engine.

While the 310 stainless steel test specimen holder is subjected to considerable attack by the hot exhaust gases, this design provides for easy removal of the test specimens and replacement of the holder when necessary.

In their location relative to the flow direction, the test specimens were subjected to appreciable gas pressure loading while a test was in progress. The pressure drop across the specimens is a measure of the loading and, for most of the tests discussed in this report, amounted to 5 lb/in.².

3. Specimen Electrocleaning

A very satisfactory technique, described by Shirley (8), was used for the removal of specimen scale or bulk oxide after exposure to hot corrosion. A schematic diagram of the apparatus for electrocleaning by a cathodic descaling process is shown in Figure 6. The test specimens, having a No. 30 drill hole at one end for hanging in the bath, were completely immersed in molten sodium hydroxide (750-790 F) and a current of about 1/3 ampere/cm² was passed through them for a period of 10 minutes. Thus, for two test specimens with a total surface area of 35.28 cm² a direct current of 12 amperes was used. This was followed by a water quench.

With new, unexposed specimens, only a negligible amount of metal is lost when subjected to this technique. Statistical analyses of data obtained during the test program also showed (18) that this method of electrocleaning had no significant effect on the measured tensile properties (ultimate tensile strength, per cent elongation, and ultimate load) of the superalloys Inconel 713C and Sierra Metal 200.

4. Specimen Modification for Tensile

As shown in Figure 5, a test specimen consisted of a coupon of superalloy 0.50 in. wide, 2.38 in. long and 0.06 in. thick. After exposure to hot corrosion in the combustor, preweighed specimens were cleaned as described in Section II-C and then reweighed to determine the weight loss.

Prior to measurement of the tensile properties, both before and after exposure to hot corrosion, the new or cleaned test specimen was filleted as shown in Figure 7. The width of the tensile specimen, 0.250 ± 0.002 in., was easily measured with a micrometer. However, when the specimen had been exposed to hot corrosion, the irregular surfaces of the top and bottom sides made the thickness more difficult to measure. Therefore, there was a minor uncertainty in the cross-sectional area to be used in the calculation of ultimate tensile strength of specimens after exposure to hot corrosion.

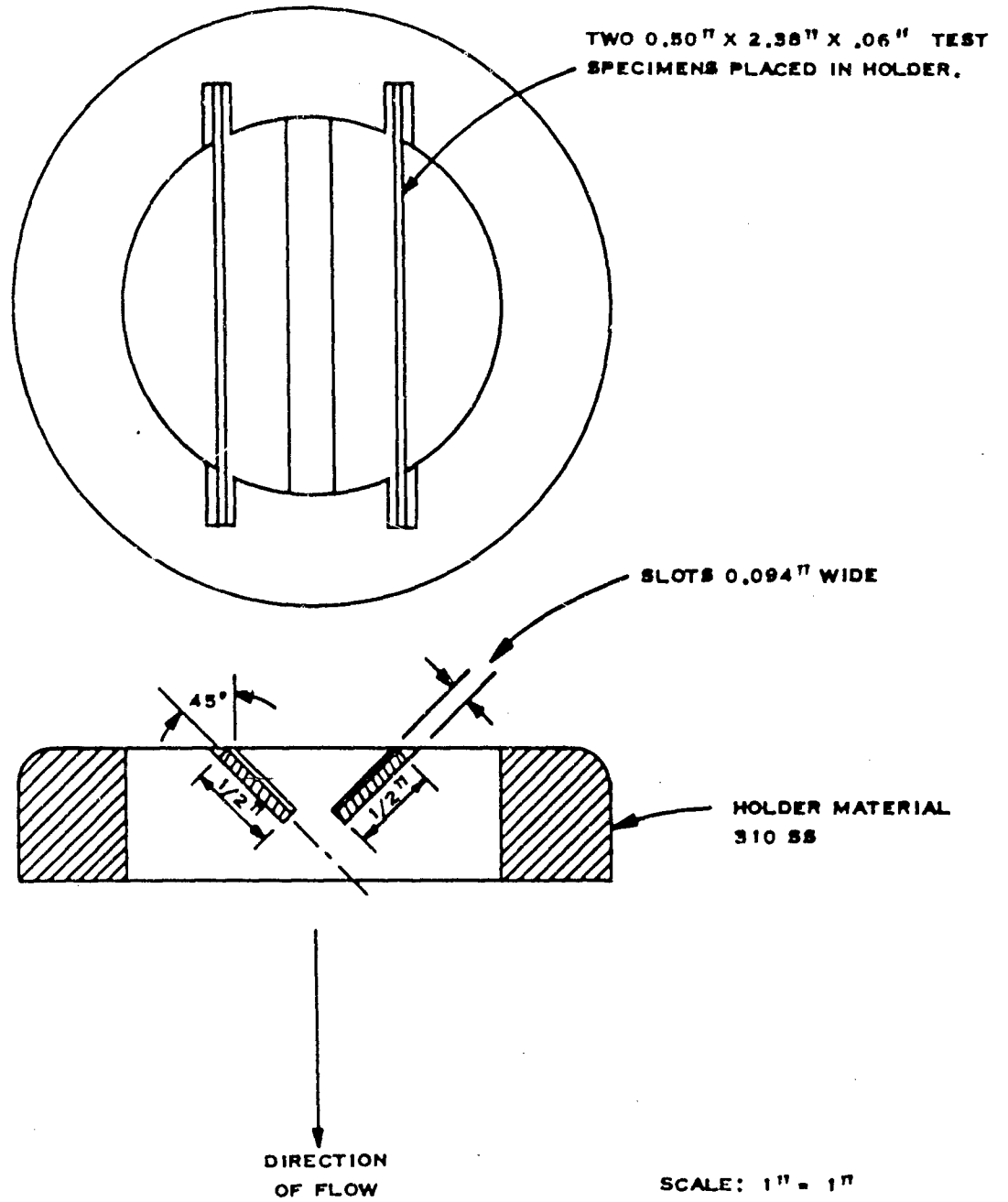


FIGURE 5
TEST SPECIMEN HOLDER FOR PHILLIPS 2-INCH COMBUSTOR

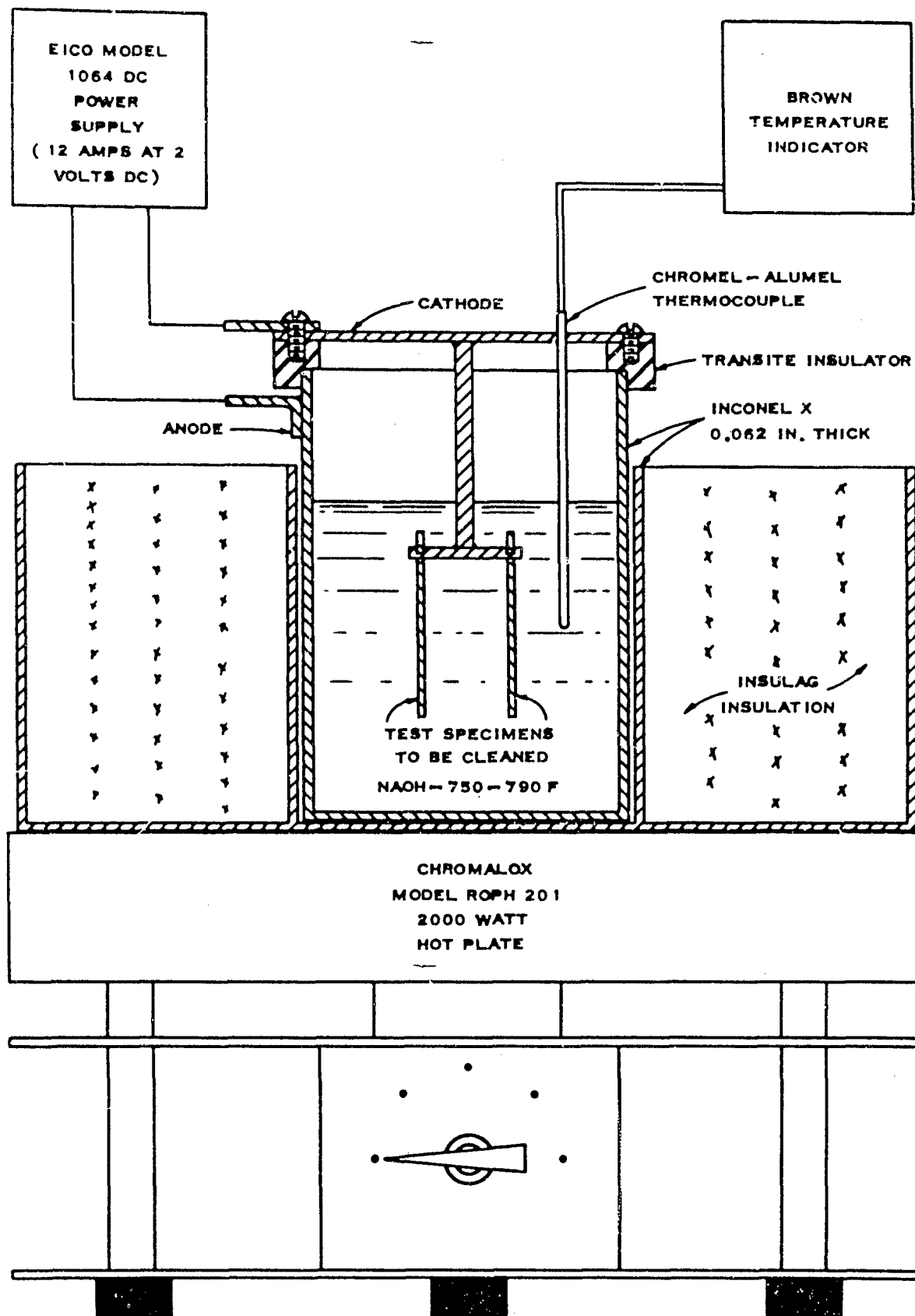


FIGURE 6
CATHODIC DESCALING APPARATUS
FOR CLEANING TEST SPECIMENS
FOLLOWING EXPOSURE TO HOT GAS CORROSION

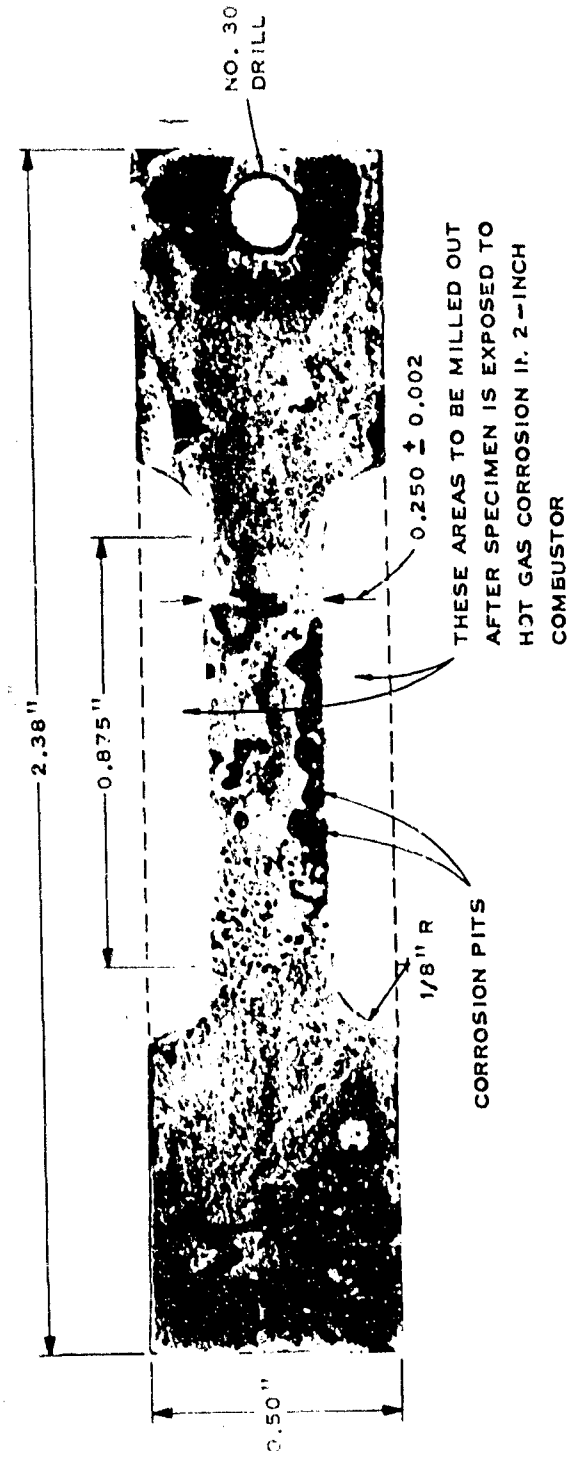


FIGURE 7
 MODIFICATION OF TEST SPECIMEN FOR TENSILE EVALUATION
 FOLLOWING EXPOSURE TO HOT GAS CORROSION

The tensile specimens were pulled in an Instron Model TTCl tensile machine operated at a crosshead travel rate of 0.1 in./min. The gauge length of the tensile specimen was 0.875 in.

B. TEST MATERIALS

1. Fuel.

a. Sulfur in Petroleum

Natural crude oil is composed of hydrocarbons, primarily. However, normally there are small amounts of organic compounds of sulfur, oxygen and nitrogen present, in addition to very small amounts of metallo-organic compounds of vanadium, nickel, iron and copper. These non-hydrocarbon constituents are usually concentrated in the higher-boiling-temperature portion of the crude oil, along with polynuclear aromatics and multi-ring cycloparaffins. Generally, they have been avoided in aviation turbine fuels by specification of fractions boiling below 550 F.

Sulfur is the exception. Decomposition of high molecular weight sulfur compounds occurs during refining operations, to add lower-boiling sulfur compounds which were not constituents of the original crude oil. Thus, a kerosine type fraction, such as JP-5, usually contains sulfides (RS), disulfides (RS₂), etc.

The amount of sulfur in crude oil varies over a range of several orders of magnitude; i.e., from about 0.05 to 5 weight per cent. South American, Near and Middle East crude oils contain, on the average, more sulfur. However, crude oils produced from a given geographical region can vary greatly.

Conventional refinery distillation of crude oil normally concentrates about 95 per cent of the sulfur in the heavy distillate fraction and residual portion. This leaves the middle distillate fraction, used for aviation turbine fuel, relatively free of sulfur. Further removal of sulfur has long constituted an important part of refinery practice to stabilize products with respect to odor, color and gum formation.

For more detailed discussions of the above information, see Reference 30.

b. Sulfur in JP-5

The sulfur content of 54 samples of grade JP-5 aviation turbine fuel, representative of production in the United States from 1957 through 1963, averaged 0.102 weight per cent, but the median value was only 0.060 weight per cent sulfur (31). These data are tabulated in Table II. It is pertinent to point out that the precision of the ASTM Lamp Method (D-1226) used by the manufacturers to obtain these data is 0.01 weight per cent sulfur, since 11 per cent of the samples were at, or below, this level. The majority of the samples, 54 per cent, were between 0.02 and 0.10 weight per cent in sulfur content. However, this left 35 per cent which approached the JP-5 specification maximum of 0.40 weight per cent sulfur.

It is of interest to note that 288 samples of the more volatile grade JP-4 aviation turbine fuel, averaged over the same period of time, showed a sulfur content of 0.044 weight per cent (31). This is 43 per cent of the average sulfur content reported for JP-5.

TABLE II

SULFUR CONTENT OF REPRESENTATIVE U.S. PRODUCTION SAMPLES OF JP-5

U.S. Bureau of Mines Petroleum Products Survey (31)

Year	<u>Total Sulfur Content, weight per cent</u>							<u>Total</u>
	<u>1957</u>	<u>1958</u>	<u>1959</u>	<u>1960</u>	<u>1961</u>	<u>1962</u>	<u>1963</u>	
	0.02	0.024	0.01	0.004	0.005	0.005	0.01	
	0.063	0.053	0.022	0.038	0.023	0.01	0.027	
	0.16	0.072	0.027	0.078	0.032	0.024	0.033	
	0.18	0.160	0.031	0.182	0.035	0.027	0.039	
	0.22	0.16	0.036	0.23	0.046	0.028	0.050	
		0.29	0.04		0.056	0.067	0.087	
			0.23		0.22	0.08	0.09	
			0.35		0.23	0.097	0.15	
					0.25	0.18	0.19	
						0.18	0.32	
						<u>0.32</u>		
Average	0.129	0.110	0.093	0.106	0.100	0.093	0.100	0.102
Median	0.16	0.116	0.034	0.078	0.046	0.067	0.069	0.060

On the basis of this and other similar information, it was decided to conduct the major program described in Section II-D of this report using test fuels having three levels of sulfur concentration. One was chosen at the maximum sulfur content of 0.40 weight per cent allowed by the specification for grade JP-5 aviation turbine fuel, since a considerable quantity of production fuel approaches this level. Another was selected at an order of magnitude less in sulfur content, 0.040 weight per cent, to represent the level characteristic of the major portion of aviation turbine fuel produced. A decrease in sulfur content of another order of magnitude, to 0.0040 weight per cent, seemed reasonable for the third fuel; however, it was felt that an even lower level would be desirable to allow testing with an essentially sulfur-free base fuel.

In the preliminary tests described in Section II-C, a fuel sulfur content of 1.0 weight per cent was used to permit comparison of the results with "sea water" ingestion with earlier results (15) obtained at this level of sulfur in the absence of "sea salt".

c. Base Fuel

The base fuel used in the preliminary tests (Section II-C) was a low sulfur JP-5 boiling range isoparaffinic fuel, having the properties shown in Table III. For most of the preliminary tests cumene was added to obtain an aromatic content at the maximum specification limit. Ditertiary butyl disulfide was added to obtain a sulfur content of 1.0 weight per cent.

The base fuel selected for use in the major program (Section II-D) was a segregated sample of production ASTM Type A aviation turbine fuel. Its physical and chemical properties of interest to this investigation are presented in Table IV. For comparison purposes, the average values of pertinent properties from the Bureau of Mines Petroleum Product Survey over the period from 1957 through 1963 are shown for grades JP-5 and JP-4 aviation turbine fuel (31). It should be noted that the physical and chemical properties of this base fuel closely approximate the averages for JP-5, with the exception of its very low sulfur content. This base fuel also was analyzed for metal content, to be certain that its iron, vanadium, nickel, and copper content were negligible; since, if present, they would concentrate as ash and might significantly alter the scale composition on the test specimen being exposed to the combustor exhaust gas.

This base fuel was essentially free of sulfur, containing only 2 parts sulfur per million parts of fuel by weight; i.e., 0.0002 weight per cent sulfur. The higher sulfur content test fuels were produced by blending to 0.040 and 0.40 weight per cent sulfur using ditertiary butyl disulfide. This dithiaalkane has been widely used in past research to obtain high sulfur content test fuels, since it is relatively inexpensive and available at adequate purity. Also, earlier work has shown organic sulfur compound type to be unimportant in hot corrosion studies (12).

TABLE IV

PHYSICAL AND CHEMICAL PROPERTIES OF BASE FUEL USED IN MAJOR PROGRAM

	<u>Test Fuel</u> <u>Base (a)</u>	<u>Average</u> <u>JP-5 (b)</u>	<u>Average</u> <u>JP-4 (b)</u>
Distillation, Temperature, F			
Initial Boiling Point	329		
5 volume per cent evaporated	344		
10 volume per cent evaporated	350	382	210
20 volume per cent evaporated	359		
30 volume per cent evaporated	368		
40 volume per cent evaporated	377		
50 volume per cent evaporated	388	413	307
60 volume per cent evaporated	400		
70 volume per cent evaporated	417		
80 volume per cent evaporated	435		
90 volume per cent evaporated	460	455	412
95 volume per cent evaporated	478		
End Point	498		
Gravity, degrees API	46.2	42.7	53.2
Gum, milligrams per 100 milliliters	0.2	1.0	1.0
Smoke Point, millimeters	26.2	23.1	28.1
Composition, weight per cent			
Sulfur	0.0002 (c)	0.10	0.04
Metals (d)			
Iron less than	0.0001		
Vanadium less than	0.0001		
Nickel less than	0.0001		
Copper less than	0.0001		
Hydrocarbon Types			
Normal Paraffins	27 (e)		
Isoparaffins	23 (e)		
Cycloparaffins	36 (e)		
Olefins	0 (e)		
Aromatics	14.0	14.3	11.2

Notes:

- (a) Segregated sample (BJ63-8-G49) of production ASTM Type A aviation turbine fuel, processed from West Texas crude and finished by hydrotreating.
- (b) U.S. Bureau of Mines Petroleum Products Survey. (31)
- (c) Higher sulfur content test fuels obtained by blending to desired sulfur level using ditertiary butyl disulfide.
- (d) X-ray fluorescence analysis.
- (e) Typical value for this product.

2. Sea Water

a. Composition

3
2) A synthetic "sea water"^(a) was used in this study. Its formulation was taken from the Standard Method of Test for Rust-Preventing Characteristics of Steam-Turbine Oil in the Presence of Water, ASTM Designation D-665-60. The components and their concentrations are shown in Table V.

Table VI compares the composition of this synthetic "sea water" with the average composition of sea water, as reported by Goldberg (32). Only the elements present in sea water at concentrations of 1 ppm, or greater, have been tabulated. Smaller concentrations of elements present in sea water are not included in the synthetic formula. It will be noted that the abundance of various elements in the synthetic formula compares very favorably with the average sea water composition. The one exception is silicon, and its exclusion from the synthetic "sea water" seems justified in the light of its reported variation in abundance from one water-mass to another by a factor of 1000, or more.

2
3
1
04 It is pertinent to point out that "sea water" will leave a residue of approximately 4.2 per cent by weight of "sea salt" upon evaporation of the water. Thus, for our purposes, a concentration of 24 parts of "sea water" per million parts of air is equivalent to a concentration of "sea salt" in air of 1 ppm. This "sea salt" contains approximately 2 per cent by weight sulfur, combined with about 20 per cent of the available sodium as sodium sulfate, Na_2SO_4 . The remaining sodium is available to combine with sulfur from the fuel to produce additional sodium sulfate, as noted by Simons, Browning and Liebhafsky (7). If the sulfur contributed by the fuel were completely scavenged from the hot gas stream, it would require a fuel sulfur content of only 0.0005 weight per cent at an air-fuel ratio of 60 to convert the excess sodium to sodium sulfate with a "sea salt" ingestion rate of 1.0 ppm in air. Thus, the amount of sodium sulfate in the ash is likely to be limited only by the total sodium content of the hot gas stream.

b. Ingestion Rate

2
level Establishing a realistic level for the concentration of sea salt in the air ingested by a gas turbine engine operating in a marine environment is difficult from the available literature. Woodstock and Gifford (33) report a concentration at 50 feet over the calm ocean near Bermuda of approximately 0.003 parts by weight of sea salt per million parts of air (ppm). Cadle (34) comments that salt particles over the ocean may at times be as concentrated as 100 particles per cubic centimeter, although one per cubic centimeter is more common. From this information, we can estimate a sea salt concentration over a rough sea of about 0.3 ppm. Of course, this level may be augmented by the vehicle. In fair agreement, unpublished data has indicated a sea salt concentration at the compressor intake of one marine application to be approximately 0.01 ppm under normal conditions, rising to 0.5 ppm in rough weather. Graves and Carleton (35), U.S. Navy Bureau of Ships, point out that marinized gas turbine engines should be capable of satisfactory operation with a sea salt ingestion rate of 1.5 ppm for a helicopter hovering at 20 feet above the ocean, with the rotor tip vortex action creating a considerable spray.

(a) "Sea water" and "sea salt" (i.e. in quotes) are used throughout this report to indicate the synthetic composition shown in Table V.

TABLE V
COMPOSITION OF ASTM D665 SYNTHETIC "SEA WATER"

<u>Salt (a)</u>	<u>Formula</u>	<u>grams per liter</u> ^(b)
Sodium Chloride	NaCl	24.54
Magnesium Chloride	MgCl ₂ ·6H ₂ O	11.10
Sodium Sulfate	Na ₂ SO ₄	4.09
Calcium Chloride	CaCl ₂	1.16
Potassium Chloride	KCl	0.69
Sodium Bicarbonate	NaHCO ₃	0.20
Potassium Bromide	KBr	0.10
Boric Acid	H ₃ BO ₃	0.03
Strontium Chloride	SrCl ₂ ·6H ₂ O	0.04
Sodium Fluoride	NaF	0.003
		<hr/>
	Total	41.953

Notes:

(a) Use cp chemicals.

(b) Use distilled water

TABLE VI

COMPOSITION OF SEA WATER

<u>Elements (a)</u>	<u>Principal Species</u>	<u>Abundance, grams per liter</u>	
		<u>Average Composition (32)</u>	<u>Synthetic "Sea Water" (ASTM D665)</u>
Oxygen	H_2O ; $O_2(g)$; SO_4^{2-}	857	857
Hydrogen	H_2O	108	108
Chlorine	Cl^-	19.0	19.8
Sodium	Na^+	10.5	11.0
Magnesium	Mg^{2+} ; $MgSO_4$	1.35	1.33
Sulfur	SO_4^{2-}	0.89	0.92
Calcium	Ca^{2+} ; $CaSO_4$	0.40	0.42
Potassium	K^+	0.38	0.39
Bromine	Br^-	0.065	0.068
Carbon	HCO_3^- ; H_2CO_3 ; CO_3^{2-} ; Organic	0.028	0.028
Strontium	Sr^{2+} ; $SrSO_4$	0.008	0.013
Boron	$B(OH)_3$; $B(OH)_2O^-$	0.005	0.005
Flourine	F^-	0.001	0.001
Silicon	$Si(OH)_4$; $Si(OH)_3O^-$	0.003 (b)	—

Notes:

- (a) Elements present at an abundance greater than 1 part per million.
- (b) Silicon varies in abundance from one water-mass to another by a factor of 1000, or more.

On the basis of this information, it was decided to conduct the major program (Section II-D) using three levels of "sea salt" ingestion. First, a corrosion base line was obtained with no "sea salt" added to the combustion system. Second, a realistic level of 1.5 ppm "sea salt" in air was obtained by the injection of synthetic "sea water" into the quench zone of the combustor, as indicated in Figure 2. Third, an accelerated corrosive effect was obtained by the ingestion of "sea water" at the level of 15.0 ppm "sea salt" in air. While the latter imposes artificially severe conditions, it is a common metallurgical practice to rely on accelerated testing for guidance.

In the preliminary tests (Section II-C), ingestion of "sea water" was at the level of 15 ppm "sea salt" in air.

3. Superalloys

In the preliminary tests, five superalloys, typical of those used for turbine blades and guide vanes in modern aircraft turbine engines, were used. Their compositions are shown in Table VII.

In the major program two different nickel-base alloys were used as test specimens during this study. The selection of Inconel 713C and Sierra Metal 200 was made to obtain cast alloys representative of materials being used for turbine blades in engines of advanced design. The chemical analyses for the heats from which the investment castings were made are shown in Table VIII. The inspection standards for these castings are shown in Table IX.

Inconel 713C has been widely used by aircraft turbine engine manufacturers for both turbine blades and turbine nozzle guide vanes. It possesses excellent strength properties up to 1800 F, and exhibits remarkable resistance to oxidation at that temperature. It is of interest to note that its introduction in 1956 led a series of cast alloys which permitted an increase in operating temperatures of about 100 F above previously available wrought materials.

Sierra Metal 200 is one of the newer cast alloys, introduced to obtain another 100 F increase in operating temperature; i.e., to 1900 F. This has required a reduction in chromium content to obtain high temperature strength properties, which has resulted in some lowering of oxidation resistance. It is of significance to note the unusually high tungsten content of this superalloy, for subsequent data show large amounts sodium tungstate in the scale of test specimens suffering catastrophic rates of corrosion.

The mean initial area of the test specimens was 17.67 cm². The mean initial weight of the Inconel 713C test specimens was 9386 milligrams, and of the Sierra Metal 200 test specimens was 9754 milligrams.

TABLE VII

COMPOSITION OF SUPERALLOY TEST SPECIMENS USED IN PRELIMINARY TESTS

<u>Alloying Elements</u>	<u>Chemical Analysis, weight per cent</u>				
	<u>Udimet 500</u>	<u>Wasp- alloy</u>	<u>Haynes Alloy 25</u>	<u>Hastelloy R-235</u>	<u>René 41</u>
Nickel	51.04	57.44	10.0	63.91	54.37
Cobalt	18.7	13.2	Balance (57.03)	0.38	10.69
Chromium	19.0	19.5	20.0	15.29	18.33
Molybdenum	4.35	4.41	--	5.48	9.69
Tungsten	--	--	15.0	--	--
Aluminum	3.10	1.23	--	2.05	1.54
Titanium	2.99	3.10	--	2.48	3.15
Manganese	<0.10	0.01	1.5	0.03	0.05
Iron	0.36	0.95	3.0	9.96	1.90
Zirconium	<0.01	0.06	--	--	--
Silicon	0.15	0.03	1.0	0.26	0.16
Boron	0.003	0.002	--	--	0.005
Sulfur	0.005	0.003	--	0.009	0.009
Carbon	0.09	0.053	0.1	0.15	0.10
Copper	<0.10	0.01	--	--	--
Phosphorus	--	0.003	--	0.001	--

TABLE VIII

COMPOSITION OF SUPERALLOY TEST SPECIMENS USED IN MAJOR PROGRAM

<u>Alloying Elements</u>	<u>Chemical Analysis, per cent</u>	
	<u>Inconel 713C</u>	<u>Sierra Metal 200</u>
Nickel	Balance (70.63)	Balance (60.34)
Cobalt	0.38	9.80
Chromium	12.93	9.14
Molybdenum	4.64	---
Tungsten	---	12.12
Aluminum	6.48	4.78
Titanium	0.82	2.00
Manganese	0.01	0.04
Iron	1.26	0.53
Zirconium	0.14	0.068
Columbium	2.25	0.99
Silicon	0.31	0.01
Boron	0.012	0.015
Sulfur	0.007	---
Carbon	0.13	0.17

TABLE IX

INSPECTION STANDARDS FOR SUPERALLOY TEST SPECIMENS USED IN MAJOR PROGRAM

1. Dimensional

- 1.1 Investment castings were finished to 0.06 in. by 0.5 in. by 2.38 in., with a tolerance of ± 0.01 in.
- 1.2 Positive roughness was removed, or reduced, by finishing to obtain a "smooth" section surface.

2. Visual

- 2.1 Negative defects which did not exceed $1/16$ in. diameter by $1/64$ in. deep, and separated by a distance equal to the diameter of the larger defect, were acceptable.
- 2.2 Evidence of mold crack, or partline, to $1/64$ in. high, or deep, was acceptable.
- 2.3 Positive roughness to $1/64$ in. high was acceptable.

3. Fluorescent Penetrant (Zyglo)

- 3.1 Cracks and through porosity were not acceptable.
- 3.2 Large faintly fluorescent areas ($1/4$ in. diameter as a guide) in which definite glowing areas do not exceed $1/16$ in. were not cause for rejection.

4. X-ray

- 4.1 Cracks were not acceptable.
- 4.2 Gas and inclusions up to $3/32$ in. in their greatest dimension were acceptable.

C. PRELIMINARY TESTS1. Procedure

In the preliminary tests (16) made before the Phillips 2-inch combustor (Figure 1) had been modified, the test specimens were constructed from the five superalloys listed in Table VII. Operation of the combustor was at an air-fuel ratio of 50 with the test specimens exposed to its near 2000 F exhaust gas stream at a pressure and flow velocity of approximately 12 atmospheres and 250 ft/sec. Synthetic "sea water" was injected directly into the primary zone of the combustor to provide a rate of 15 parts of "sea salt" per million parts of mass air throughput. The fuel used was the base fuel (Table III) with 1.0 per cent added sulfur and blended with 25 weight per cent cumene for all except one test where the cumene was omitted. Cumene was included in the fuel to promote carbon formation and thus provide conditions favorable to the reduction (15) of protective oxide films on the test specimens.

Prewedged test specimens were placed in the holder shown in Figure 5. The duration of the tests was twelve hours, obtained by running six 2-hour intervals. After each 2-hour period, the specimens were cathodically cleaned, as described in Section II-A3, and then reweighed.

2. Test Results

The data expressed as milligrams of accumulated weight loss (both specimens) per square inch of exposed area are given in Table X and are shown as a function of test duration in Figure 8.

TABLE XRESULTS OF PRELIMINARY HOT CORROSION TESTS (a)

<u>Alloy</u>	<u>Test Fuel (b)</u>	<u>Accumulated Metal Loss, mg/cm²</u>					
		<u>2 hr.</u>	<u>4 hr.</u>	<u>6 hr.</u>	<u>8 hr.</u>	<u>10 hr.</u>	<u>12 hr.</u>
Udimet 500	Aromatic added	7.5	26.2	35.7	49.7	62.4	90.5
	No added-aromatic	3.3	17.8	36.6	58.3	79.0	109.5
Waspalloy	Aromatic added	1.4	9.2	20.8	30.3	45.2	63.7
Haynes Alloy 25	Aromatic added	9.9	25.4	50.0	83.0	97.2	110.4
Hastelloy R-235	Aromatic added	5.2	19.9	51.8	108.0	181.6	239.4
René 41	Aromatic added	54.9	65.5	79.2	90.5	107.8	148.4

(a) Combustor Operating Conditions: P = 350 in. Hg abs.; V = 250 ft/sec; IAT = 900 F; EGT = 1950 - 2000 F.

(b) JP-5 type isoparaffinic base fuel (Table III) plus 1.0 weight per cent sulfur. When aromatics were added they consisted of 25 weight per cent cumene.

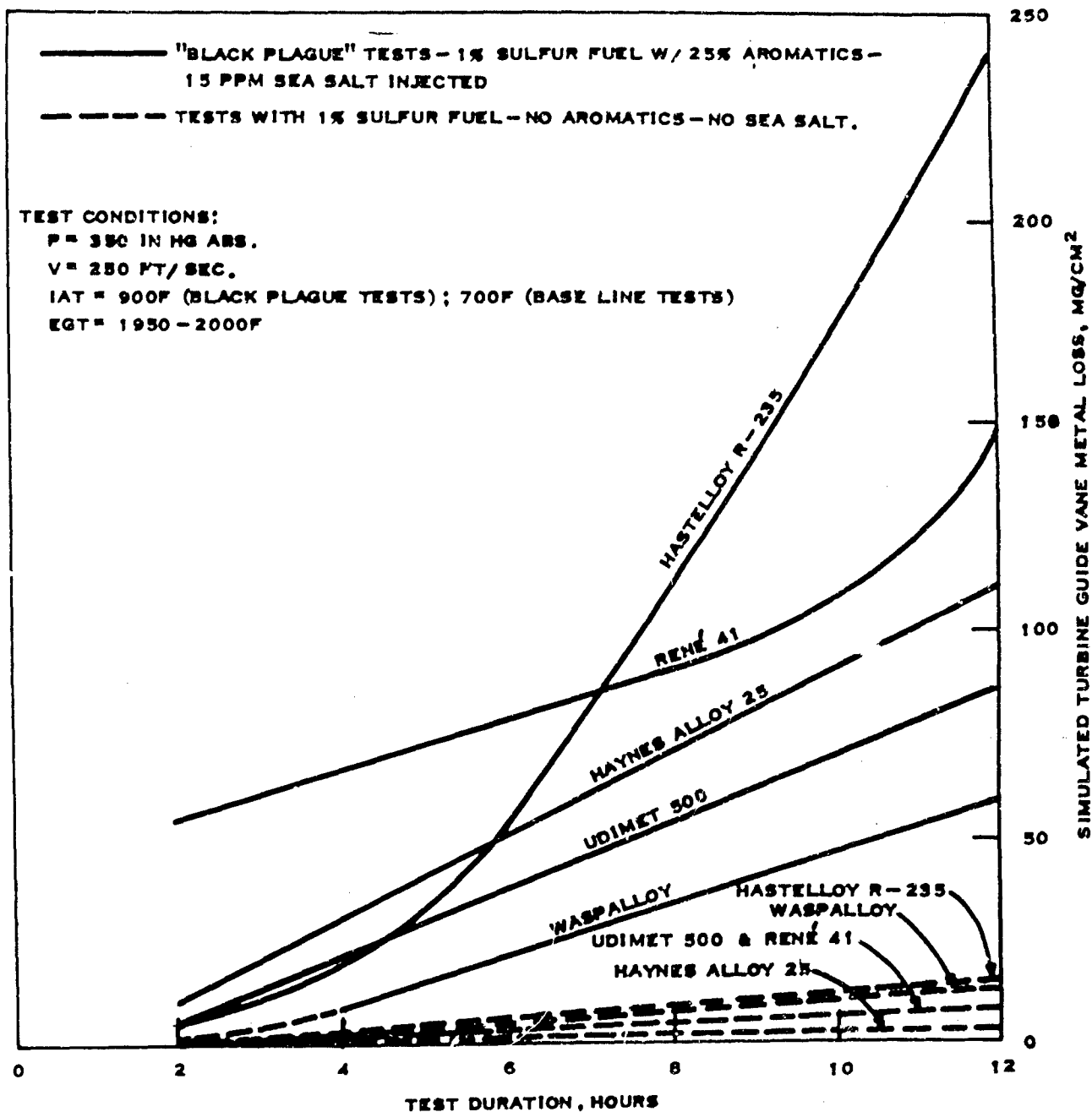


FIGURE 8
 TURBINE GUIDE VANE METAL LOSS AS A FUNCTION OF TEST DURATION
 FOR EXPOSURE TO SULFUR AND/OR SEA SALT LADEN ATMOSPHERES

Comparisons of the metal weight losses from Udimet 500 specimens, with and without cumene added to the fuel, indicates that the presence of the aromatic did not accelerate corrosion as might have been expected. Presumably, if hot corrosion was preceded by reduction by carbon of protective chromium oxide films, there was sufficient carbon formation by the fuel in the absence of the aromatic.

In Figure 8, data previously obtained (15) on the effect of 1.0 per cent sulfur in the absence of "sea salt" are also shown. It is seen that the "sea salt" greatly accelerated hot corrosion. Under the test conditions, the alloys were rated (8 to 12 hours test duration) in the following order of increasing metal weight loss: Waspalloy, Udimet 500, Haynes Alloy 25, René 41 and Hastelloy R-235. At shorter test durations, the first four alloys fell in the same order but the position of the last, Hastelloy R-235, improved relative to the others. The higher weight loss from Hastelloy R-235 at the longer test times is in general accord with previous reports (10) of high corrosion of alloys containing 15 per cent or less chromium when exposed to "sea salt" at elevated temperatures.

D. MAJOR PROGRAM

1. Procedure

In the major program on the effects of sulfur and "sea salt" on hot corrosion, made after the Phillips 2-inch combustor (Figure 2) had been modified, the test specimens were constructed of Inconel 713C and Sierra Metal 200 (Table VIII). The operating conditions selected as representative of modern, high performance aircraft are shown in Table XI under the column heading 2000 F. It is seen that operation was at a pressure of 15 atmospheres, an inlet air temperature of 1000 F, an air-fuel ratio of 56 and an exhaust gas temperature closely approaching 2000 F. The resultant test specimen temperature was near 1830 F and the flow velocity over the specimens was 500 ft/sec. Under these conditions, synthetic "sea water" was injected at the rates 0.0, 1.5 and 15 ppm "sea salt" with fuel sulfur contents of 0.0002, 0.040 and 0.40 weight per cent.

The tests were conducted in accordance with a statistically designed program. Duplicate tests were run on each alloy with each of the nine possible combinations of sulfur and sea water concentrations. In each test, two specimens of the same superalloy were exposed to hot gases from the combustor. The eighteen tests were run at random on each alloy.

The procedure consisted of a five-hour cyclic test with 55 minutes of exposure of the test specimens to hot gases followed by 5 minutes with the fuel turned off. On completion of a test, the specimens were cathodically cleaned, as described in Section II-A3, for determination of the weight loss. The tensile properties (ultimate tensile strength, ultimate load and per cent elongation) were measured after preparing the specimens for this purpose as described in Section II-A4.

Photomicrographs of the specimens were made for examination to determine the depth and type of the corrosion attack.

TABLE XI

OPERATING CONDITIONS OF PHILLIPS 2-INCH COMBUSTOR

<u>Test Variables</u>	<u>Test Conditions (a)</u>		
	<u>2000 F</u>	<u>1750 F</u>	<u>1500 F</u>
<u>Temperature, degrees Fahrenheit</u>			
Exhaust Gas	1993 ± 15	1746 ± 11	1498 ± 7
Profile (b)	210	190	110
Test Specimens	1830	1720 (c)	1590 (e)
Combustor Inlet Air	1000 ± 10	900 ± 10	800 ± 10
<u>Pressure, atmospheres</u>			
Combustor Inlet Air	15.0 ± 0.1	15.0 ± 0.1	15.0 ± 0.1
Combustor Drop.	0.6	0.8	1.0
Test Specimen Drop.	0.3	0.4	0.5
<u>Mass Flow Rate, pounds per hour</u>			
Air	5480 ± 40	6120 ± 40	6840 ± 40
Fuel.	98	90	81
Air-Fuel Ratio.	56	68	84
<u>Flow Velocity, feet per second</u>			
Combustor Reference (d)	200	210	220
Exhaust Gas (e)	270	270	270
at Test Specimens (f)	500	500	500
Combustion Efficiency, per cent (g)	100	100	100
Test Duration, hours (h)	5.00±0.01	5.00±0.01	5.00±0.01

Notes:

- (a) Average values, with standard deviation shown for control points.
- (b) Maximum variation between four thermocouples on equal area centers.
- (c) Test specimens probably reflecting flame radiation to give fictitiously high readings with optical pyrometer.
- (d) Cold flow, based on 2.66 in.² exit area in flame tube.
- (e) Based on 3.36 in.² area at outlet from combustor.
- (f) Based on 1.80 in.² unblocked area in test specimen holder.
- (g) Calculated using mean specific heats and temperature at exhaust gas core to minimize error from heat loss to water cooled wall.
- (h) Operating cycle of 55 minutes at test condition, followed by 5 minutes with fuel off.

2. Test Results

Statistical methods (36, 37) were used in the analysis of the data obtained under the 2000 F test conditions for determination of the effect of sulfur and "sea salt", separately and together, on metal weight losses and changes in tensile properties as the result of hot corrosion of Inconel 713C and Sierra Metal 200.

The significance of test specimen weight losses and changes in tensile properties was established by analyses of variance, made at a confidence level of 95 per cent (18).

The summarized results are shown in Tables XII and XIII.

3. Discussion

a. Oxidation and Erosion

The weight losses found when no "sea salt" and 0.0002 weight per cent fuel sulfur were present indicate little oxidation and erosion. The weight loss was 1.3 mg/cm² from the Inconel 713C specimens while that from the Sierra Metal 200 specimens was 6.8 mg/cm² during the five hour tests. However, Inconel 713C specimens, having an initial tensile strength of 121,600 lb/in.², showed appreciable bowing (one-eighth in.) in the direction of gas flow. This indicates that the specimens were under considerable stress during exposure to the hot gases. Sierra Metal 200 specimens, having an initial tensile strength of 136,000 lb/in.², showed little or no bowing.

b. Sulfur Corrosion

In the absence of "sea salt" in the air, increasing fuel sulfur content over the range from 0.0002 to 0.40 weight per cent did not significantly affect the weight loss or tensile properties of Inconel 713C. This is shown in the photographs of Figure 9 and in the data plots of Figures 10, 11 and 12.

Under similar conditions, the weight loss from Sierra Metal 200 specimens increased slightly with increase in fuel sulfur content from 0.0002 to 0.040 weight per cent but decreased on further increase in sulfur content to 0.40 weight per cent. This is illustrated in the photographs of Figure 13 and in the plots of Figures 14 and 15. In Figure 16, it is shown that, in the absence of "sea salt", increase in fuel sulfur content had no significant effect on the tensile properties of Sierra Metal 200.

It can be concluded that, under the 2000 F operating conditions, and in the absence of "sea salt", fuel sulfur content had essentially no effect on the hot corrosion of Inconel 713C and Sierra Metal 200.

c. "Sea Salt" Corrosion

In the essential absence of sulfur in the fuel (0.0002 weight per cent sulfur), metal weight loss from Inconel 713C was not increased by the presence of 1.50 ppm "sea salt" in the combustor air but was markedly increased by the presence of 15.0 ppm "sea salt". This is indicated graphically in Figures 10 and 11. The photographs of Figure 9 show that metal loss was characterized by patches of attack and pitting, i.e., localized corrosion taking the form of cavities at the surface.

TABLE XII
SUMMARY OF WEIGHT LOSS AND TENSILE PROPERTY DATA ON

INCONEL 713C TEST SPECIMENS

(2000 F TEST CONDITIONS)

A. METAL WEIGHT LOSS, MG.

Sulfur in Fuel, Wt. %	Weight Loss, mg (Geometric Means)		
	"Sea Salt" in Air, ppm		
	0.0	1.50	15.0
0.0002	10.1 ≤ 22.7 ≤ 45.6	9.3 ≤ 18.7 ≤ 37.6	357 ≤ 717 ≤ 1440
0.040	8.2 ≤ 16.4 ≤ 33.0	49.5 ≤ 99.4 ≤ 200	431 ≤ 866 ≤ 1740
0.40	6.2 ≤ 12.5 ≤ 25.0	66.5 ≤ 134 ≤ 268	863 ≤ 2130 ≤ 4290

lower confidence limit ≤ geometric mean ≤ upper confidence limit

Analyses of variance indicated a significant sulfur x "sea salt" interaction. Comparisons of ratios of weight losses for (1) sulfur concentrations with fixed "sea salt" concentrations and (2) "sea salt" concentrations with fixed sulfur concentrations indicated the following:

- (1) At 0.0 ppm "sea salt", fuel sulfur concentration did not affect weight loss.
- (2) At 1.50 ppm "sea salt", weight loss was significantly lower with 0.0002 per cent fuel sulfur than with 0.040 or 0.40 per cent fuel sulfur.
- (3) At 15.0 ppm "sea salt", weight loss was significantly lower with 0.0002 per cent fuel sulfur than with 0.40 per cent sulfur.
- (4) At a constant level of sulfur content, weight loss increased with increase in "sea salt" concentration except that at 0.0002 per cent sulfur, there was no significant difference on increasing "sea salt" from 0.0 to 15.0 ppm.
- (5) Changes in "sea salt" concentration had a much greater effect on weight loss than changes in percentage sulfur. The maximum increase for a change in fuel sulfur was 7 times for an increase from 0.0002 to 0.40 per cent sulfur at 1.50 ppm "sea salt" while the maximum increase for a change in "sea salt" was 170 times for an increase from 0.0 to 15.0 ppm "sea salt" at 0.40 per cent fuel sulfur.

TABLE XIII (Cont'd)

B. TENSILE PROPERTIES

Sulfur in Fuel, Wt. %	Ultimate Tensile Strength, (a) $\text{lb/in.}^2 \times 10^{-3}$			Per Cent Elongation (a) "Sea Salt" in Air, ppm			Ultimate Load (a), $\text{lb} \times 10^{-3}$		
	0.0	1.50	15.0	0.0	1.50	15.0	0.0	1.50	15.0
0.0002	121.0	122.5	116.8	7.21	9.92	5.58	1.945	1.975	1.660
0.040	121.2	122.2	110.8	6.61	7.52	5.05	1.852	1.905	1.585
0.40	131.8	117.8	114.5	9.32	5.67	4.87	2.062	1.790	1.440
"Sea Salt" Mean	124.7	120.8	114.0	7.71	7.71	5.17	1.953	1.890	1.562

(a) Values for new metal specimens were: Ultimate tensile strength = 121.6×10^3 lb/in.^2 ; Per cent elongation = 7.86 per cent; Ultimate load = 1.879×10^3 lb.

Analyses of variance and comparisons of means with calculated least significant differences indicated the following:

- (1) Change in sulfur content of the fuel had no significant effect on tensile properties.
- (2) Change in "sea salt" concentration (a) from 0.0 to 1.50 ppm had no significant effect, (b) from 0.0 to 15.0 ppm had a significant effect on all three measured tensile properties such that each decreased with increase in "sea salt" concentration.
- (3) There was no significant sulfur x "sea salt" interaction.

TABLE XIII

SUMMARY OF WEIGHT LOSS AND TENSILE PROPERTY DATA ON SIERRA METAL 200 TEST SPECIMENS (2000 F TEST CONDITIONS)

A. METAL WEIGHT LOSS, MG.

Sulfur in Fuel, Wt. %	Weight Loss, mg (Geometric Means)		
	"Sea Salt" in Air, ppm		
	0.0	1.50	15.0
0.0002	50.7 ≤ 120 ≤ 282	762 ≤ 1790 ≤ 4240	1760 ≤ 4150 ≤ 9790
0.040	262 ≤ 617 ≤ 1470	207 ≤ 485 ≤ 1150	930 ≤ 2190 ≤ 5280
0.40	42.8 ≤ 101 ≤ 238	108 ≤ 256 ≤ 603	191 ≤ 450 ≤ 1060

lower confidence limit ≤ geometric mean ≤ upper confidence limit

Analyses of variance indicated a significant sulfur x "sea water" interaction. Comparisons of ratios of weight loss for (a) sulfur concentrations with fixed "sea salt" concentrations and (b) "sea salt" concentrations with fixed sulfur concentrations indicated the following:

- (1) At 0.0 ppm "sea salt", weight loss increased significantly with increase in fuel sulfur from 0.0002 to 0.040 per cent and decreased with increase in fuel sulfur from 0.040 to 0.40 per cent.
- (2) At 1.50 ppm "sea salt", weight loss with 0.040 or 0.40 per cent sulfur was significantly less than with 0.0002 per cent sulfur.
- (3) At 15.0 ppm "sea salt", weight loss with 0.40 per cent sulfur was significantly less than with 0.0002 or 0.040 per cent sulfur.
- (4) With increasing sulfur concentration, weight loss decreased significantly or was directionally lower except for a significant increase in weight loss with increase in sulfur from 0.0002 to 0.040 per cent at 0 ppm "sea salt".
- (5) At 0.0002 per cent sulfur, weight loss increased significantly on increasing "sea salt" from 0.0 to either 1.50 or 15.0 ppm.
- (6) At 0.040 per cent sulfur, weight loss increased significantly on increasing "sea salt" from 0.0 to 15.0 or from 1.50 to 15.0 ppm.
- (7) At 0.40 per cent sulfur, weight loss increased significantly on increasing "sea salt" from 0.0 to 15.0 ppm.
- (8) With increasing "sea salt" concentration, weight loss increased significantly or was directionally higher except for a non-significant decrease with increase in "sea salt" from 0.0 to 1.50 ppm at 0.040 per cent sulfur.

(Continued)

TABLE XIII (Continued)

B. TENSILE PROPERTIES (a)

Sulfur in Fuel, Wt. %	Ultimate Tensile Strength, (b) lb/in. ² x 10 ⁻³			Per Cent Elongation (b) "Sea Salt" in Air, ppm			Ultimate Load, lb x 10 ⁻³		
	0.0	1.50	15.0	0.0	1.50	15.0	0.0	1.50	15.0
0.0002	124.0	110.5	78.0	16.75	12.25	9.00	1.820	1.318	0.484
0.040	111.0	111.2	59.2	15.00	14.75	7.25	1.542	1.586	0.605
0.40	109.0	108.5	106.0	14.75	14.75	11.75	1.622	1.511	1.612
"Sea Salt" Mean	---	---	---	15.5	13.9	9.3	---	---	---

(a) Examination of the break, after pulling, indicated a crack with 5 of the 12 specimens exposed to 15 ppm "sea salt" and with 2 of the 12 specimens exposed to 1.50 ppm "sea salt".

(b) Values for new metal specimens were: Ultimate tensile strength = 136.0 x 10³ lb/in.²; Per cent elongation = 17.1 per cent; Ultimate load = 2.056 x 10³ lb.

Analyses of variance and comparisons with calculated least significant differences indicated the following:

- (1) There was a significant sulfur x "sea salt" interaction effect on ultimate tensile strength and ultimate load but not on per cent elongation.
- (2) At all levels of "sea salt", sulfur concentration had no significant effect on per cent elongation.
- (3) At 0.0 and 1.50 ppm "sea salt", sulfur concentration had no significant effect on ultimate tensile strength and ultimate load.
- (4) At 15.0 ppm "sea salt", ultimate tensile strength and ultimate load were significantly lower with 0.0002 and 0.040 than with 0.40 per cent sulfur.
- (5) At 15.0 ppm "sea salt", per cent elongation was significantly lower than with 0.0 and 1.50 ppm "sea salt". It was also directionally lower at 1.50 ppm than at 0.0 ppm "sea salt".
- (6) At 0.0002 per cent sulfur, ultimate tensile strength was significantly lower with 15 ppm than with 0.0 or 1.50 ppm "sea salt" and ultimate load decreased significantly on increase in "sea salt" from 0.0 to 1.50 to 15.0 ppm.
- (7) At 0.040 per cent sulfur, ultimate tensile strength and ultimate load were significantly lower with 15.0 than with 0.0 or 1.50 ppm "sea salt".
- (8) At 0.40 per cent sulfur, "sea salt" concentration had no significant effect on ultimate tensile strength or ultimate load.

SULFUR
IN FUEL,
WT %

0

SEA SALT IN AIR, PPM

1.50

15.0



0.0002



0.040



0.40



NEW TEST SPECIMEN



FIGURE 9
PHOTOGRAPH OF INCONEL 713C TEST SPECIMENS
AFTER EXPOSURE TO HOT GAS CORROSION IN PHILLIPS 2 - INCH COMBUSTOR
AT 2000 F TEST CONDITION

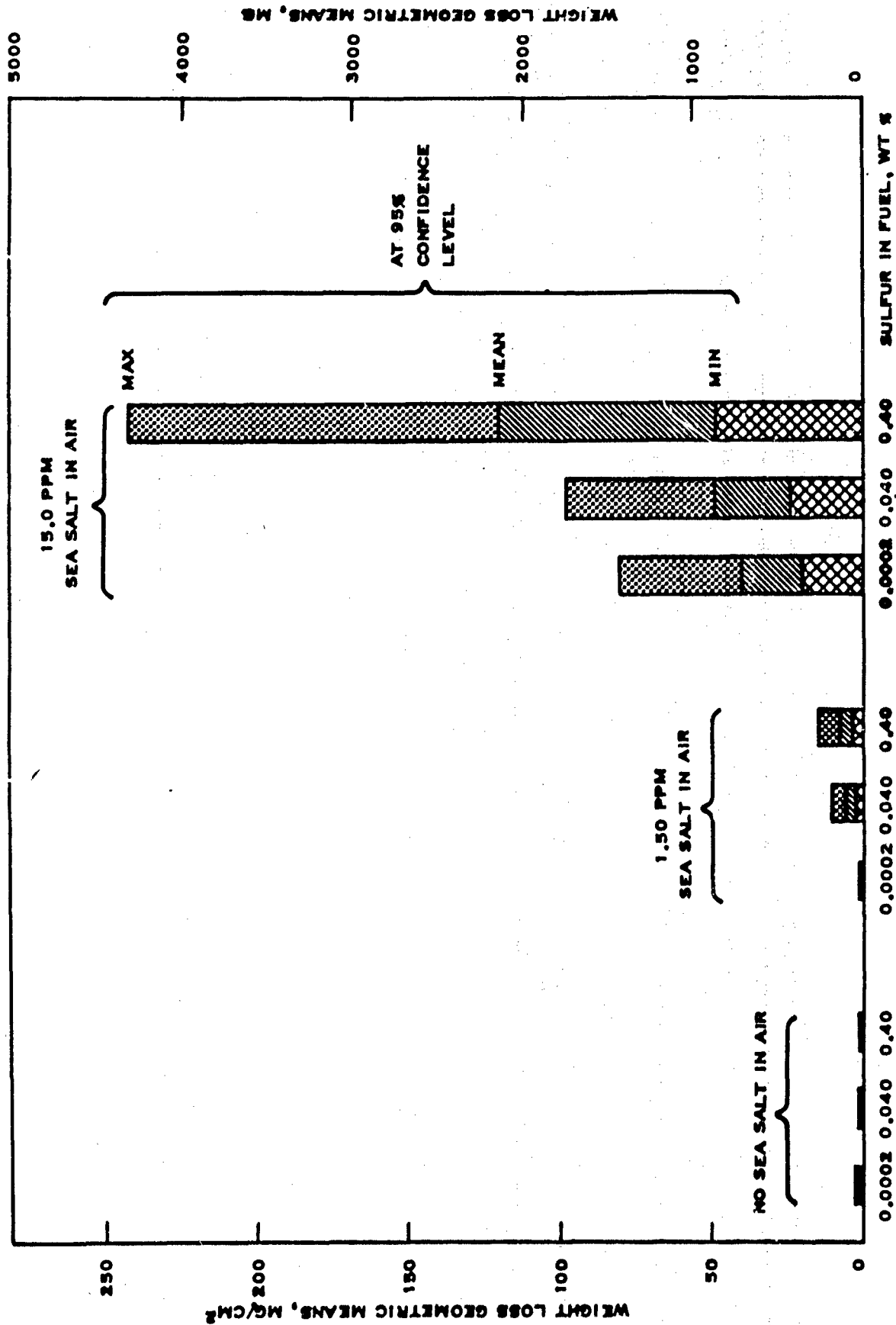


FIGURE 10
EFFECT OF SULFUR AND SEA SALT ON INCONEL 713C TEST SPECIMEN WEIGHT LOSS
AS A RESULT OF EXPOSURE TO HOT GAS CORROSION IN PHILLIPS 2-INCH COMBUSTOR
AT 2000 F TEST CONDITION

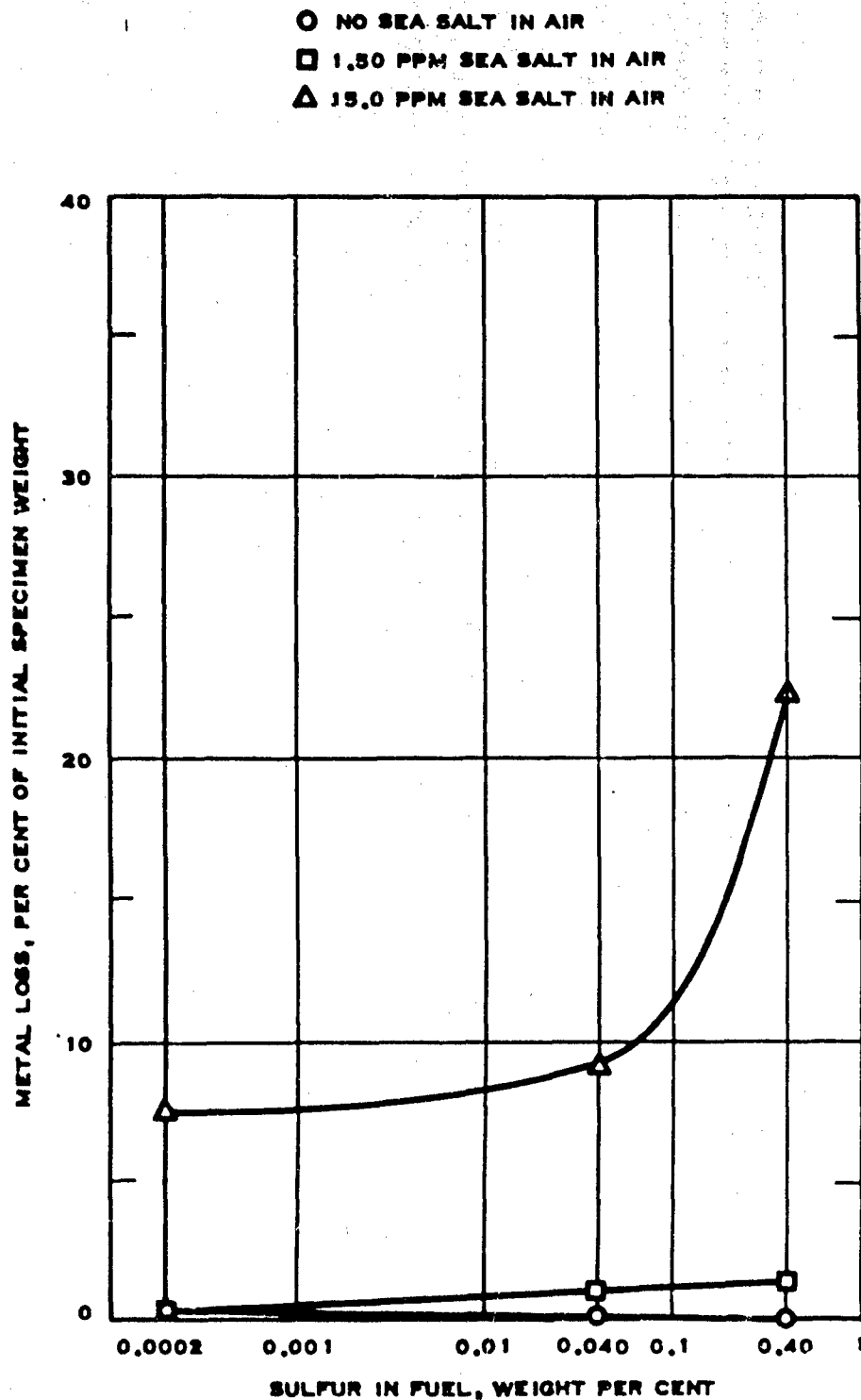


FIGURE 11
EFFECT OF SULFUR AND SEA SALT ON INCONEL 713C TEST SPECIMEN MEAN WEIGHT LOSS
AS A RESULT OF EXPOSURE TO HOT GAS CORROSION IN PHILLIPS 2-INCH COMBUSTOR
AT 2000 F TEST CONDITION

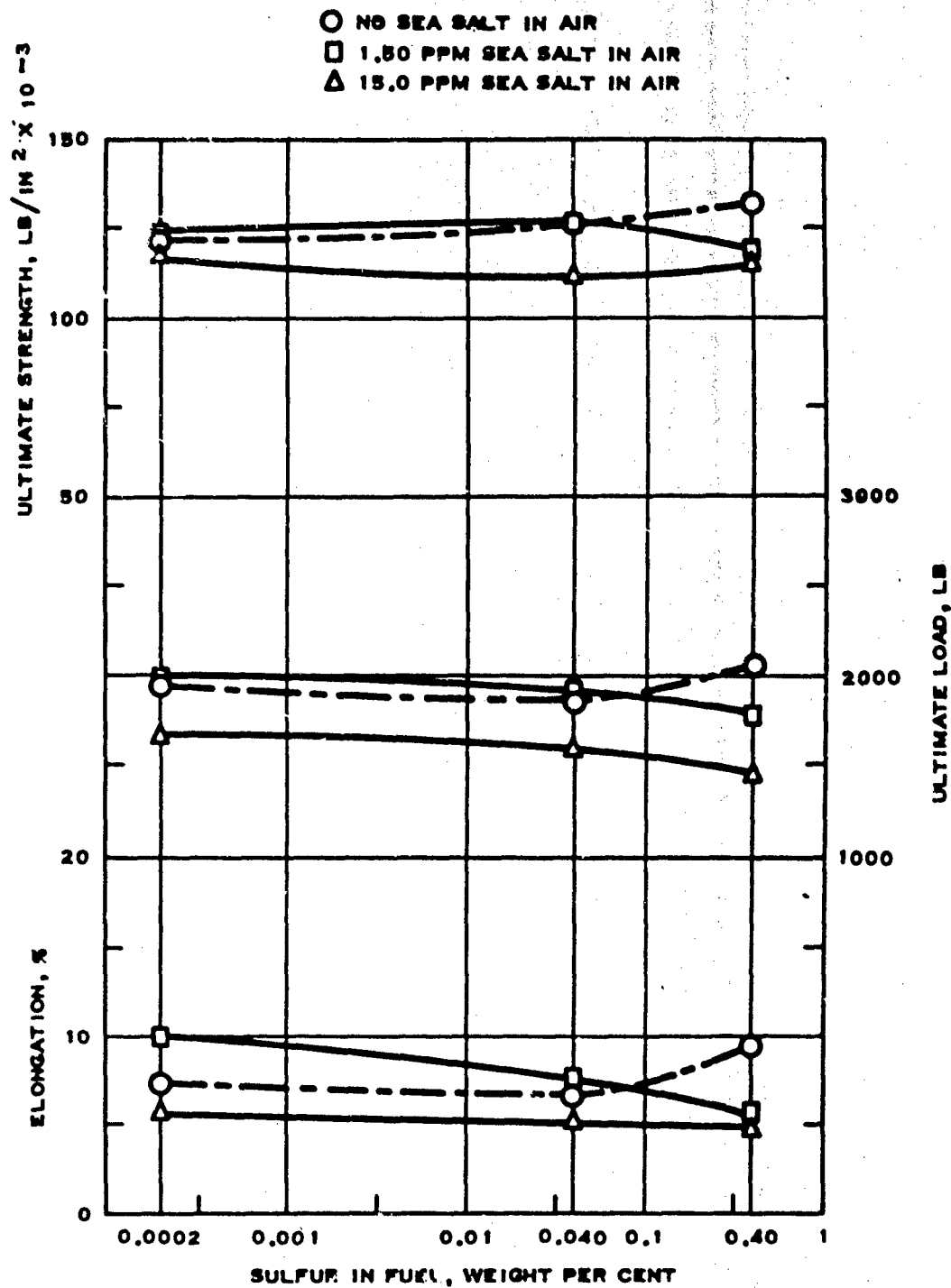


FIGURE 12
EFFECT OF SULFUR AND SEA SALT ON INCONEL 713C TEST SPECIMEN TENSILE PROPERTIES
AFTER EXPOSURE TO HOT GAS CORROSION IN PHILLIPS 2-INCH COMBUSTOR
AT 2000 F TEST CONDITION

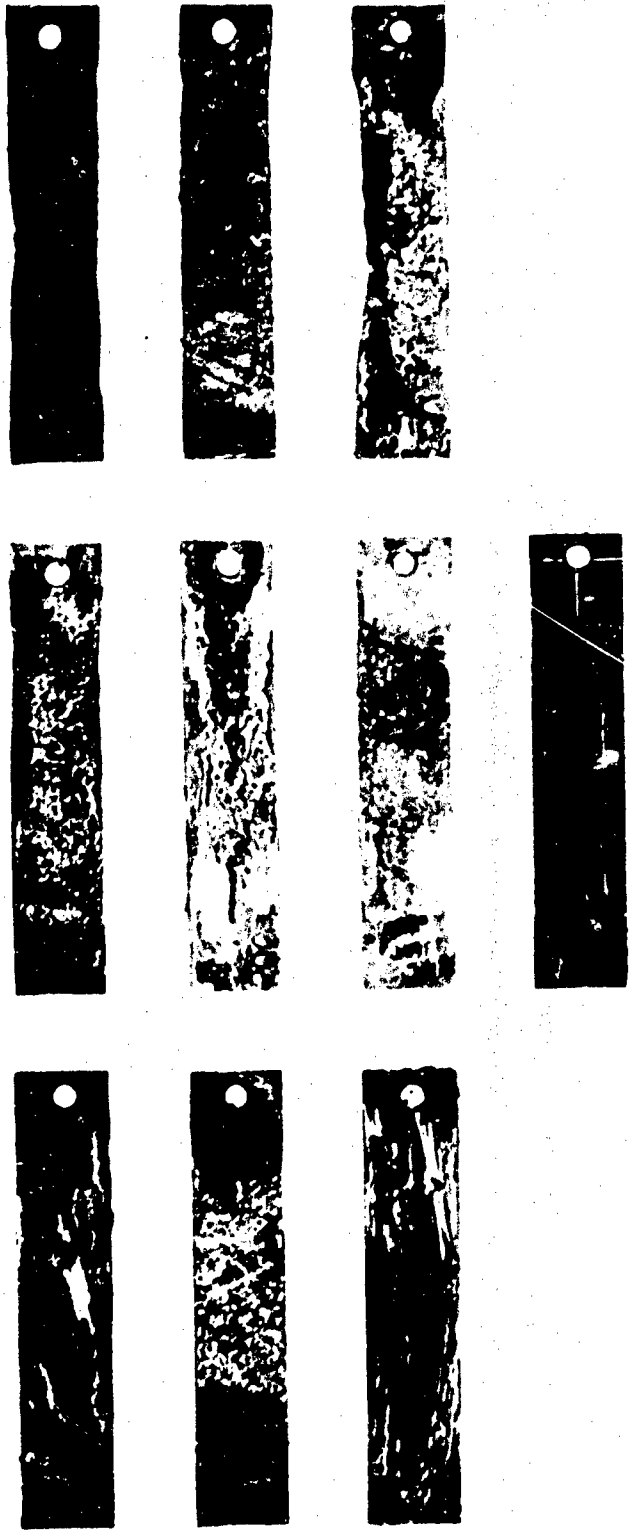
SULFUR
IN FUEL,
WT %

0

SEA SALT IN AIR, PPM

1.50

15.0



0.0002

0.040

0.40

NEW TEST SPECIMEN

FIGURE 13
PHOTOGRAPHS OF SIERRA METAL 200 TEST SPECIMENS
AFTER EXPOSURE TO HOT GAS CORROSION IN PHILLIPS 2 - INCH COMBUSTOR
AT 2000 F TEST CONDITION

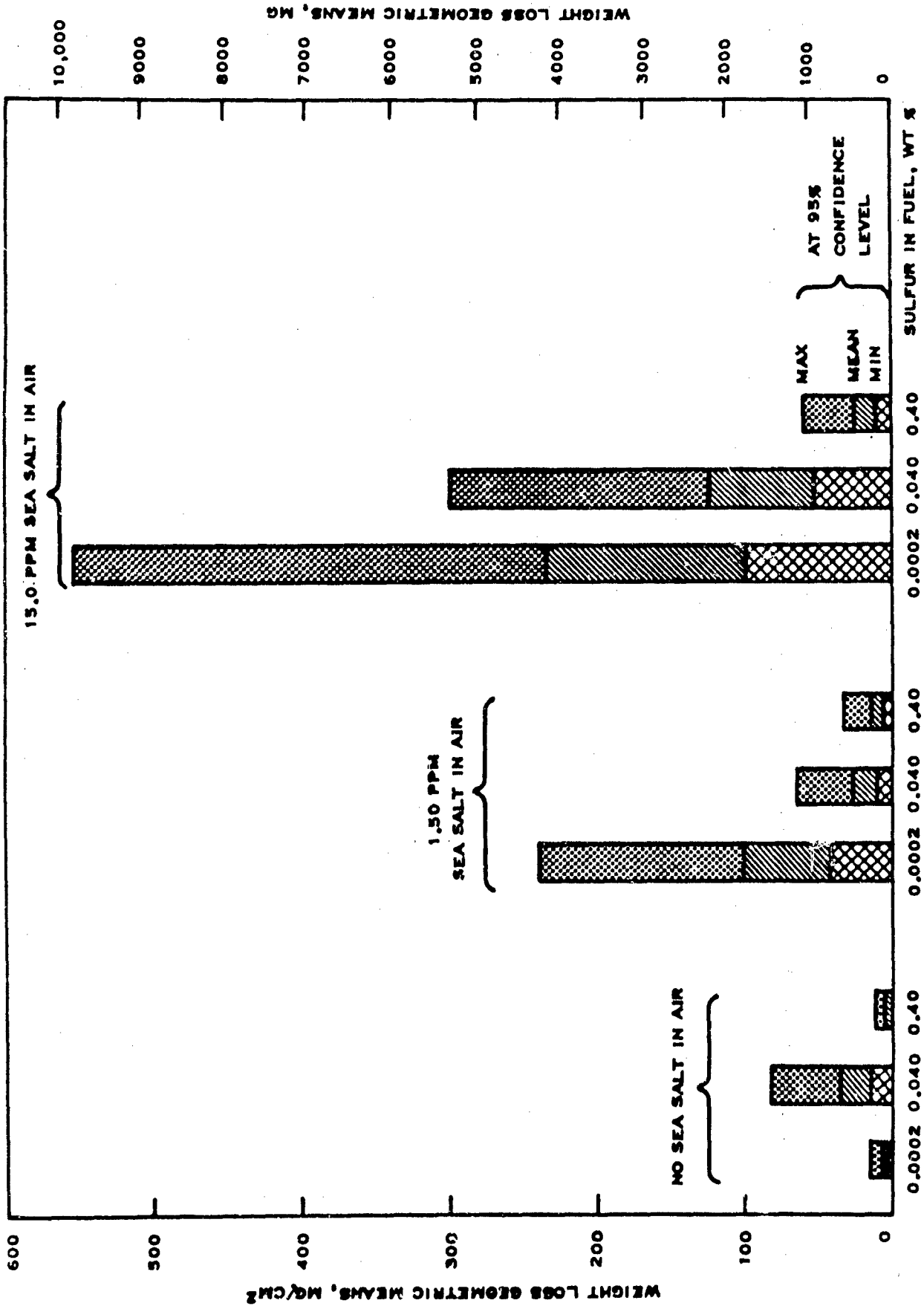


FIGURE 14
 EFFECT OF SULFUR AND SEA SALT ON SIERRA METAL 200 TEST SPECIMEN WEIGHT LOSS
 AS A RESULT OF EXPOSURE TO HOT GAS CORROSION IN PHILLIPS 2 - INCH COMBUSTOR
 AT 2000 F TEST CONDITION

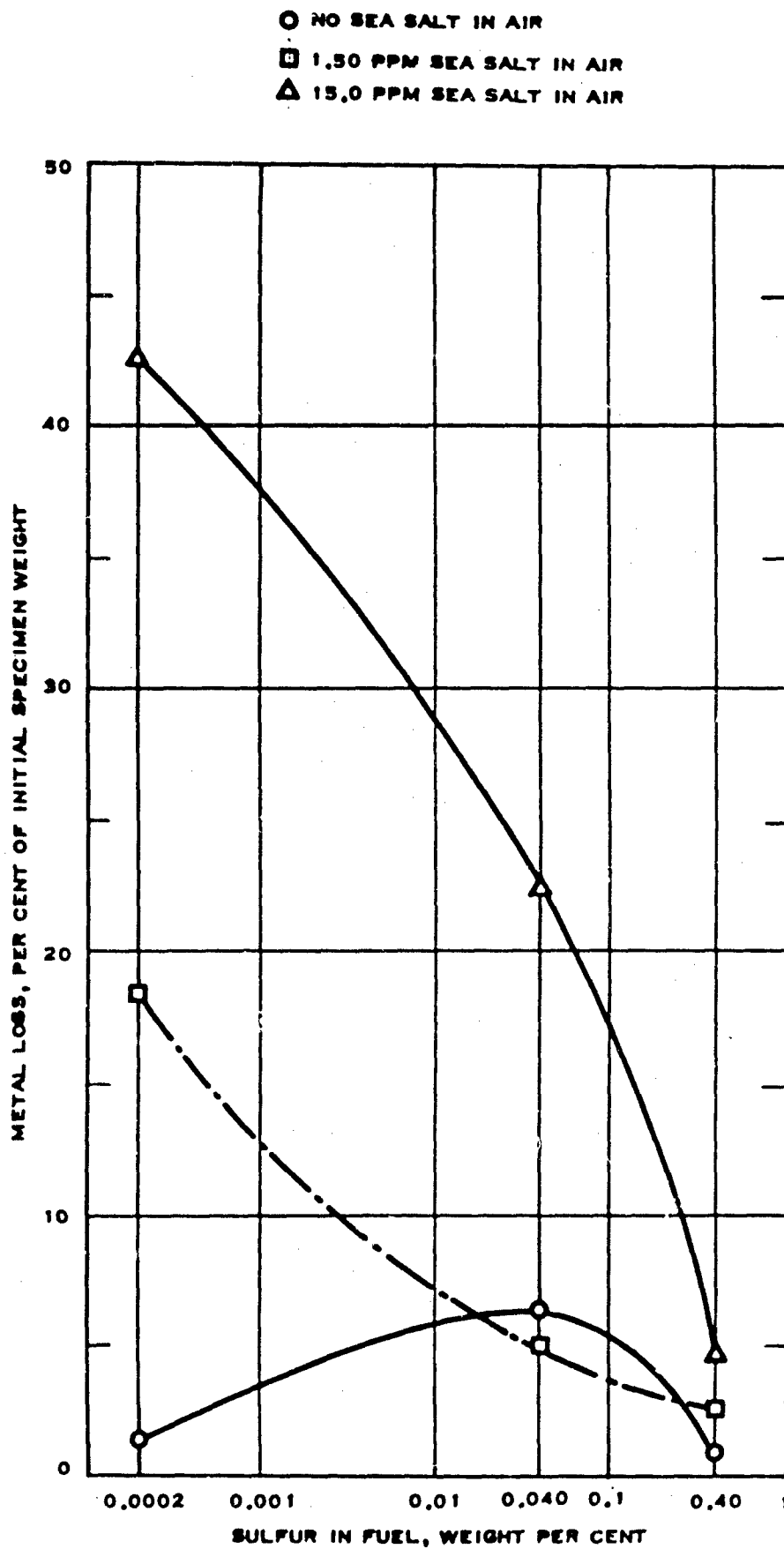


FIGURE 15

EFFECT OF SULFUR AND SEA SALT ON SIERRA METAL 200 TEST SPECIMEN MEAN WEIGHT LOSS AS A RESULT OF EXPOSURE TO HOT GAS CORROSION IN PHILLIPS 2 - INCH COMBUSTOR AT 2000 F TEST CONDITION

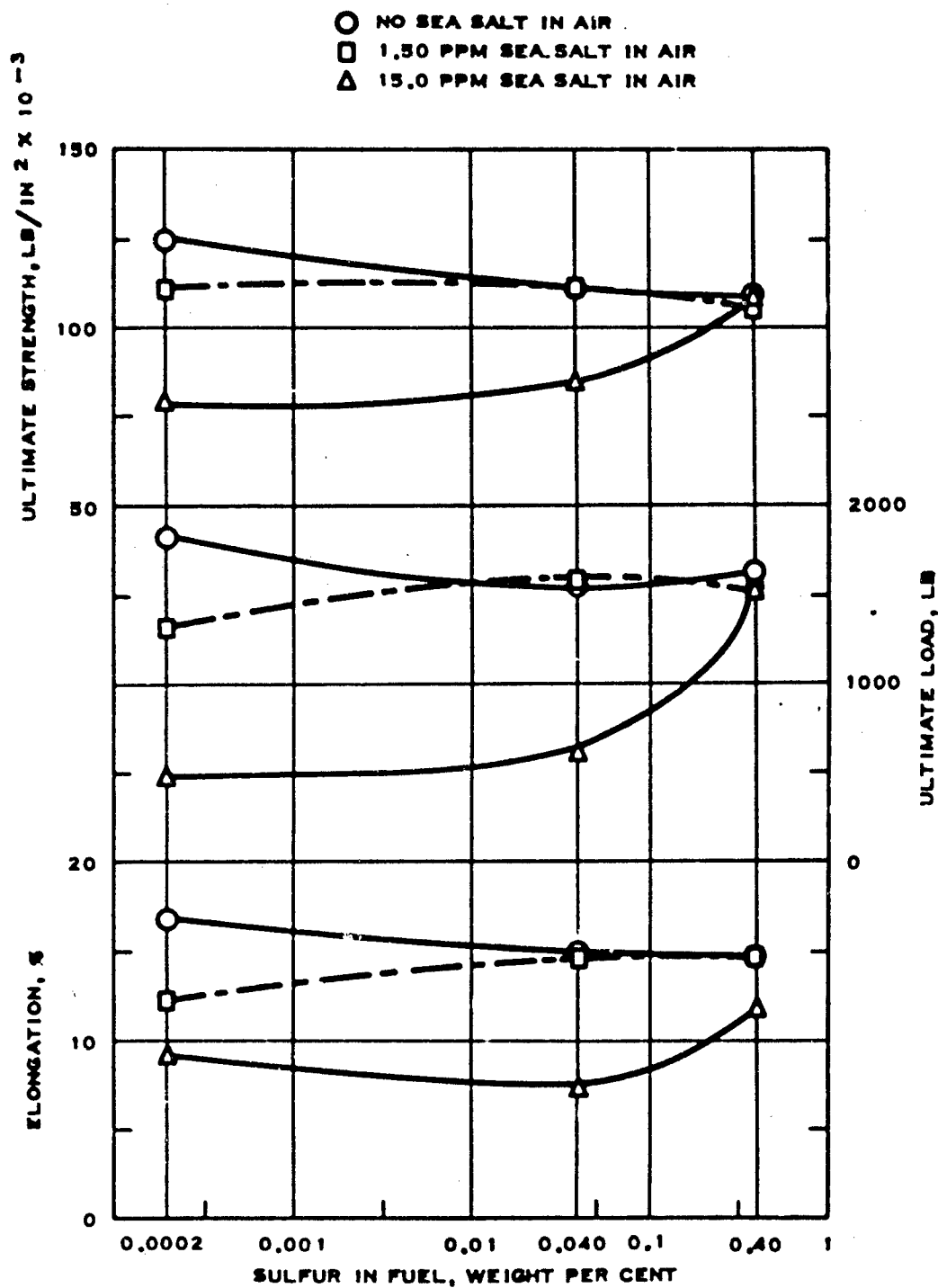


FIGURE 16
EFFECT OF SULFUR AND SEA SALT ON SIERRA METAL 200 TEST SPECIMEN TENSILE
PROPERTIES AFTER EXPOSURE TO HOT GAS CORROSION IN PHILLIPS 2-INCH COMBUSTOR
AT 2000 F TEST CONDITION

In Figure 12, it may be seen that in the essential absence of sulfur, there was no directional trend in change of tensile properties of Inconel 713C with increase in "sea salt" concentration. This indicates that "sea salt" attack was at the surface of the metal with no deep intergranular penetration.

With only 0.0002 weight per cent sulfur in the fuel, metal weight loss from Sierra Metal 200 increased rapidly with increase in concentration of "sea salt" in the combustor air as illustrated in Figures 14 and 15. The photograph of Figure 13 shows that this loss was characterized by metal wastage and thinning of the test specimen indicating gross attack of the metal on a broad front.

As shown in Figure 16, with essentially no sulfur present in the fuel, there is a loss in tensile properties as "sea salt" is added to the combustor air. This indicates that there was preferential attack at the grain boundaries, introducing localized stress concentrations and resulting in corrosion fatigue.

From the above metal weight loss data, it is obvious that high (41 mg/cm^2 or 7.6 per cent for the 5-hour test) hot corrosion can occur with Inconel 713C, and excessive (235 mg/cm^2 or 42.7 per cent for the 5-hour test) hot corrosion can occur with Sierra Metal 200 in a saline atmosphere with essentially sulfur-free fuel under 2000 F test conditions.

d. Combined Sulfur-"Sea Salt" Corrosion

It has been shown in Section II-D2 that there was a significant sulfur x "sea salt" interaction on metal weight loss from both Inconel 713C and Sierra Metal 200. Referring to Figures 10 and 11, it is seen that, in the case of Inconel 713C, the highest level of hot corrosion occurred when "sea salt" in the combustor air and sulfur in the fuel were both at their maximum concentrations.

Figure 12 shows no combined sulfur-"sea salt" effect on the tensile properties of Inconel 713C.

In the case of Sierra Metal 200, Figure 14 and 15 show that maximum metal weight loss occurred when "sea salt" in the combustor air was at its maximum and sulfur in the fuel at its minimum concentration.

In Figure 16, it is shown that sulfur had an inhibiting effect on the change in tensile properties of Sierra Metal 200.

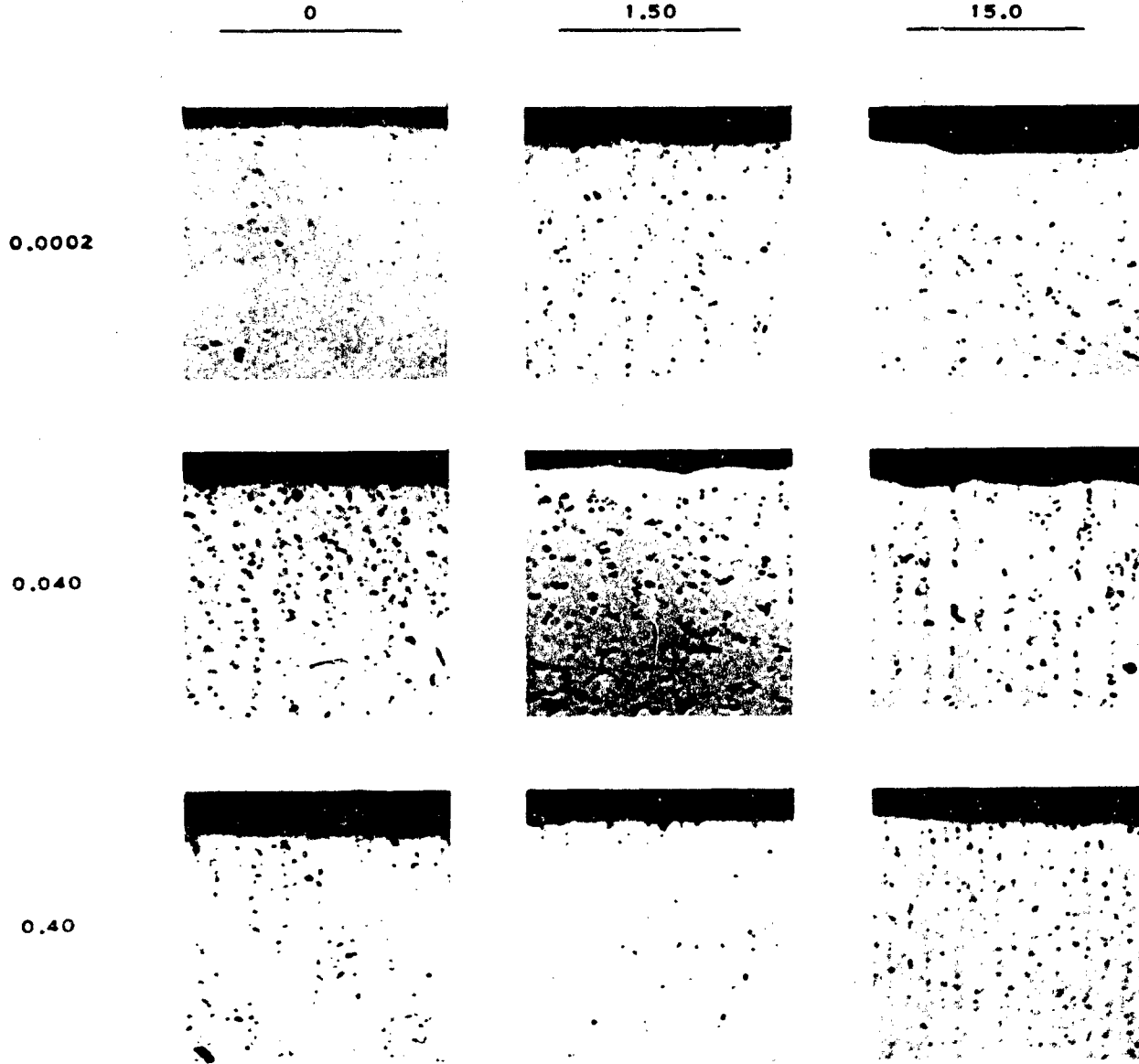
From these data, it can be observed that sulfur and "sea salt" can have varied effects on hot corrosion with sulfur in the presence of "sea salt" promoting corrosion of Inconel 713C and inhibiting corrosion of Sierra Metal 200 at the 2000 F operating conditions.

e. Metallography

In order to determine whether hot corrosion experienced at the 2000 F test condition was a deep intergranular penetration photomicrographs of the specimens were made. Figures 17 (at 100 X) and 18 (at 600 X) show photomicrographs of Inconel 713C after exposure to various test conditions and after cathodic cleaning. It may be noted that surface oxidation was general, with

SULFUR
IN FUEL,
WT %

SEA SALT IN AIR, PPM



MAGNIFICATION-100X, POLISHED, UNETCHED

FIGURE 17
PHOTOMICROGRAPHS AT 100X OF INCONEL 713C TEST SPECIMENS
AFTER EXPOSURE TO HOT GAS CORROSION IN PHILLIPS 2 - INCH COMBUSTOR
AT 2000 F TEST CONDITION

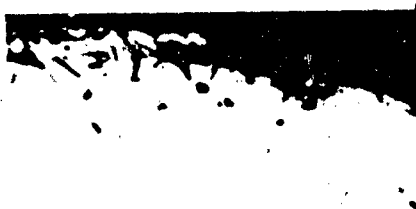
SULFUR
IN FUEL,
WT %

SEA SALT IN AIR, PPM

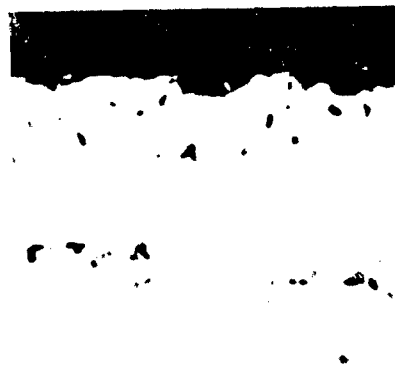
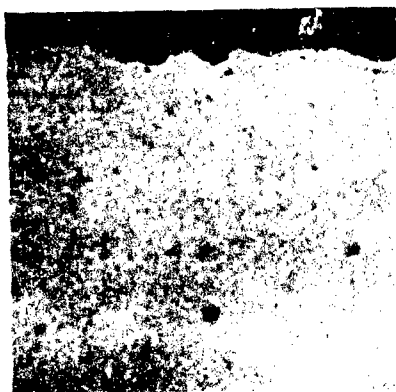
0

15.0

0.0002



0.40



MAGNIFICATION - 600X, POLISHED, UNETCHED

FIGURE 18
PHOTOMICROGRAPHS AT 600X OF INCONEL 713C TEST SPECIMENS
AFTER EXPOSURE TO HOT GAS CORROSION IN PHILLIPS 2 - INCH COMBUSTOR
AT 2000 F TEST CONDITION

no preferential attack on the grain boundaries of the stress-corrosion type. The hot corrosion appears to attack the entire surface of the specimen.

Photomicrographs of the Sierra Metal 200 specimens after exposure to hot corrosion at the 2000 F test conditions are shown in Figures 19 (at 100 X) and 20 (at 600 X). It may be noted that with 15 ppm "sea salt" at the various levels of sulfur, hot corrosion attack was several grains deep. There is some evidence of sulfur attack, as shown by the gray specks at the metal-scale interface in Figure 20, under the high "sea salt" ingestion conditions. This material is usually identified as chromium sulfide. The photomicrographic evidence of relatively deep attack plus the reduction in tensile strength suggests that the "sea salt" affected the internal structure of the Sierra Metal 200.

4. Conclusions

The following statements can be made concerning the effects of sulfur in the fuel and "sea salt" in the air on the hot corrosion of the superalloys Inconel 713C and Sierra Metal 200 under the conditions described in Section II-D1.

1. Oxidation and erosion were minor in the absence of sulfur and "sea salt".
2. Sulfur had little or no effect on hot corrosion in the absence of "sea salt".
3. "Sea salt" accelerated hot corrosion, even in the absence of sulfur, in some instances to catastrophic levels.
4. Sulfur x "sea salt" interactions were significant; but, while hot corrosion of Inconel 713C was accelerated, hot corrosion of Sierra Metal 200 was inhibited.
5. Decreasing sulfur concentration in the fuel from the current JP-5 specification maximum of 0.40 to 0.040 weight per cent, did not reduce hot corrosion in the presence of "sea salt" significantly.

SULFUR
IN FUEL,
WT %

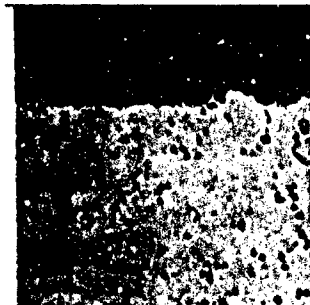
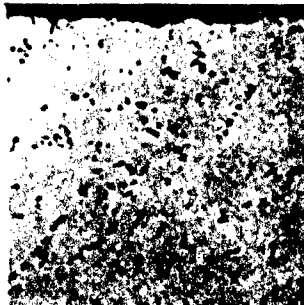
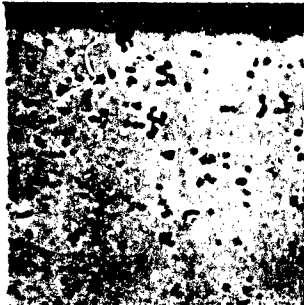
SEA SALT IN AIR, PPM

0

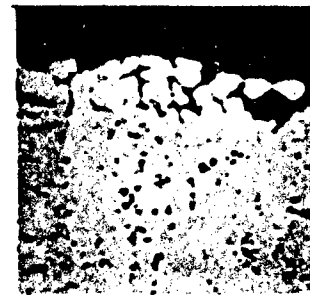
1.50

15.0

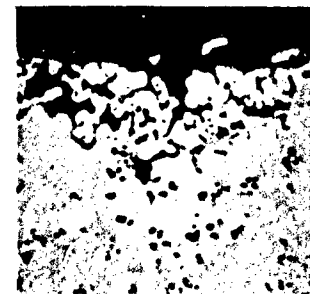
0.0002



0.040



0.40



MAGNIFICATION-100X, POLISHED, UNETCHED

FIGURE 19
PHOTOMICROGRAPHS AT 100X OF SIERRA METAL 200 TEST SPECIMENS
AFTER EXPOSURE TO HOT GAS CORROSION IN PHILLIPS 2 - INCH COMBUSTOR
AT 2000 F TEST CONDITION

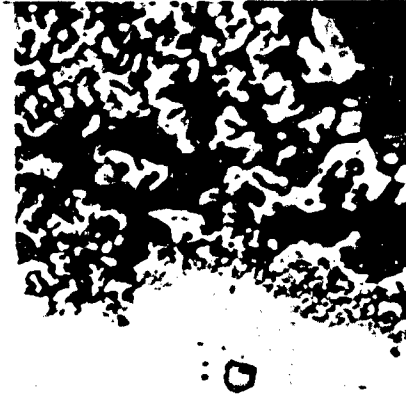
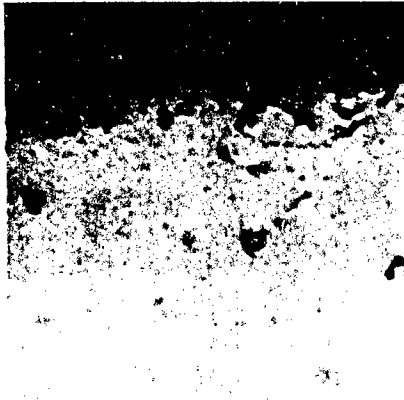
SULFUR
IN FUEL,
WT %

SEA SALT IN AIR, PPM

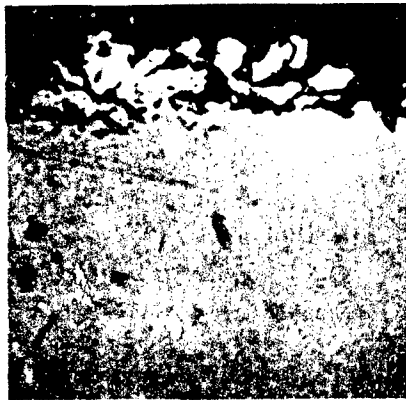
0

15.0

0.0002



0.40



MAGNIFICATION - 600X, POLISHED, UNETCHED

FIGURE 20
PHOTOMICROGRAPHS AT 600X OF SIERRA METAL 200 TEST SPECIMENS
AFTER EXPOSURE TO HOT GAS CORROSION IN PHILLIPS 2 - INCH COMBUSTOR
AT 2000 F TEST CONDITION

E. SUPPLEMENTARY TESTS

To obtain information on the mechanism of hot corrosion, a limited number of supplementary tests were made to evaluate the effect of temperature on weight loss and composition of the scale and to study the effect of sodium on hot corrosion in an essentially sulfur-free system. X-ray diffraction analyses were also made of the scale from some of the specimens from the 2000 F tests.

1. Effect of Temperature on Hot Corrosion

In the investigation of the effect of temperature on hot corrosion, tests similar to those described in Section II-D1, were run at exhaust gas temperatures of 1500, 1750 and 2000 F under the conditions listed in Table XI. The temperatures 1500 and 1750 bracket the freezing point, 1623 F, of sodium sulfate (Na_2SO_4). They were selected on the basis of the premise that it is important whether the corrosive agent is in its solid or liquid phase. This selection may have been somewhat arbitrary since sodium chloride freezes at 1434 F and the 45/55 per cent eutectic of sodium sulfate-sodium chloride freezes at 1153 F.

In the tests, Inconel 713C specimens were used, the sulfur content of the fuel was 0.40 weight per cent and the "sea salt" concentration in the combustor air was 15.0 ppm. A single test was made at each temperature and one specimen was used for weight loss measurement and the other for X-ray diffraction analyses of the scale and for photomicrographs. The test data are given in the following Table XIV.

TABLE XIV

EFFECT OF EXHAUST GAS TEMPERATURE ON HOT CORROSION OF INCONEL 713C

<u>Exhaust Gas Temp., F</u>	<u>X-ray Diffraction Analyses of Scale</u>	<u>Metal Loss, Wt. per cent</u>
1500	Na_2SO_4 (Thenardite), MgO (Periclase)	10.0
1750	MgO (Periclase), Na_2SO_4 (Thenardite), Ni, Fe (Josephinite)	0.4
2000	NiO (Bunsenite), MgO (Periclase), Na_2SO_4 (Form III)	25.8

As shown in this table, metal weight loss did not increase linearly with temperature. This suggests that a change in the mechanism of hot corrosion is involved. Photographs of the specimens before and after cathodic cleaning are shown in Figure 21. The amount and appearance of the deposits as well as the scale or deposit composition are different at the low and high exhaust gas temperatures. At 1500 F, there was a thick coating of scale on the uncleaned specimen and the weight loss was 10 per cent. This temperature is below the freezing points of Na_2SO_4 and MgO which accounts for the heavy build-up of deposits from the "sea salt". No material could be identified as a corrosion product. At 1750 F, the scale was very thin and the metal loss was very low (0.4 per cent). Since this temperature is above the freezing point of Na_2SO_4 , a major portion of the deposit was washed from the specimen by the high velocity exhaust gases. The minor amount of Josephinite may have resulted from contamination from other metal in the burner system since the weight loss was low. At 2000 F, the coating of scale was thin, but the attack on the specimen was heavy as indicated by the weight loss and the photograph of the cathodically cleaned specimen. This high metal weight loss (25.8 per cent) was associated with a change in scale composition with the major constituent

15.0 PPM SEA SALT IN AIR
0.40 WT % SULFUR IN FUEL

1500 F TEST CONDITION



UNCLEANED



CATHODICALLY CLEANED
925 MG METAL LOSS

1750 F TEST CONDITION



UNCLEANED



CATHODICALLY CLEANED
43 MG METAL LOSS

2000 F TEST CONDITION



UNCLEANED



CATHODICALLY CLEANED
2766 MG METAL LOSS

FIGURE 21
PHOTOGRAPHS OF INCONEL 713C TEST SPECIMENS
AFTER EXPOSURE TO HOT GAS CORROSION IN PHILLIPS 2 - INCH COMBUSTOR
AT VARIOUS TEMPERATURES

being NiO and with Na₂SO₄ changing from Thenardite to Form III. The large effect of temperature shown above merits further investigation.

Photomicrographs (at 600 X) of the heavily corroded test specimens at 1500 F and 2000 F are shown in Figure 22. The attack at 1500 F is characteristic of sulfidation, with randomly distributed internal gray globules of chromium sulfide. However, at 2000 F, where the metal is no longer covered by a heavy layer of sodium sulfate, there is little evidence of sulfidation. Generally, a black oxide lace is found at the surface of the metal; however, in some areas, as shown, the attack is led by a very fine grained structure of sulfides. This 2000 F specimen differs from that shown in Figure 18, in that it was not cathodically cleaned. These findings indicate that the characteristic sulfidation attack at 1500 F gives way to gross oxidation at higher temperatures where the metal is no longer covered by a heavy deposit of sodium sulfate. However, the patches of attack, with pitting at 2000 F still indicate localized areas of sulfidation.

2. X-Ray Diffraction Analysis

X-ray diffraction analyses were made of the scale on Inconel 713C specimens, tested under the 2000 F conditions with (a) 0.040 per cent fuel sulfur, 15.0 ppm "sea salt", (b) 0.40 per cent fuel sulfur, 15 ppm "sea salt" and (c) 0.40 per cent fuel sulfur, 1.50 ppm "sea salt". X-ray diffraction patterns were identical for all of these conditions. The deposits were chiefly Bunsenite (NiO). Other weaker diffraction lines were not identified. There was no evidence, from the X-ray diffraction analyses, of sulfide compounds in the corrosion products. This does not eliminate the possibility of the presence of sulfides since X-ray diffraction techniques are somewhat insensitive to small concentrations of sulfides and sulfides, if present, would be expected only adjacent to the metal where an overlay of deposit provides protection from oxygen in the gas stream. Further investigations are needed in this area.

More extensive X-ray diffraction data were obtained on corrosion products, under the 2000 F operating conditions, from Sierra Metal 200. These data are given in Table XV.

TABLE XV

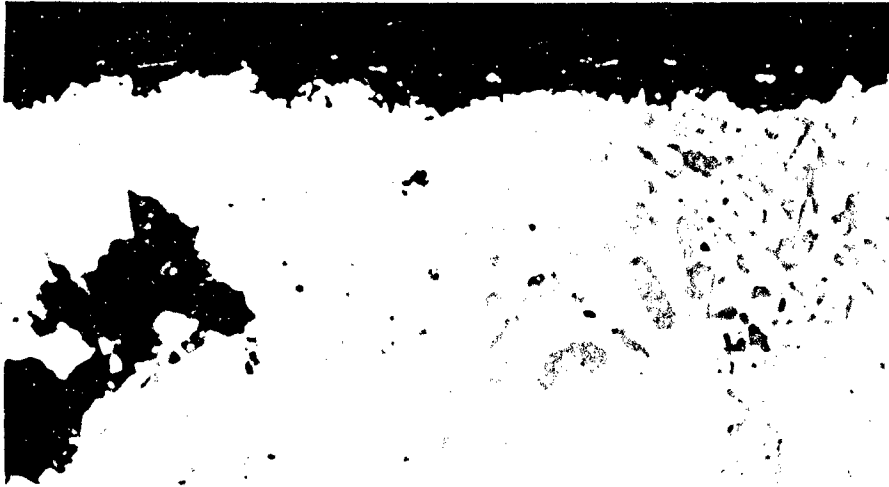
X-RAY DIFFRACTION ANALYSIS OF SIERRA METAL 200 CORROSION PRODUCTS

Sulfur, %	"Sea Salt", ppm		
	0.0	1.50	15.0
0.0002	No XRD data (2% wt. loss)	NiO (a), Na ₂ WO ₄ (b) Fe(AlCr) ₂ O ₄ (c) (18% wt. loss)	NiO, Na ₂ WO ₄ Fe(AlCr) ₂ O ₄ (45% wt. loss)
0.040	No XRD data (7% wt. loss)	NiO Fe(AlCr) ₂ O ₄ (5% wt. loss)	NiO, Na ₂ WO ₄ Fe(AlCr) ₂ O ₄ (22% wt. loss)
0.40	Ni, Fe (d) γ-Fe ₃ O ₄ (1% wt. loss)	NiO Fe(AlCr) ₂ O ₄ (2% wt. loss)	NiO Fe(AlCr) ₂ O ₄ (5% wt. loss)

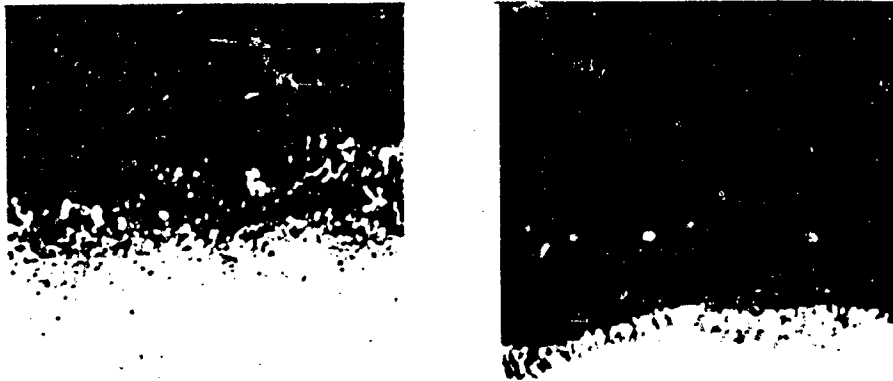
(a) NiO - Bunsenite; (b) Na₂WO₄ - Sodium Tungstate; (c) Fe(AlCr)₂O₄ - Aluminian Chromite; (d) Ni, Fe - Josephinite; γ-Fe₃O₄ - Magnetite

15.0 PPM SEA SALT IN AIR
0.40 WT % SULFUR IN FUEL

1500 F TEST CONDITION



2000 F TEST CONDITION



MAGNIFICATION - 600 X , POLISHED, UNETCHED

FIGURE 22
PHOTOMICROGRAPHS OF INCONEL 713C TEST SPECIMENS
AFTER EXPOSURE TO HOT GAS CORROSION IN PHILLIPS 2 - INCH COMBUSTOR
AT VARIOUS TEMPERATURES

Shown with the X-ray diffraction analysis data are metal weight losses which occurred under the sulfur x "sea salt" conditions indicated. In all cases where "sea salt" was present NiO was the major constituent of the scale. Of particular interest is the occurrence of sodium tungstate (Na_2WO_4) whenever the weight loss was 18 per cent or above. In the essential absence of sulfur, Na_2WO_4 is formed with 1.50 ppm "sea salt" in the combustor air; however, with 0.040 per cent sulfur in the fuel Na_2WO_4 is not present and metal weight loss is greatly reduced. Likewise, with 15.0 ppm "sea salt", increasing fuel sulfur from 0.040 to 0.40 per cent eliminated Na_2WO_4 and markedly reduced weight loss. From these observations, it may be postulated that sulfur in the fuel reacts with "sea salt" in the combustor air to prevent the formation of Na_2WO_4 .

A more complete investigation of corrosion products might show the reason for the obvious differences in sulfur x "sea salt" attack and elucidate the differences in the mechanism.

3. Sodium Corrosion

In the study of the effect of sodium on hot corrosion, tests were run under the 2000 F conditions described in Section II-D1 with essentially sulfur-free fuel (0.0002 weight per cent or 2 ppm). Sodium was introduced in the form of "sea salt", sodium chloride or sodium hydroxide. The "sea salt" concentration was 15 ppm in the combustor air. The other sources of sodium were introduced in concentrations to maintain equivalent sodium content, namely 9 ppm of sodium chloride and 6 ppm of sodium hydroxide. The data obtained are shown in Table XVI.

TABLE XVI

EFFECT OF VARIOUS SODIUM CONTAINING COMPOUNDS ON HOT GAS CORROSION

<u>Additive</u>	<u>Additive Concentration</u>	<u>Sulfur In Fuel</u>	<u>Super Alloy</u>	<u>Weight Loss, %</u>	<u>X-Ray Diffraction Analysis of Scale</u>
None (a)	None	2 ppm	713C	0.2	---
"Sea Salt" (a)	15 ppm in air	2 ppm	713C	8.7	---
Sodium Chloride (b)	9 ppm in air	2 ppm	713C	14.2	NiO, $\text{Fe}(\text{AlCr})_2\text{O}_4$
None (a)	None	2 ppm	SM 200	1.2	---
"Sea Salt" (a)	15 ppm in air	2 ppm	SM 200	42.7	NiO, Na_2WO_4 , $\text{Fe}(\text{AlCr})_2\text{O}_4$
Sodium Chloride (b)	9 ppm in air	2 ppm	SM 200	43.7	NiO, Na_2WO_4 , $\text{Fe}(\text{AlCr})_2\text{O}_4$
Sodium Hydroxide (b)	6 ppm in air	2 ppm	SM 200	100(c)	NiO, Na_2WO_4 , $\text{Fe}(\text{AlCr})_2\text{O}_4$

(a) Base line data.

(b) Added at a concentration to obtain a comparable level of sodium as found in "sea salt".

(c) About 90 per cent of the specimen was corroded away in four hours at which time the test was terminated.

It is seen that substitution of sodium chloride for "sea salt" increases hot corrosion of Inconel 713C. This suggests that materials present in "sea salt" such as non-aggressive alkaline earths or passive sulfates retard the corrosive attack of sodium. Nickel oxide and aluminian chromite [$\text{Fe}(\text{AlCr})_2\text{O}_4$] were identified by X-ray diffraction of the deposits when sodium chloride was introduced in the combustor air, with NiO being the major component.

With Sierra Metal 200, substitution of sodium chloride for "sea salt" had essentially no effect on metal weight loss. However, sodium hydroxide, NaOH, was much more severe than "sea salt" or sodium chloride with respect to metal weight loss. It is interesting to note that the same corrosion products were identified by X-ray diffraction for each of the three sodium systems. This suggests that the same mechanism of attack was involved in all three cases. While the mechanism of NaOH attack is unknown, it may be that excessive corrosion was caused by active oxygen from sodium peroxide, Na₂O₂, or it may be that sodium hydroxide forms a fused salt of greater solubility for the protective scale and thus clears the base metal for accelerated attack.

From these data it is quite apparent that catastrophic corrosion may be experienced in an essentially sulfur-free environment.

F. RECOMMENDATIONS

This study was made to determine whether the maximum sulfur limit of 0.4 weight per cent, currently allowed in grade JP-5 aviation turbine fuel, is a safe level for the protection of turbine blade alloys used in advanced engines. If not, information was sought to show whether a reduction in the sulfur specification limit would alleviate hot corrosion significantly. However, the complex interaction found with ingested "sea water" does not allow for either recommendation without additional information.

This study does not indicate a need for precipitate action to reduce the maximum sulfur limit of 0.4 weight per cent, currently allowed in grade JP-5 aviation turbine fuel. Both of the nickel-base alloys used in this study showed good resistance to oxidation, erosion, and sulfidation - in the absence of "sea salt". However, catastrophic "sea salt" corrosion was encountered with both superalloys, in some instances. A significant sulfur x "sea salt" interaction was shown by both superalloys; but, while hot corrosion of Inconel 713C was accelerated, hot corrosion of Sierra Metal 200 was inhibited. The catastrophic level of corrosion encountered with Inconel 713 C at high "sea salt" x sulfur concentrations was reduced to a negligible level by a drop in exhaust gas temperature from 2000 to 1750 F, indicating the prime importance of operating temperature. Therefore, it is recommended that this study be extended to obtain more complete data, covering additional superalloys, evaluated over a range in exhaust gas temperature.

Details of a program for this purpose have been outlined (18). The proposal is to employ a statistically designed program to study the hot corrosion of Inco 713C, SM-200, IN-100, Udimet 500, WI 52 and Inco 713C coated with Misco No. MDC-1 with exhaust gas temperatures of 1800, 2000 and 2200 F, a combustor inlet air pressure of 15.0 atmospheres and an exhaust gas velocity of 500 ft/sec at the location of the test specimens. It is planned to use fuel sulfur contents of 0.0002, 0.040 and 0.40 and "sea salt" concentrations of 0 and 10.0 ppm in the combustor air.

Measurements of weight loss and change in tensile properties and metallographic evaluation would be supplemented by analysis of corrosion products using X-ray diffraction, X-ray fluorescence and emission spectroscopy. In addition, measurements of exhaust gas temperature by thermocouples, and subsequent calculation of combustion efficiency, would be augmented by determination of exhaust gas composition using gas chromatography.

Six, rather than two, specimens would be exposed to hot gases in each test using three test specimen holders stacked in series and successively rotated to prevent channeling of gas flow. This system of cascade testing would subject downstream specimens to corrosion products not normally in the exhaust gas, as would be the case in a multi-stage turbine.

Another modification of the procedure used in the studies described in the present report would be an improved method of preparing specimens for measurement of tensile properties. Reduction to cross section would be accomplished by drilling a 1/8 in. diameter hole in the center of the specimen rather than by filleting. Thus, the usually more highly corroded edges would be retained. This would permit a more sensitive evaluation of over-all damage, reflecting both intergranular attack and loss in cross-sectional area.

III. FLAME RADIATION

A. TEST EQUIPMENT

1. Phillips Microburner

The Phillips Microburner (38) was developed to provide a bench-scale apparatus for measuring the combustion characteristics of hydrocarbon fuels under turbulent flow conditions simulating those in aircraft turbine engines. It has been used primarily for measuring the combustor deposit (carbon) and smoke (soot) forming tendencies of aviation turbine fuels (38), and to a limited extent for determining flame radiation characteristics of such fuels (22).

The Microburner is shown in the photograph of Figure 23 and in Figure 24. It consists of a Vycor glass tube 1.5 inches in diameter, and eight inches long, supported by the metal base shown in Figure 25. Air at elevated temperature is admitted through this base where the air is split into about 75 per cent tangential flow and 25 per cent axial flow by means of a swirl ring and axial air inlets. The fuel is introduced under nitrogen pressure and is atomized by discharging it from an orifice type fuel nozzle into the highly turbulent axial air stream. This normally results in essentially complete vaporization of the fuel before it enters the combustion zone.

The fuel vaporizer tube is positioned in the Vycor combustion chamber by means of a taper cut on its lower end which mates with a female-tapered tube holder placed at the center of the swirl ring. This mounting permits easy removal of the tube for replacement or for weighing when deposits are being measured.

Initial ignition is by means of a miniature spark plug swept by propane vapor. A schematic diagram of the flow system and instrumentation is shown in Figure 26, while Figure 27 shows the control panel.

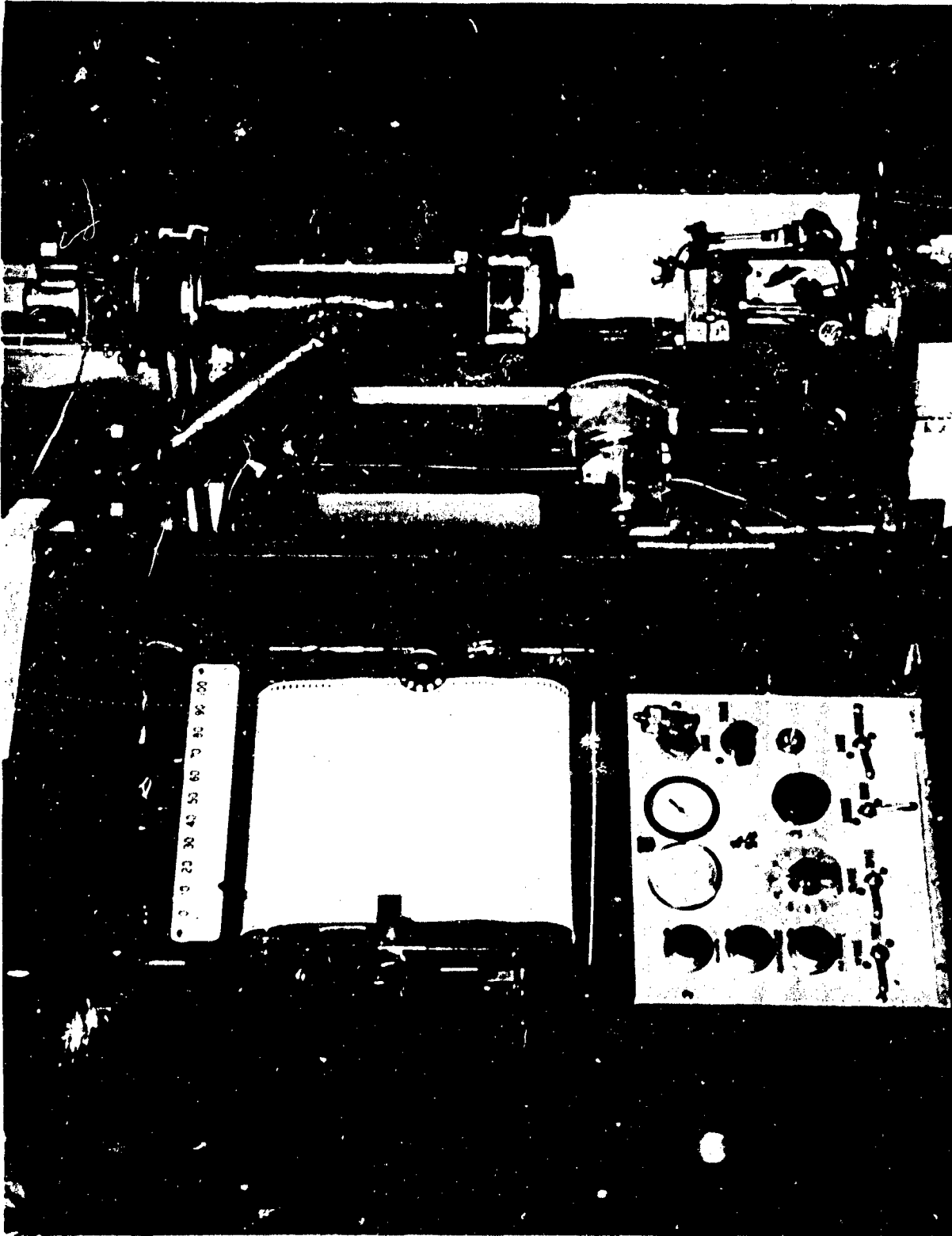


FIGURE 23
PHILLIPS MICROBURNER AND AUXILIARY EQUIPMENT
FOR STUDY OF FLAME RADIATION

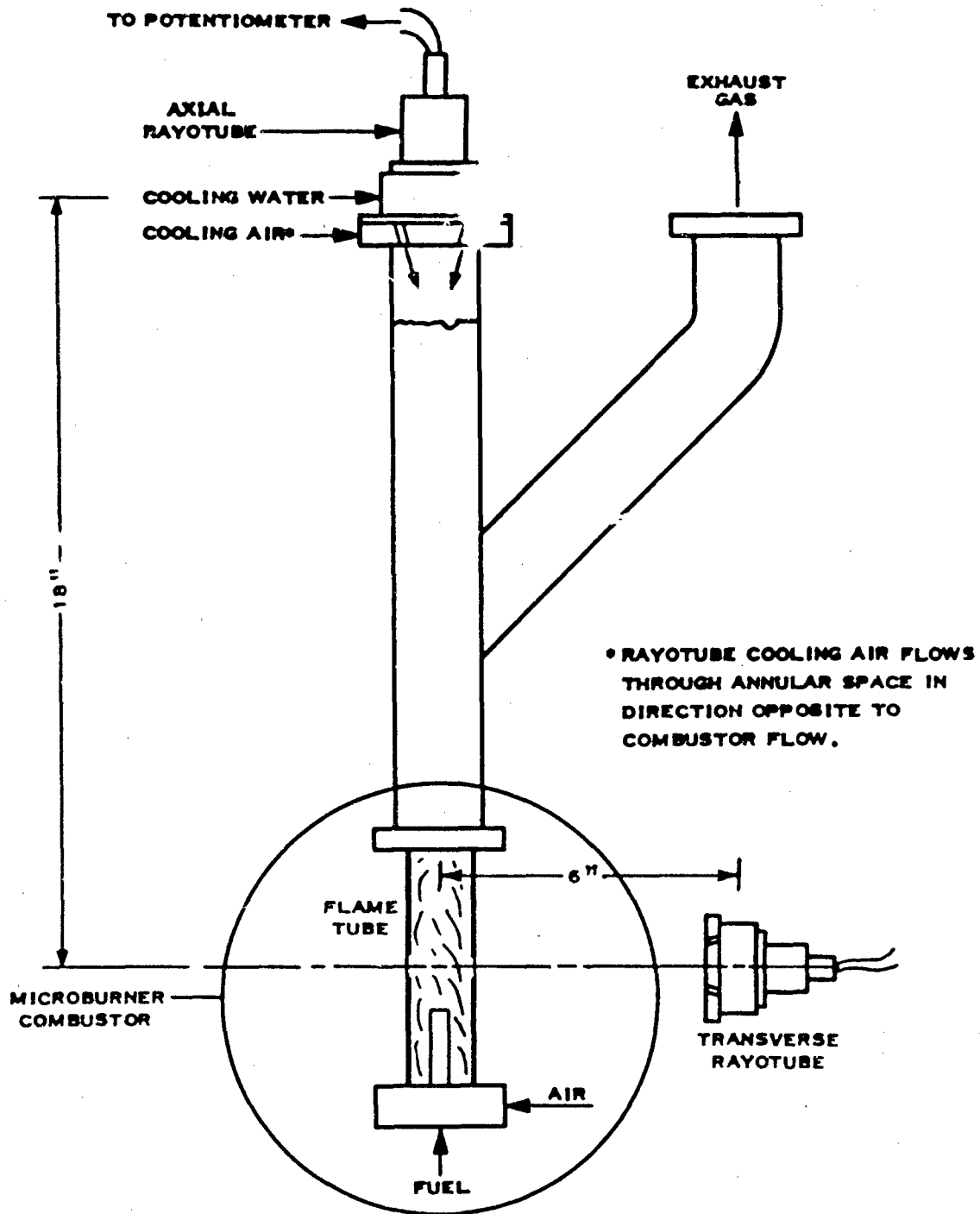


FIGURE 24
PHILLIPS MICROBURNER SET UP FOR MEASUREMENT OF FLAME RADIATION

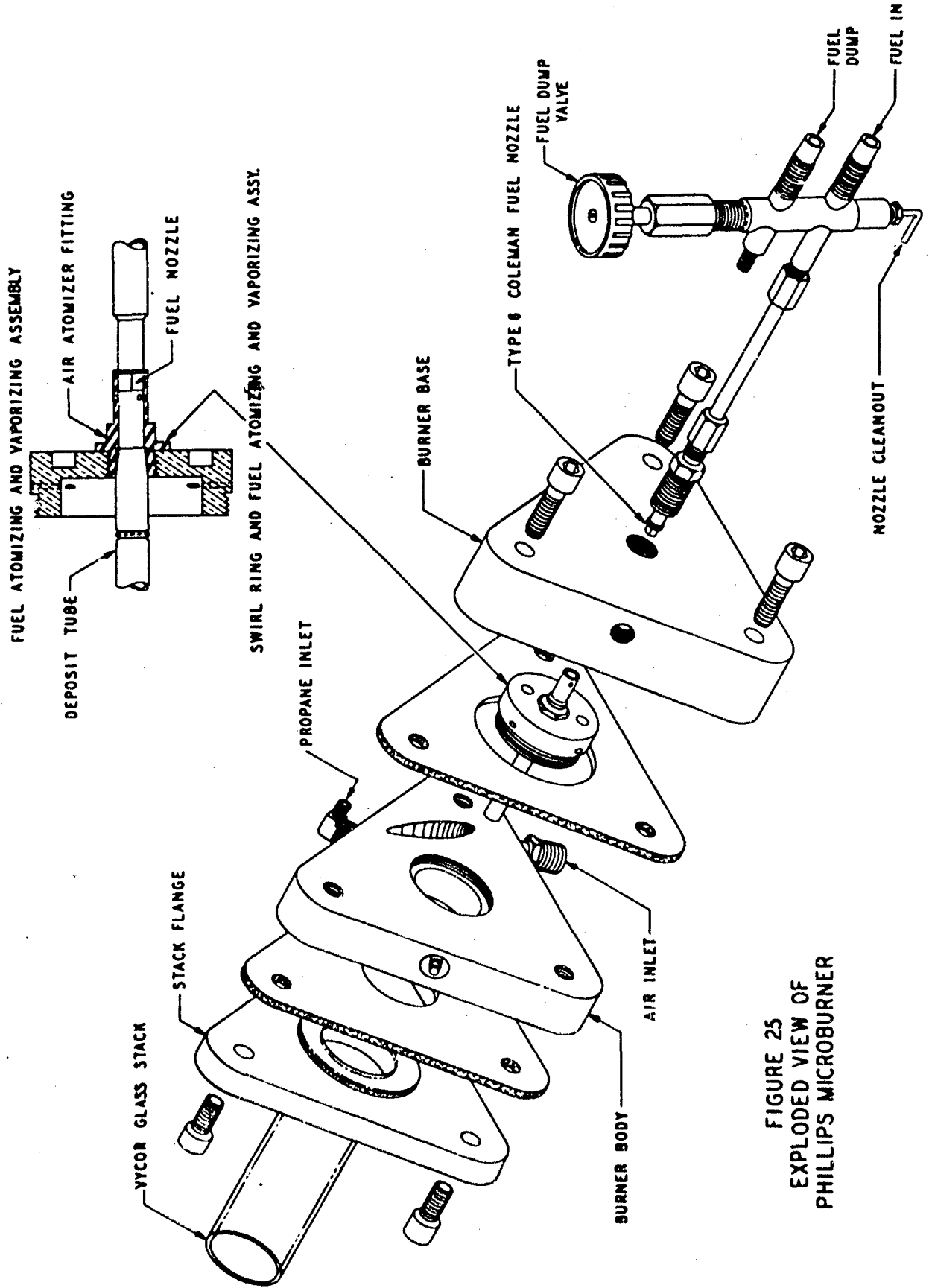


FIGURE 25
EXPLODED VIEW OF
PHILLIPS MICROBURNER

- 2 MOTOR VALVE - AIR SUPPLY PRESSURE
- 3 PRESSURE CONTROLLER - SUPPLY PRESSURE
- 4 ORIFICE - TOTAL GRAVIMETRIC AIR FLOW RATE
- 5 DIFFERENTIAL PRESSURE CELL - TOTAL FLOW RATE
- 6 DIFFERENTIAL MANOMETER - ORIFICE PRESSURE DROP
- 7 MOTOR VALVE - TOTAL AIR FLOW RATE
- 8 DIFFERENTIAL PRESSURE CELL - PRIMARY AIR PRESSURE SENSING.
- 9 MOTOR VALVE - AIR BLEED TO SECONDARY AIR LINE TO CONTROL PRIMARY AIR PRESSURE
- 10 DUAL PRESSURE CONTROLLER-CONTROLLING TOTAL AIR FLOW RATE AND PRIMARY AIR PRESSURE
- 11 DP CELL LOAD & LOCK VALVE
- 12 PRECISION DIAL MANOMETER - PRIMARY AIR PRESSURE
- 13 ROTAMETER - PRIMARY AIR
- 14 PRIMARY AIR FLOW RATE CONTROL VALVE
- 15 PRIMARY AIR ELECTRIC PREHEATER
- 16 BURNER BASE PRESSURE GAUGE
- 17 PHILLIPS MICROBURNER, MODEL 5
- 18 FUEL DUMP VALVE
- 19 FUEL FLOW RATE CONTROL VALVE
- 20 FUEL ROTAMETER
- 21 FUEL TANK
- 22 NITROGEN BLEED VALVE
- 23 PRECISION DIAL MANOMETER - NITROGEN PRESSURE
- 24 NITROGEN PRESSURE REGULATOR
- 25 PROPANE VALVE

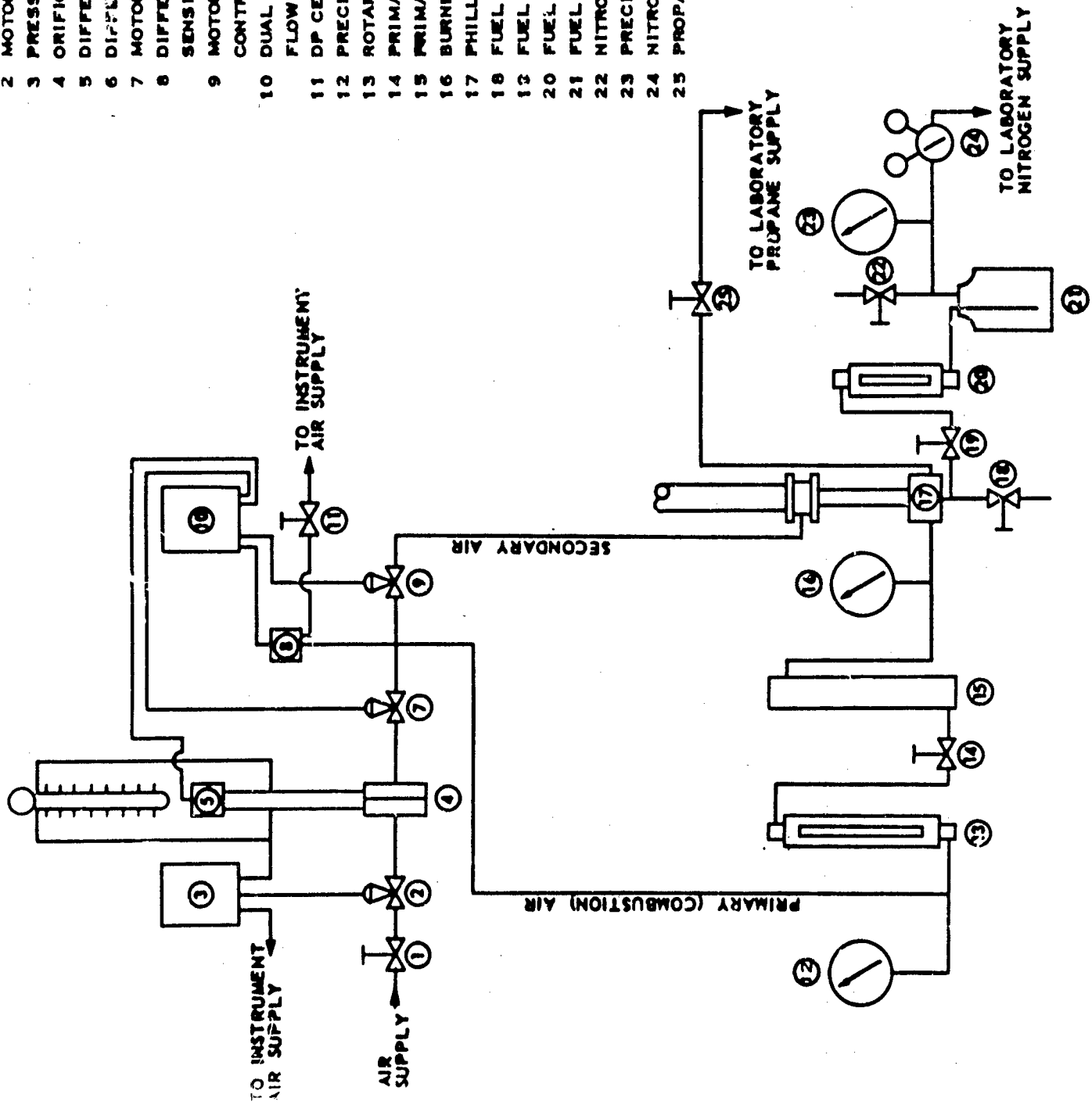


FIGURE 26

SCHMATIC FLOW DIAGRAM OF PHILLIPS MICROBURNER TEST FACILITY

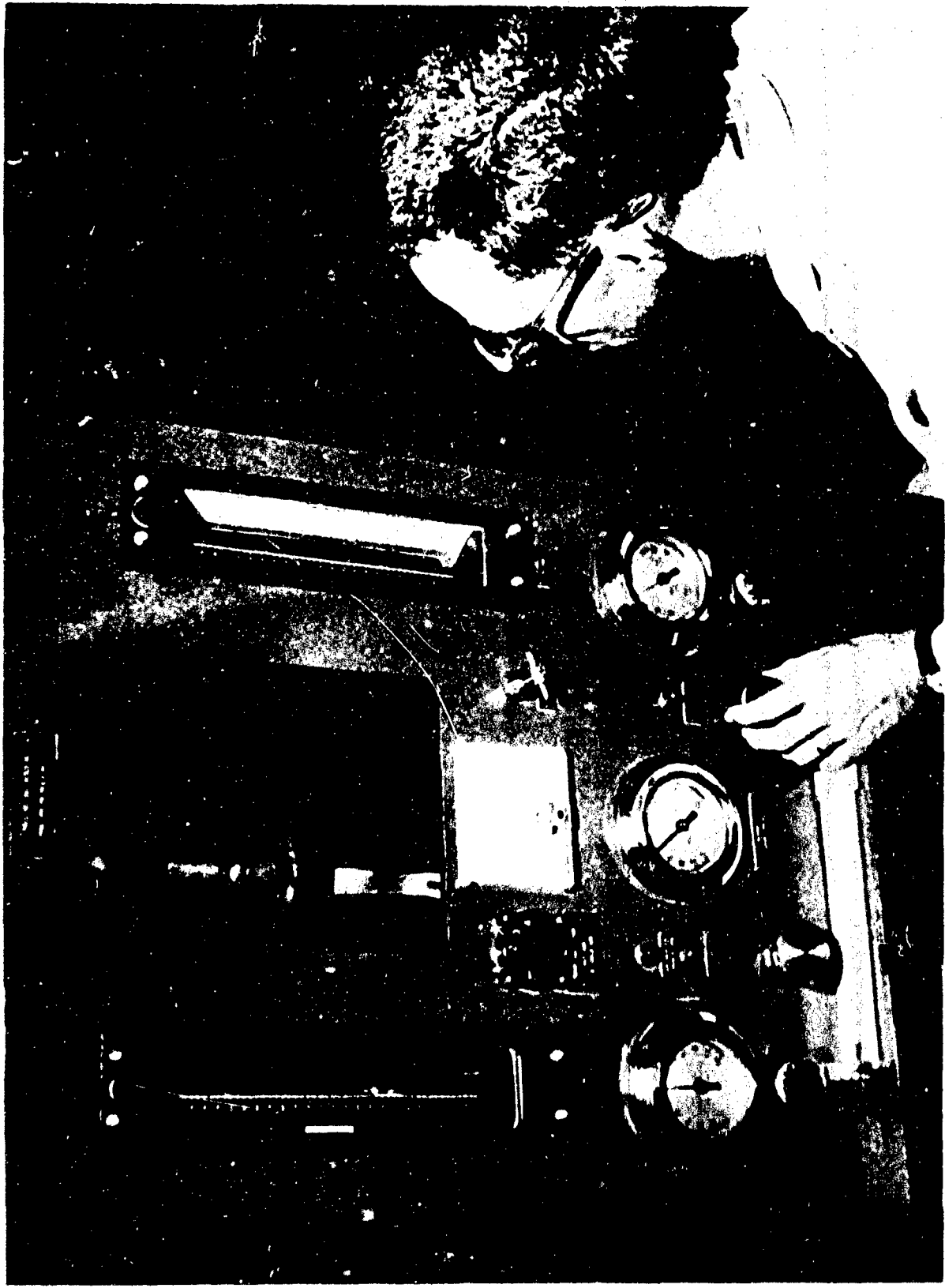


FIGURE 27
PHILLIPS MICROBURNER AND CONTROL PANEL

Figure 28 indicates the flow pattern in the vaporizer tube and combustion chamber. The atomized and largely vaporized fuel and the axial air are emitted from the vaporizer tube. On emerging from the tube, the mixture enters the axial back-flow of hot exhaust gases and is further mixed and vaporized. The normally fuel-rich mixture is carried into the tangential air stream where a combustible mixture is formed. As a result of the helical pattern of flow, a back-flow is established along the axis. This induced free vortex flow pattern establishes a seat for the flame in the low-velocity region of flow reversal and the flame becomes anchored near the base of the burner.

The Phillips Microburner simulates the primary combustion zone of an aircraft turbine engine combustor. It can be operated on fuels of widely varying characteristics under a broad range of operating conditions at atmospheric pressure.

2. Equipment for Flame Radiation Measurements

Leeds and Northrup No. 8898 fast-response double-mirror Rayotubes were employed in conjunction with a Leeds and Northrup Speedomax Type G potentiometric recorder to measure total radiant energy from the flames. The Rayotubes have "total radiation" thermocouple-type detectors, and were modified by the use of sapphire windows to allow transmission of significant flame radiation out to a wavelength of 5 microns (30).

One Rayotube (18-inch focal length) was mounted directly above the Microburner, as shown in Figure 24. It viewed the flame from an axial position, through the exhaust gas. This location simulates that of the turbine in an aircraft turbine engine. It provided a flame depth varying from a few inches to about a foot, with the longer flames being obtained at richer fuel-air mixtures. While the greater depth of flame increased emissivity, the increased concentration of combustion products, especially soot, in the exhaust gas tended to mask flame radiation by absorption. Thus, the total radiant energy measured at this axial position is a complex product of flame emission and combustion product absorption.

A second Rayotube (6-inch focal length), also shown in Figure 24, was placed to measure flame radiation from a transverse location, across the flame tube. This location simulates that of the combustor liner in an aircraft turbine engine. A direct view of the flame was obtained through a 0.5 in. diameter hole in the combustor wall; thus, avoiding cut-off of transmission of infrared radiation at wavelengths greater than about 2 microns by the Vycor glass (20). Another 0.5 in. diameter hole in the wall opposite the view port minimized wall radiation effects.

The Rayotubes contain an internal thermal shunt to compensate for their temperature coefficient. In addition, error caused by transient changes in Rayotube housing temperature were minimized by the use of water-cooled jackets (Leeds and Northrup Std. 13296-A). These water-cooled mountings also served to stabilize the Rayotubes below their maximum operating temperature of 300 F.

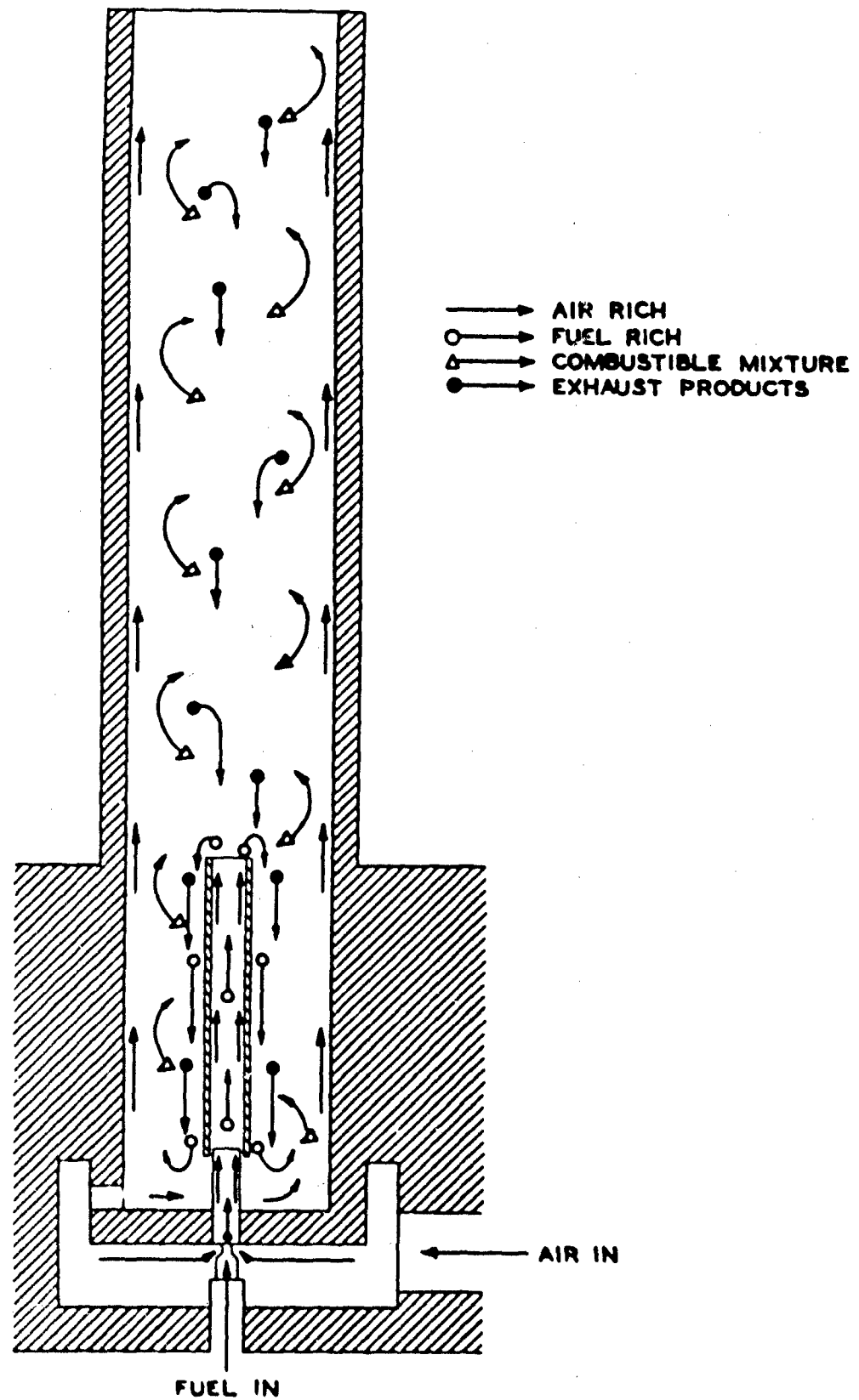


FIGURE 28

LOW PATTERN THROUGH COMBUSTION CHAMBER-PHILLIPS MICROBURNER

An air nozzle (Leeds and Northrup Std. 3296-U) was used as part of the mountings to flush the sapphire windows of the Rayotubes with clean, dry air and prevent deposit of combustion products. Such deposits on these windows would decrease the sensitivity of the Rayotubes and result in error, with total radiant energy measurements being low in value. Therefore, these windows were inspected, by cleaning with lens tissue, after each run as a precautionary measure.

The apparatus used for calibration of the Rayotube and potentiometer combination is shown in Figure 29. The black body target was designed in accordance with Reference 39 to insure a uniform emissivity approaching one. The target was enclosed in a muffle furnace, controlled at the desired temperatures, which were measured by means of a chromel-alumel thermocouple and Brown potentiometer. The Rayotube was focused on the black body target at controlled temperature and the generated emf was recorded by the Speedomax for development of the temperature-millivoltage calibration.

Values of total radiant energy corresponding to the observed temperatures were calculated from the Stefan-Boltzmann Law, using

$$W = 1.797 \times 10^{-8} T^4$$

where W = radiant energy flux per unit area, Btu/ft²/hr
 T = absolute temperature of source in degrees Kelvin
and 1.797×10^{-8} = Stefan-Boltzmann constant, Btu/ft²/deg⁴/hr.

B. TEST HYDROCARBONS

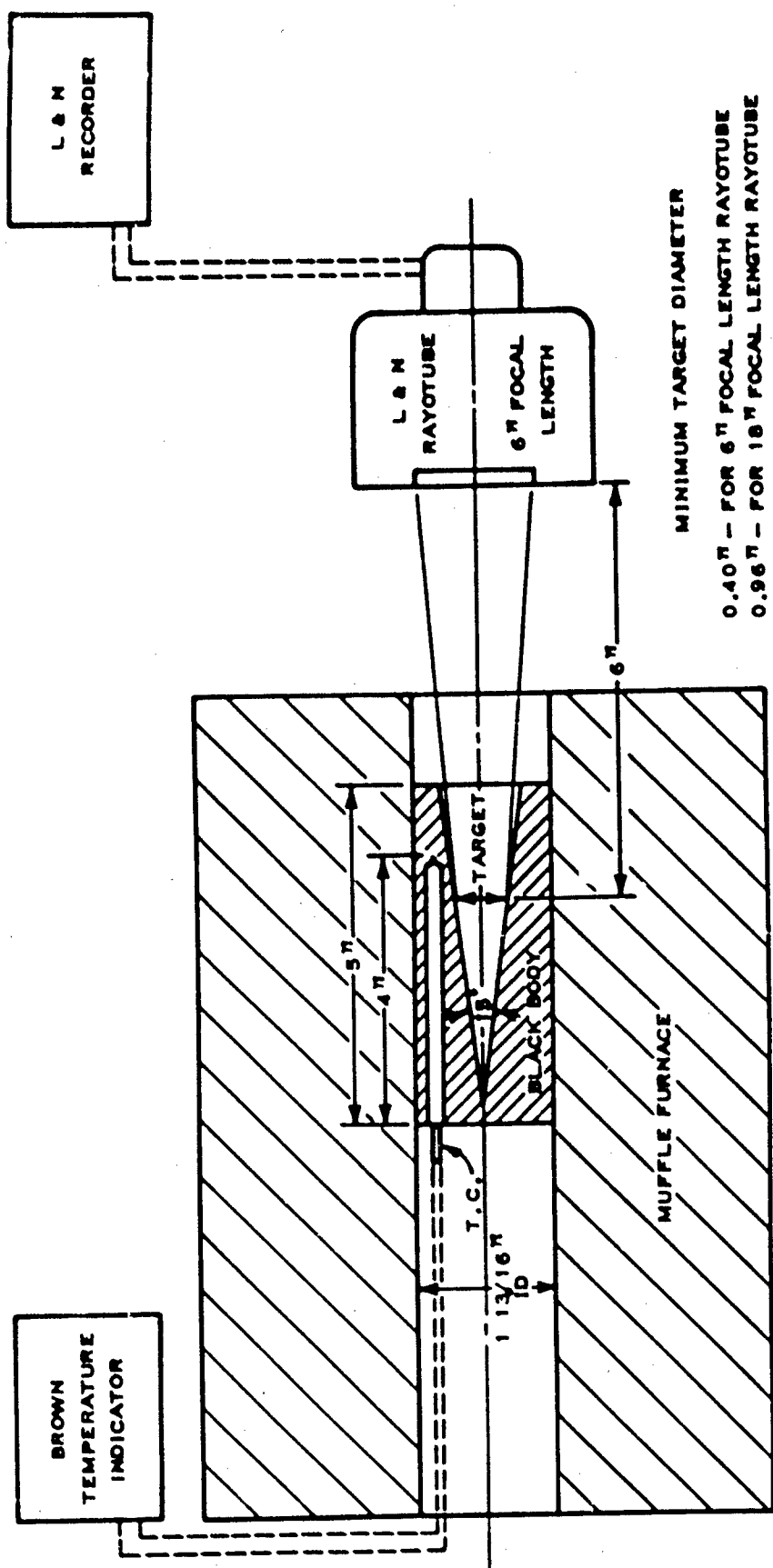
The hydrocarbons used in the Microburner for studies of flame radiation are listed in Table XVII together with the available physical and chemical properties.

The hydrocarbons were selected to cover a wide range in molecular structure and boiling point, as well as significant fuel properties such as hydrogen content, heat of combustion, Luminometer Number, and ASTM Smoke Point. This is illustrated in Figures 30 and 31 where Luminometer Number and hydrogen content, respectively, are plotted against boiling point.

Similar plots are not presented for heat of combustion and Smoke Point because the former correlates reasonably closely with hydrogen content and the latter with Luminometer Number over the range where Smoke Point is applicable.

C. TEST PROCEDURE

Preliminary experiments were made to choose operating conditions for the Microburner tests such that all of the test hydrocarbons could be burned satisfactorily over a wide range of fuel-air mixture ratios. This led to the selection of an inlet air temperature of 500 F with a cold flow reference velocity of 26 ft/sec (air flow of 0.0101 lb/sec).



BLACK BODY MATERIAL
H - W CHROME CASTABLE

FIGURE 29
APPARATUS FOR CALIBRATION OF L & N RAYOTUBES

SCALE: 3/8" = 1"

TABLE XVII
PHYSICAL AND CHEMICAL PROPERTIES OF TEST HYDROCARBONS

Phillips Sample Number	Compound	Formula	Purity, Mol %	Boiling Point, °F	API Gravity	Aniline Point, °F	Refractive Index at 68 °F	Net Heat of Combustion, Btu/lb.	Hydrogen Content, Wt. %	Luminometer Number	ASTM Smoke Point, cm
NORMAL PARAFFINS											
A13	n-Hexane	C ₆ H ₁₄	99	156	81.6	155.5	1.3759	19,233	16.38	226	Over 50
A10	n-Heptane	C ₇ H ₁₆	99	209	74.1	157.5	1.3883	19,157	16.10	209	Over 50
A17	n-Octane	C ₈ H ₁₈	99	258	65.7	159.1	1.3970	19,100	15.88	197	Over 50
A32	n-Decane	C ₁₀ H ₂₂	99	345	61.4	170.6	1.4129	19,020	15.59	170	Over 50
A33	n-Dodecane	C ₁₂ H ₂₆	99	421	56.6	182.9	1.4222	18,966	15.39	166	Over 50
A34	n-Tetradecane	C ₁₄ H ₃₀	99	488	53.2	192.7	1.4298	18,927	15.24	152	Over 50
A29	n-Tetradecane (Cetane)	C ₁₄ H ₃₀	99	548	50.9	202.7	1.4350	18,898	15.13	149	Over 50
A4	n-Decane-n-Pentadecane Mixture	C ₁₀ H ₂₂	98.5	421 ^b	56.0	182.4	1.4228	18,900	15.1	159	Over 50
A35	n-Decane Concentrate	C ₁₀ H ₂₂	84.7	338 ^b	56.9	159.1	1.4191	18,800	15.0	118	Over 50
A36	n-Decane-n-Pentadecane Concentrate	C ₁₀ H ₂₂	80	428 ^b	52.6	170.4	1.4291	18,750	14.9	112	50
ISOPARAFFINS											
A18	3-Methylpentane	C ₆ H ₁₄	99	146	80.4	151.3	1.3770	19,218	16.38	177	Over 50
A37	2, 2-Dimethylbutane (Neohexane)	C ₆ H ₁₄	99	123	85.0	123.2	1.3698	19,161	16.38	Too Volatile	48.8
A38	Dimethylhexanes (Mixed 2, 4-, and 2, 5-)	C ₈ H ₁₈	99	225 ^b	70.3	164.5	1.3948	19,000	15.88	135	Over 50
A9	2, 2, 4-Trimethylpentane (Isooctane)	C ₈ H ₁₈	99	211	71.7	175.1	1.3923	19,065	15.88	100	41.6
A20	2, 3, 4-Trimethylpentane	C ₈ H ₁₈	99	236	64.3	154.3	1.4050	19,080	15.88	120	50
A30	2, 2, 4, 4, 6, 8, 8-Heptamethyl-nonane	C ₁₀ H ₂₂	99	458 ^b	48.0	200.2	1.4402	19,100	15.13	74	33.2
B6	Isoundecane (Soltrol 130)	C ₁₁ H ₂₄	98	366 ^b	55.3	184.4	1.4235	18,900	15.5	99	41.8
B7	Isotridecane (Soltrol 170)	C ₁₃ H ₂₈	97	435 ^b	50.6	194.6	1.4336	18,950	15.1	91	38.7
CYCLOPARAFFINS											
A14	Cyclohexane	C ₆ H ₁₂	99	177	49.9	87.8	1.4264	18,676	14.37	130	Over 50
A21	Methylcyclopentane	C ₆ H ₁₂	99	161	56.8	91.4	1.4098	18,768	14.37	76	33.0
A19	1, 2-Dimethylcyclohexane (Mixed Isomers)	C ₈ H ₁₆	99	255 ^b	48.1	101.2	1.4320	18,600	14.37	95	33.9
A39	Diethylcyclohexanes	C ₁₀ H ₂₀	95.7	339 ^b	44.3	132.3	1.4401	18,600	14.37	90	33.9
A40	Deca-hydronaphthalene (Decalin-Mixed Isomers)	C ₁₀ H ₁₈	98.7	372 ^b	27.7	92.8	1.4764	18,250	13.12	49	22.9
A41	Methyl deca-hydronaphthalene (Methyl Decalins)	C ₁₁ H ₂₀	99.6	418 ^b	33.9	130.2	1.4644	18,350	13.24	47	21.4
A42	Tetracyclododecane (Dimethanodecalin)	C ₁₂ H ₁₈	99.3	446 ^b	7.1	87.7	1.5200	17,950	11.18	16	10.9
A43	Isopropyl bicyclohexyl	C ₁₅ H ₂₈	96.5	531	27.9	142.2	1.4825	18,350	13.54	54	23.0
OLEFINS											
A22	1-Hexene	C ₆ H ₁₂	99	146	77.4	73.0	1.3889	19,132	14.37	105	40.1
A44	1-Octene	C ₈ H ₁₆	99	250	64.7	90.5	1.4096	19,033	14.37	110	47.8
A23	4-Methyl-2-pentene (Mixed Isomers)	C ₆ H ₁₂	99	135	78.5	95.9	1.3889	18,450	14.37	71	28.3
A45	2, 2, 4-Trimethyl-2-pentene (Diisobutylene)	C ₈ H ₁₆	99	215	65.4	108.6	1.4098	18,904	14.37	63	25.9
A12	Cyclohexene	C ₆ H ₁₀	99	181	42.4	-4.0	1.4470	18,483	12.27	71	31.1
A24	4-Vinyl-cyclohexene-1	C ₈ H ₁₂	99	262	38.2	Crystals at +7	1.4641	17,900	11.18	37	18.8
A46	Phenylethylene (Styrene)	C ₈ H ₈	99	293	24.2	Crystals at -10	1.5469	17,418	7.74	2.7	6.2
AROMATICS											
A11	Benzene	C ₆ H ₆	99	176	29.0	Crystals at -2	1.5011	17,259	7.74	11	8.1
A15	Methylbenzene (Toluene)	C ₇ H ₈	99	231	31.4	Crystals at -40	1.4974	17,424	8.75	3	7.0
A25	1, 4-Dimethylbenzene (Para-Xylene)	C ₈ H ₁₀	99	281	32.3	-22	1.4960	17,347	9.49	-2	7.4
A26	Ethylbenzene	C ₈ H ₁₀	99	277	31.2	Crystals at -20	1.4959	17,596	9.49	2	6.8
A47	Diethylbenzene (Mixed Isomers)	C ₁₀ H ₁₄	99	352 ^b	31.5	Crystals at +2	1.4959	17,750	10.51	9	6.6
A27	Sec-Butylbenzene (2-Phenylbutane)	C ₁₀ H ₁₄	99	344	32.3	Crystals at -2	1.4900	17,851	10.51	15	6.2
A16	Tetra-hydro-naphthalene (Tetralin)	C ₁₀ H ₁₂	99	397 ^b	14.6	Crystals at -24	1.5395	17,400	9.15	0	6.6
A31	1-Methylnaphthalene	C ₁₁ H ₁₀	99	472	7.3	Crystals at -22	1.6151	16,900	7.09	-14	5.1
A48	Methylnaphthalene Concentrate (Mixed Isomers)	C ₁₁ H ₁₀	75	480 ^b	6.8	Crystals at -30	1.6142	16,800	7.1	-13	5.0

(a) All values of API Gravity and Refractive Index were directly measured. When these values agreed closely with accepted literature values and the estimated purity was high, literature data are given for boiling point, net heat of combustion, and aniline point where available, and hydrogen content is calculated from the chemical formula. When the hydrocarbon consisted of a mixture or where there were no accepted literature values, the purity and all properties were measured. All Luminometer numbers and Smoke points were also measured.

(b) Average boiling points.

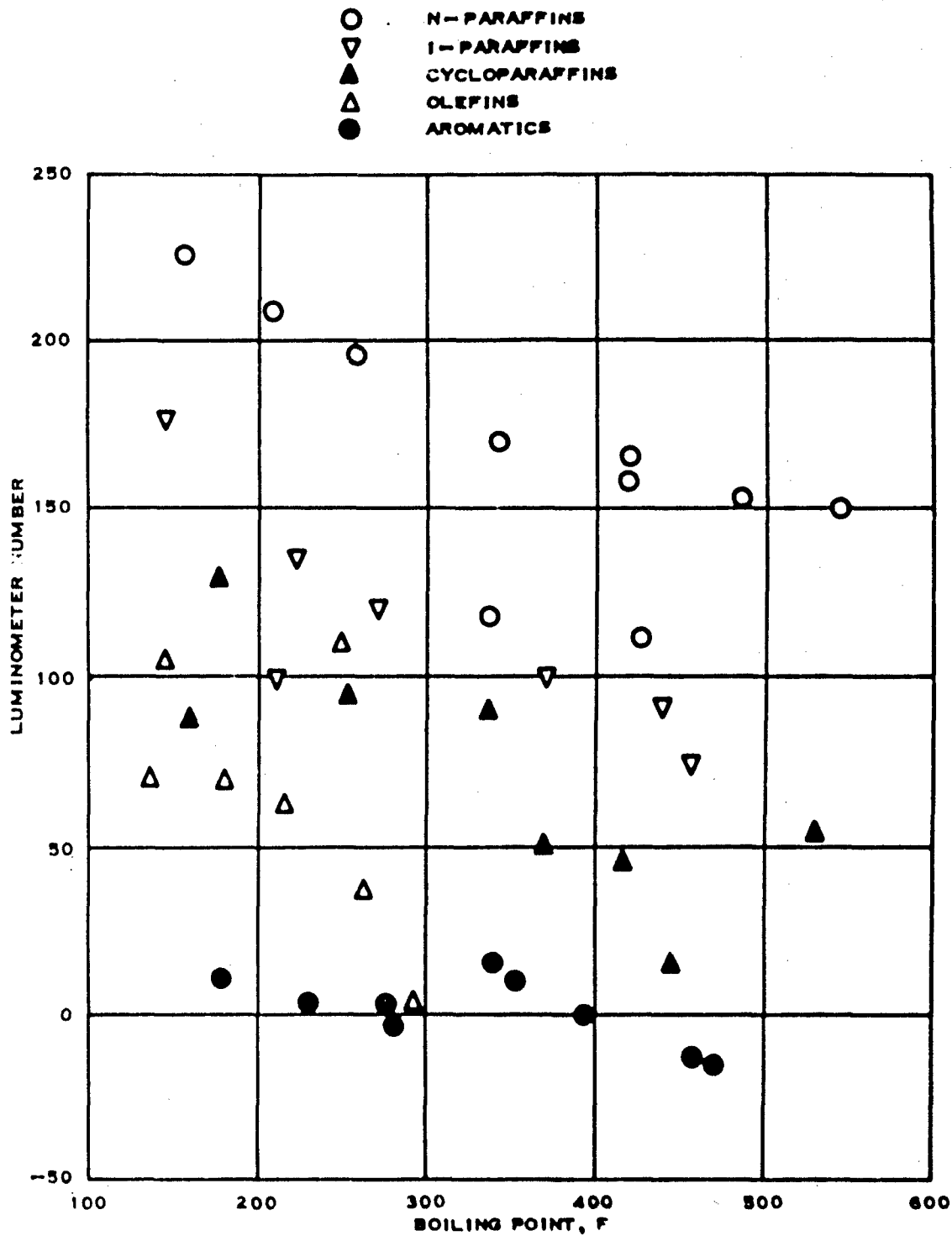


FIGURE 30
 SPREAD IN LUMINOMETER NUMBER OVER BOILING
 RANGE OF HYDROCARBONS USED IN MICROBURNER
 STUDIES OF FLAME RADIATION

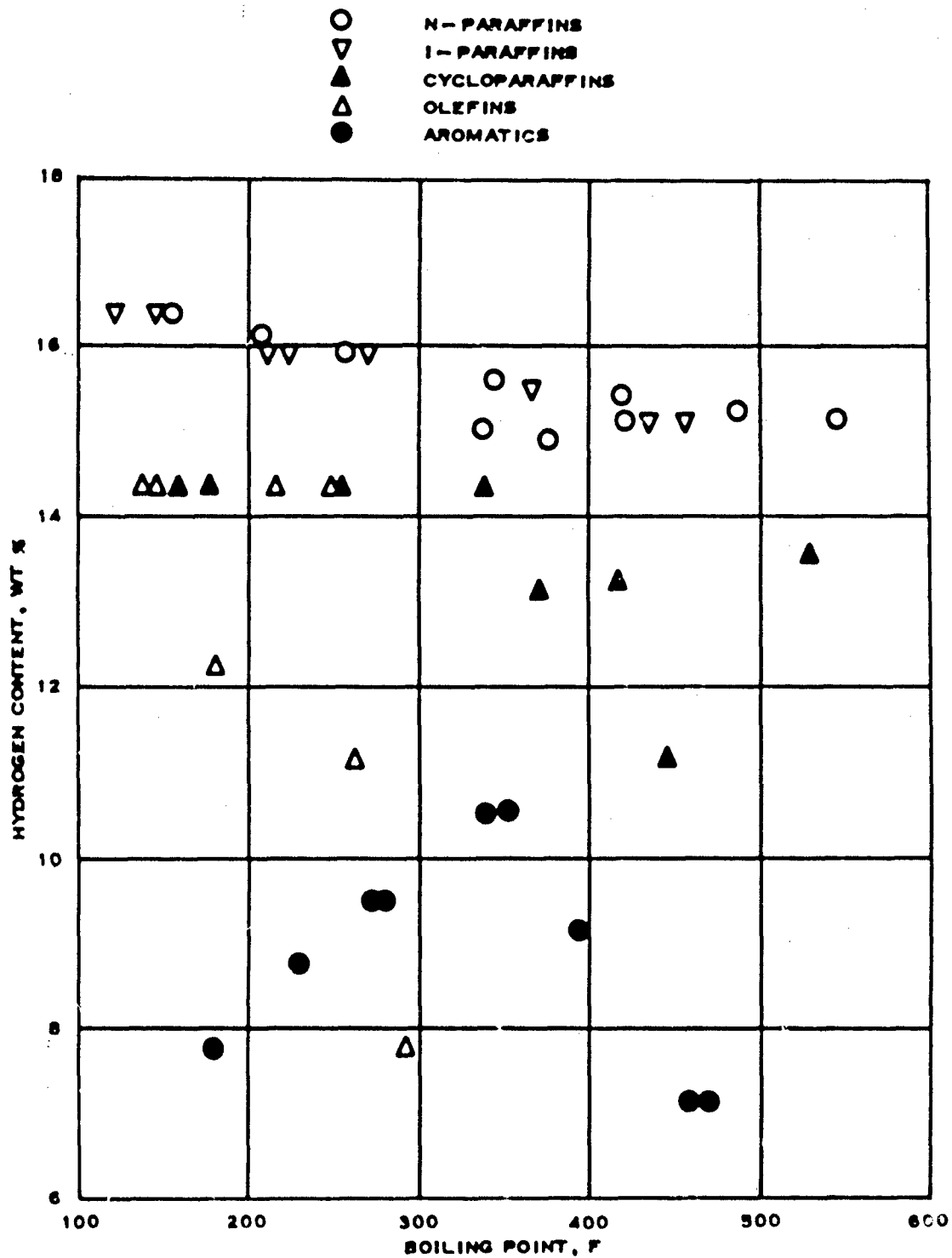


FIGURE 31
SPREAD IN HYDROGEN CONTENT OVER BOILING RANGE
OF HYDROCARBONS USED IN MICROBURNER STUDIES
OF FLAME RADIATION

Prior to measurements of flame radiation, the fuel rotameter was calibrated with each hydrocarbon to develop curves of rotameter reading against fuel flow in lb/sec. In the tests, fuel flow was varied so that the supplied fuel-air mixture ratio ranged from a maximum of about 0.09 to 0.13, depending upon the fuel flow obtained at the 150 mm limit of the Brooks rotameter scale, or lower if dictated by fuel performance characteristics, to the leanest mixture that would permit stable burning. The limiting lean mixtures varied from about 0.01 to 0.04 fuel-air mixture ratio.

Paraffin fuels exhibited visually blue flames under these operating conditions. While flames of aromatic fuels were blue at their lean limit, they were already brilliantly luminous at stoichiometric. Figures 32, 33 and 34 partially show these differences although, in the absence of color, the marked difference between isooctane and toluene at the lean limit and toluene at stoichiometric is not as striking as it was in fact.

In the preliminary experiments, it was found that greater repeatability was obtained in total radiant energy values when measurements were made on decreasing fuel-air mixture ratios. Subsequently, with the Rayotube and Speedomax recorder in operation, burning was first stabilized at the maximum fuel rotameter setting. The rotameter setting was then reduced 10 mm and the burning again allowed to stabilize. This procedure was continued until stable burning could no longer be obtained and the flame blew out.

With each fuel duplicate runs were made for measurements of total radiant energy, both transversely and axially. The reported data are based on the averages of the two runs which were made consecutively and which were usually in good agreement.

From the observed experimental data expressed in terms of rotameter readings and millivoltage recordings, fuel-air mixture ratio, percentage stoichiometric and corresponding total radiant energies for the flames were calculated.

D. TEST RESULTS

Typical plots of flame radiation as a function of percentage stoichiometric fuel-air mixture ratio are shown in Figures 35 and 36. Comparison of these two figures shows that axial total radiant energy is greater than transverse total radiant energy, because of the greater flame depth viewed by the Rayotube installed above the Microburner.

It was also observed in some cases, as shown for the aromatic hydrocarbon, benzene, in Figures 35 and 36 that the amount of transverse total radiant energy leveled off at a maximum while the axial total radiant energy passed through a maximum. This results from absorption of radiant energy from the high temperature flame by the cooler combustion products. At rich fuel-air mixtures, aromatic hydrocarbons generally produce significant amounts of soot, which approaches a black body in its radiant energy absorption characteristics. Therefore, the more soot in the cooler combustion products, the more effectively the total radiant energy detector is screened from the flame radiation.



FIGURE 32
PHILLIPS MICROBURNER FLAME
WITH ISOCTANE AT LEAN LIMIT

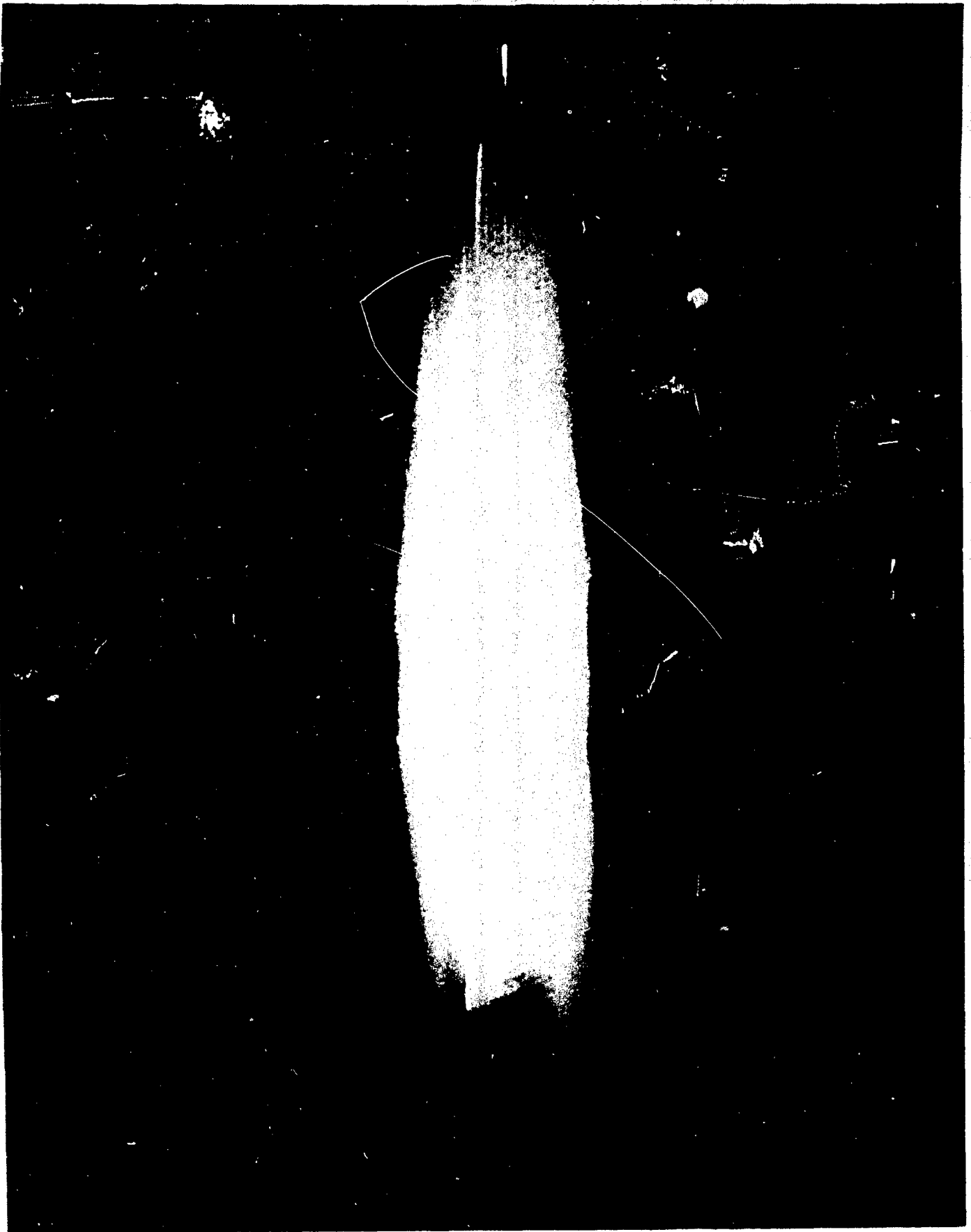


FIGURE 33
PHILLIPS MICROBURNER FLAME
WITH TOLUENE AT LEAN LIMIT

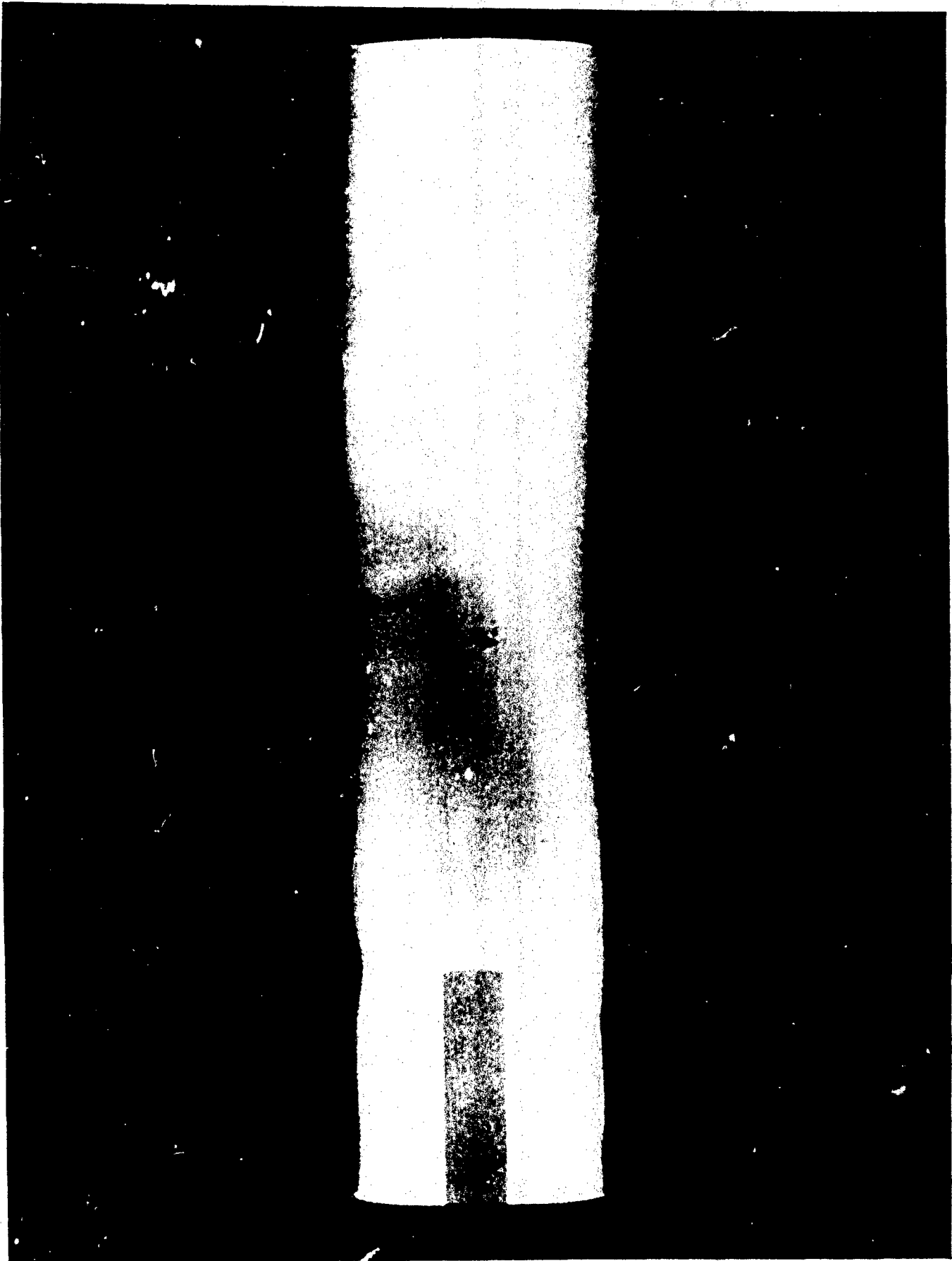


FIGURE 34
PHILLIPS MICROBURNER FLAME
WITH TOLUENE AT STOICHIOMETRIC
AIR - FUEL MIXTURE

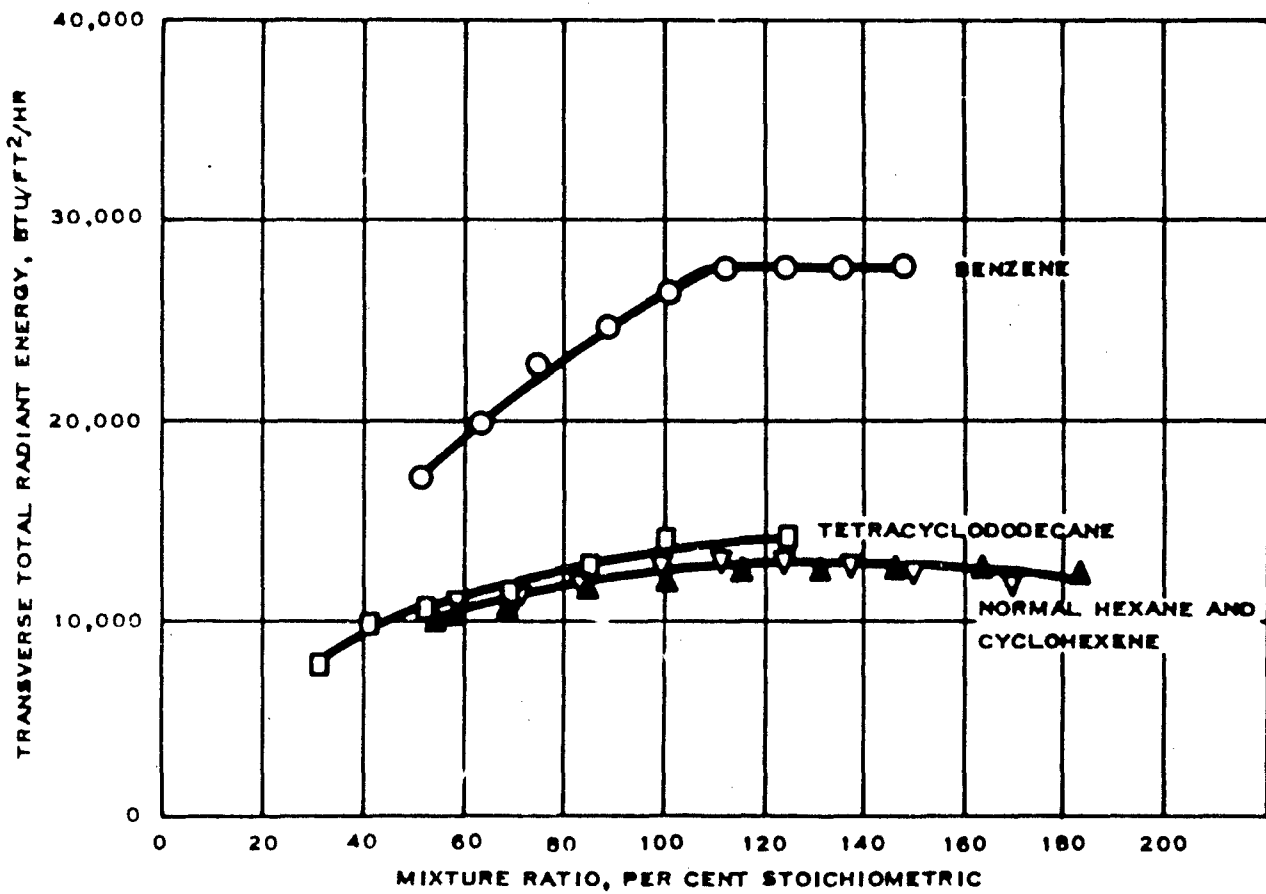


FIGURE 35
 EXAMPLES OF THE CHANGE IN TRANSVERSE FLAME
 RADIATION WITH FUEL - AIR MIXTURE RATIO

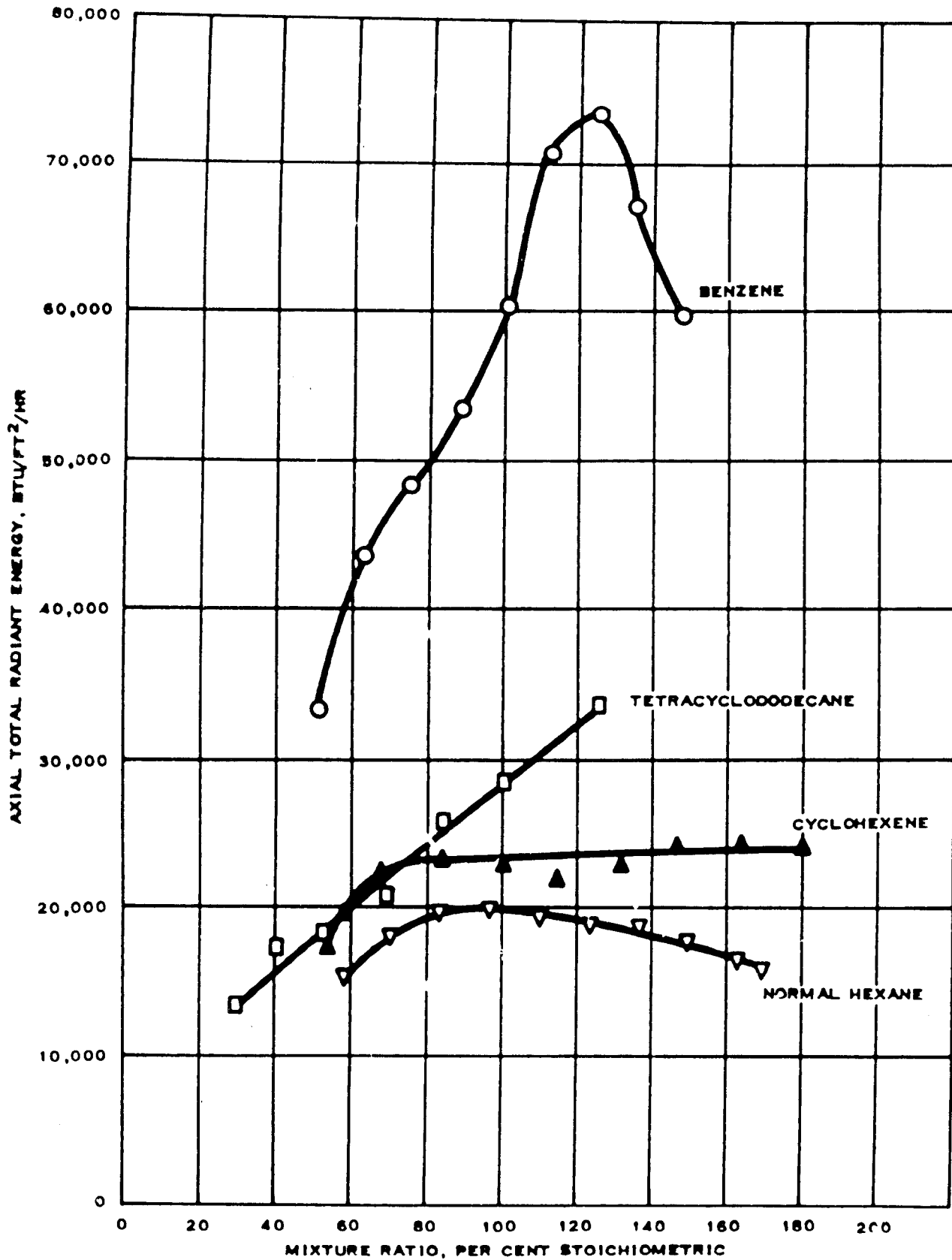


FIGURE 36
 EXAMPLES OF THE CHANGE IN AXIAL FLAME RADIATION
 WITH FUEL - AIR MIXTURE RATIO

Plots similar to those of Figures 35 and 36, but on a more open scale, were made for all of the hydrocarbons and values of total radiant energy were read from them at a series of even percentages of stoichiometric. These smoothed values are given in Tables XVIII and XIX.

E. DISCUSSION

1. Effect of Hydrocarbon Type

The curves of total radiant energy plotted against percentage stoichiometric for the normal- and iso-paraffins, the mono- and bi-cycloparaffins and the straight and branch chain olefins are roughly similar to those shown in Figures 35 and 36 for normal hexane. The curves for the aromatics are of the same general type as those for benzene.

This is illustrated in Figure 37 for transverse measurements of flame radiation. In this figure all of the paraffins and all of the olefins except the aromatic olefin, styrene, fall in a narrow band of total radiant energies at a low level and there is relatively little change in level with change in fuel-air mixture ratio. The alkylbenzenes and tetralin (a bicyclic aromatic with one saturated and one unsaturated ring) fall at a higher level within another narrow band which overlaps the band for paraffins and olefins at low percentages stoichiometric but which lies increasingly above the latter at higher percentages stoichiometric. At a still higher level lie the still steeper curves for benzene and the olefinic aromatic, styrene. Above these are the curves for the bicyclic aromatics with two unsaturated rings, methylnaphthalene and methylnaphthalene concentrate.

Somewhat the same general picture is shown for axial measurements of flame radiation in Figure 38. However, here the lower band includes only the normal- and iso-paraffins, the mono- and bi-cycloparaffins, and the straight and branch chain olefins. Separate curves are shown for the two cycloolefins, cyclohexene and 4-vinyl-cyclohexene-1, and for the tetracycloparaffin, tetracyclododecane, which fall intermediate between the lower band and the aromatics. Also there is a considerably broader band for the alkylbenzenes and tetralin and much less differentiation between those aromatics (ethylbenzene and toluene) at the top of alkylbenzene band and benzene and styrene which lie at the bottom of the top band of Figure 38. Again the methylnaphthalene flames exhibit the highest total radiant energies with those from the pure methylnaphthalene being appreciably greater than those from the methylnaphthalene concentrate.

2. Effect of Hydrocarbon Properties

Luminometer Number and Smoke Point are used in aviation turbine fuel specifications for control of burning quality and hydrogen content has been proposed (21, 40) for this purpose. A fourth property, net heat of combustion, correlates reasonably well with hydrogen content. Accordingly, it is of interest to determine the extent of the effect of variations in these properties on flame radiation in the Phillips Microburner.

TABLE XVIII

ACIAL FLAME RADIATION AT VARIOUS FUEL-AIR MIXTURE RATIOS

Total Radiant Energy, $\text{W}/\text{ft.}^2/\text{hr.} \times 10^{-3}$ at Stated Mixture Ratios, % Stoichiometric

Compound	40	50	60	70	80	90	100	110	120	130	140	150	160	170	180	190
NORMAL PARAFFINS																
n-Heptane	-	-	15.3	17.7	19.3	19.8	19.7	19.5	19.2	18.8	18.3	17.6	16.7	15.7	-	-
n-Octane	14.7	15.6	17.0	18.7	20.3	21.2	21.1	20.7	20.4	20.0	19.7	19.4	19.2	19.0	18.6	18.3
n-Nonane	12.5	13.5	14.9	16.3	17.7	18.9	19.3	19.3	18.8	18.4	18.0	17.7	17.4	17.2	17.0	-
n-Decane	13.2	13.6	14.5	16.0	17.5	18.8	19.4	19.3	18.9	18.4	17.9	17.6	17.2	17.0	-	-
n-Dodecane	11.8	12.7	13.6	15.1	17.2	18.6	19.0	18.9	18.5	18.0	17.6	-	-	-	-	-
n-Tetradecane	15.0	16.3	17.4	18.6	19.3	18.8	18.2	17.8	17.6	17.4	17.2	17.0	16.9	16.6	16.4	16.3
n-Hexadecane (Cetane)	12.4	14.0	15.4	16.6	18.0	18.7	18.8	18.7	18.4	18.0	17.7	17.5	17.4	17.4	-	-
n-Decane, n-Pentadecane Mixture	11.9	12.2	13.0	14.6	16.2	17.6	18.2	18.4	18.2	17.6	17.3	-	-	-	-	-
n-Decane Concentrate	11.8	12.5	13.6	15.3	17.1	18.6	19.3	19.3	18.9	18.5	18.2	17.8	17.4	17.0	-	-
n-Decane, n-Pentadecane Concentrate	12.4	13.7	15.3	17.2	18.4	19.2	19.9	19.9	19.3	18.9	-	-	-	-	-	-
ISOPARAFFINS																
1-Methylpentane	12.4 ^a	12.7	15.4	18.3	19.3	19.3	18.9	18.6	18.2	17.8	17.6	17.3	16.9	15.6	16.3	-
2, 2-Dimethylbutane (Isobutane)	15.5	18.8	19.8	20.0	19.7	19.3	18.9	18.4	18.0	17.6	17.2	17.0	-	-	-	-
Dimethylbenzenes (Mixed 2, 4- and 2, 5-)	12.8	13.1	14.4	16.0	17.7	18.8	19.0	18.8	18.4	18.0	17.6	17.3	17.0	16.7	16.5	16.2
2, 2, 4-Trimethylpentane (Isooctane)	-	-	16.4	17.6	18.6	19.2	19.4	19.2	18.8	18.3	18.0	17.6	17.3	17.0	-	-
2, 3, 4-Trimethylpentane	12.0	13.0	14.5	16.1	17.6	18.8	19.4	19.2	18.8	18.3	17.9	17.6	17.3	17.0	16.8	16.6
2, 2, 4, 4, 6, 6, 8, 8-Heptamethyl-nonane	13.7	14.2	14.9	15.8	16.9	18.1	19.5	20.4	20.7	20.6	20.4	20.0	19.5	19.1	18.8	18.6
Isoundecane (Soltrol 130)	12.3	13.2	15.1	17.1	18.4	19.4	19.9	19.9	19.4	19.1	18.8	-	-	-	-	-
Isotridecane (Soltrol 170)	12.9	13.5	14.7	17.3	19.0	19.8	20.0	19.9	19.5	19.2	19.0	18.8	18.6	18.4	18.0	17.8
CYCLOPARAFFINS																
Cyclohexane	-	14.1	16.0	17.8	19.3	20.0	20.0	19.8	19.6	19.3	19.0	18.7	18.3	17.8 ^a	-	-
Methylcyclopentane	-	12.6	14.2	16.4	18.0	18.9	19.7	19.1	18.4	18.1	17.8	17.6	17.3	17.0	16.6	-
1, 2-Dimethylcyclohexanes (Mixed Isomers)	-	15.8	17.3	18.8	19.6	19.6	19.3	18.8	18.3	17.9	17.6	17.2	16.9	16.6	-	-
Diethylcyclohexanes	12.4	13.7	15.7	17.6	19.2	20.1	20.0	19.5	19.1	18.7	18.5	18.1	17.8	17.7	17.6	-
Decalin (Mixed Isomers)	13.3	14.4	15.7	17.1	18.9	20.7	21.3	21.6	21.8	21.9	22.0	22.1	22.2	-	-	-
Methyldecalins	12.6	14.2	15.8	17.4	18.9	19.8	20.2	20.0	19.4	-	-	-	-	-	-	-
Tetrahydronaphthalene	15.5	17.7	19.8	22.0	24.2	26.3	28.4	30.4	32.3	-	-	-	-	-	-	-
Isopropyl bicyclohexyl	12.2	12.9	14.0	16.0	18.2	19.1	19.6	19.8	19.9	19.6	19.4	-	-	-	-	-
OLEFINS																
1-Heptene	-	15.4	18.5	19.7	20.4	20.8	20.9	20.8	20.3	19.7	19.3	19.0	18.8	18.6	18.4	18.0
1-Octene	13.3	13.7	14.8	16.5	18.0	19.1	19.4	19.2	18.8	18.5	18.2	18.0	17.7	17.5	17.3	17.2
4-Methyl-2-pentene (Mixed Isomers)	-	14.0	17.5	18.8	20.7	21.0	20.2	19.6	19.4	19.2	19.0	18.8	-	-	-	-
2, 2, 4-Trimethyl-1-pentene (Diisobutylene)	-	14.3	15.4	17.0	18.6	19.9	20.6	20.5	20.1	19.9	19.7	19.6	19.5	19.4	19.4	19.0
Cyclohexene	-	-	20.5	22.6	25.0	25.2	25.3	25.4	25.6	25.8	25.8	25.8	26.0	26.0	26.0	-
4-Vinyl-cyclohexene-1	16.6	17.3	18.3	20.7	23.9	25.6	26.4	27.0	27.4	27.7	-	-	-	-	-	-
Phenylethylene (Styrene)	25.3	32.2	39.7	46.6	52.7	59.6	65.5	72.0	75.2	75.1	74.1	68.5	63.1	57.0	-	-
AROMATICS																
Benzene	-	33	40.6	45.8	50.0	53.9	59.0	67.5	72.9	70.7	64.8	59.9	-	-	-	-
Methylbenzene (Toluene)	25.0	30.7	36.5	42.4	47.1	52.1	58.2	64.0	67.8	67.1	65.7	59.2	-	-	-	-
1, 4-Dimethylbenzene (Para-Xylene)	22.8	24.3	28.2	36.0	40.3	44.1	47.8	52.0	58.0	62.4	63.2	62.6	60.9	58.6	-	-
Ethylbenzene	21.7	26.9	32.5	38.1	42.7	48.2	53.4	59.3	66.3	67.9	67.7	65.9	62.6	59.6	56.7	-
Diethylbenzene (Mixed Isomers)	24.6	26.1	30.5	34.6	38.6	42.5	46.6	50.5	57.5	63.5	64.2	64.0	62.3	59.0	-	-
Sec-Butylbenzene (2-Phenylbutane)	19.4	22.0	26.3	30.8	34.8	37.7	40.1	43.3	48.8	52.8	55.0	56.6	56.2	52.2	-	-
Tetra-Hydro-naphthalene (Tetralin)	15.7	18.2	21.1	24.9	29.9	36.7	42.7	45.3	48.8	-	-	-	-	-	-	-
1-Methylnaphthalene	-	34.5	52.7	59.9	66.5	71.3	76.7	82.3	88.0	93.7	99.3	-	-	-	-	-
Methylnaphthalene Concentrate (Mixed Isomers)	-	37.7	49.0	54.9	58.4	64.3	68.7	74.3	74.8	74.0	72.8	71.2	68.0	64.5	-	-

(a) Curve slightly extrapolated.

TABLE XXI

TRANSVERSE FLAME RADIATION AT VARIOUS FUEL-AIR MIXTURE RATIOS

Compound	Total Radiant Energy, Btu/Ft. ² /hr. x 10 ⁻³ at Stated Mixture Ratio, % Stoichiometric															
	40	50	60	70	80	90	100	110	120	130	140	150	160	170	180	190
NORMAL PARAFFINS																
n-Hexane	-	-	10.9	11.4	11.9	12.4	12.9	13.1	13.2	13.0	12.8	12.5	12.2	11.9	-	-
n-Heptane	8.6	10.2	10.8	11.3	11.7	12.0	12.4	12.5	12.6	12.7	12.7	12.5	12.2	12.0	11.8	11.5
n-Octane	9.3	10.4	11.1	11.6	12.2	12.4	13.0	13.4	13.5	13.6	13.7	13.6	13.5	13.4	13.2	12.8
n-Decane	10.4	10.9	11.5	12.0	12.4	12.9	13.3	13.6	14.1	14.3	14.4	14.4	14.3	14.1	-	-
n-Dodecane	9.8	10.8	11.4	11.7	12.0	12.4	12.6	12.8	13.0	13.2	13.2	-	-	-	-	-
n-Tetradecane	9.8	10.3	11.0	11.6	12.1	12.5	12.9	13.2	13.2	13.2	13.2	13.0	12.9	12.6	11.9	10.9
n-Hexadecane (Cetane)	10.3	10.8	11.1	11.5	11.8	12.3	12.9	13.4	13.6	14.0	13.2	13.3	13.3	13.3	-	-
n-Decane-n-Pentadecane Mixture	10.1	10.7	11.1	11.5	11.9	12.4	12.9	13.4	13.6	13.6	13.6	-	-	-	-	-
n-Decane Concentrate	10.4	10.9	11.4	12.0	12.4	12.9	13.3	13.8	14.0	14.3	14.4	14.4	14.3	14.1	-	-
n-Decane-n-Pentadecane Concentrate	9.5	10.4	11.4	11.9	12.4	12.7	12.9	13.0	13.0	13.0	-	-	-	-	-	-
ISOPARAFFINS																
3-Methylpentane	9.6 ^a	10.1	10.8	11.7	12.4	12.7	13.0	13.2	13.2	13.0	12.8	12.6	12.3	12.1	-	-
2, 2-Dimethylbutane (Neohexane)	10.3	11.3	12.0	12.4	12.7	12.8	13.0	13.0	12.7	12.3	11.8	11.2 ^a	-	-	-	-
Dimethylhexanes (Mixed 2, 4- and 2, 5-)	9.2	9.9	10.3	10.8	11.4	12.2	12.8	13.1	13.2	13.2	13.1	12.9	12.6	12.2	11.6	11.0
2, 2, 4-Trimethylpentane (Isooctane)	-	-	11.7	12.5	13.0	13.8	13.5	13.6	13.5	13.2	12.5	12.5	12.0	11.2	-	-
2, 3, 4-Trimethylpentane	8.0	9.4	10.6	11.4	12.0	12.5	12.9	13.2	13.4	13.5	13.4	13.3	13.0	12.7	12.3	12.0
2, 2, 4, 4, 6, 8, 8-Heptamethyl-nonane	9.7	10.2	10.6	11.0	11.4	11.7	12.0	12.2	12.3	12.4	12.5	12.4	12.4	12.2	11.9	11.6
Isodecane (Soltrol 130)	9.6	10.6	11.5	12.2	12.8	13.2	13.3	13.3	13.4	13.3	13.3	13.2	13.0 ^a	-	-	-
Isotridecane (Soltrol 170)	9.4	10.2	11.2	11.9	12.6	13.0	13.2	13.4	13.6	13.7	13.6	13.4	13.1	12.7	12.2	-
CYCLOPARAFFINS																
Cyclohexane	10.6	11.0	11.4	11.8	12.1	12.5	13.0	13.2	13.3	13.3	13.3	13.3	13.2	12.9 ^a	-	-
Methylcyclopentane	-	-	11.2 ^a	11.9	12.5	13.1	13.5	13.7	13.7	13.6	13.6	13.4	13.1	12.8	12.5	12.2 ^a
1, 2-Dimethylcyclohexanes (Mixed Isomers)	9.8	10.2	10.6	11.1	11.5	11.8	12.2	12.4	12.4	12.4	12.4	12.2	11.8	10.8	-	-
Diethylcyclohexanes	9.8	11.2	12.0	12.6	13.1	13.5	13.8	14.0	14.1	14.2	14.2	14.0	14.0	13.6	13.6	-
Decalin (Mixed Isomers)	9.5	10.3	11.0	11.6	12.2	12.7	13.2	13.6	13.8	14.0	14.0	14.0	14.0	14.0	-	-
Methyldecalins	9.0	10.2	11.1	11.9	12.7	13.3	13.5	13.6	13.5	-	-	-	-	-	-	-
Tetracyclododecane	9.4	10.5	10.9	11.4	12.2	13.0	13.5	13.8	14.0	-	-	-	-	-	-	-
Isopropyl bicyclohexyl	9.6	10.4	11.0	11.2	11.7	12.3	13.0	13.2	13.5	13.6	13.6	-	-	-	-	-
OLEFINS																
1-Hexene	-	10.5	11.4	12.0	12.2	12.4	12.6	12.8	13.0	13.1	13.2	13.3	13.4	13.4	13.4	13.3
1-Octene	9.6	10.2	10.9	11.5	12.0	12.5	13.0	13.4	13.7	13.9	14.1	14.1	14.0	14.0	13.9	13.5
4-Methyl-2-pentene (Mixed Isomers)	-	10.4	11.2	12.0	12.6	13.1	13.6	13.9	14.0	14.0	13.9	13.6 ^a	-	-	-	-
2, 2, 4-Trimethyl-1-pentene (Diisobutylene)	-	-	11.7	11.9	12.2	12.5	12.9	13.4	13.6	13.7	13.7	13.7	13.6	13.5	13.1	11.4
Cyclohexene	-	-	10.4	11.0	11.5	11.8	12.1	12.4	12.6	12.7	12.8	12.8	12.6	12.4	12.4	-
4-Vinyl-cyclohexene-1	-	9.1 ^a	9.8	10.4	11.1	11.7	12.3	12.8	13.4	13.9	14.5	14.6	14.8	14.8	-	-
Phenylethylene (Styrene)	10.9	13.8	16.1	18.1	20.0	22.0	24.0	26.0	27.8	29.2	30.1	30.8	31.3 ^a	-	-	-
AROMATICS																
Benzene	-	-	16.8 ^a	18.5	20.4	22.5	24.2	25.9	27.2	27.6	27.6	27.6 ^a	-	-	-	-
Methylbenzene (Toluene)	10.0	12.0	13.4	14.6	15.8	16.8	17.8	18.8	19.8	20.6	21.4	22.1	-	-	-	-
1, 4-Dimethylbenzene (Para-Xylene)	10.8	12.2	13.6	14.6	15.3	16.0	17.0	18.1	19.0	19.8	20.4	20.9	21.0	21.0	21.0	-
Ethylbenzene	10.3	11.9	13.0	14.1	15.2	16.4	17.9	19.4	20.5	21.6	22.3	22.6	22.9	23.1	23.3	-
Diethylbenzene (Mixed Isomers)	10.5	11.2	12.0	12.8	13.8	15.0	16.0	17.0	18.0	18.8	19.5	20.1	20.5	20.8	-	-
Sec-Butylbenzene (2-Phenylbutane)	10.6	11.9	12.8	13.4	13.8	14.2	14.7	15.4	15.8	16.0	16.7	17.3	17.6	17.8	-	-
Tetra-Hydro-naphthalene (Tetralin)	9.4	10.0	10.4	11.1	12.1	13.4	15.3	16.3	17.0	-	-	-	-	-	-	-
1-Methylnaphthalene	-	18.2	23.3	26.5	28.7	30.5	31.8	32.9	34.0	35.2	36.5	-	-	-	-	-
Methylnaphthalene Concentrate (Mixed Isomers)	9.3	13.5	17.1	21.1	24.1	26.7	28.8	30.5	31.9	33.0	34.0	35.0	35.9	36.6	37.3	-

(a) Curve slightly extrapolated.

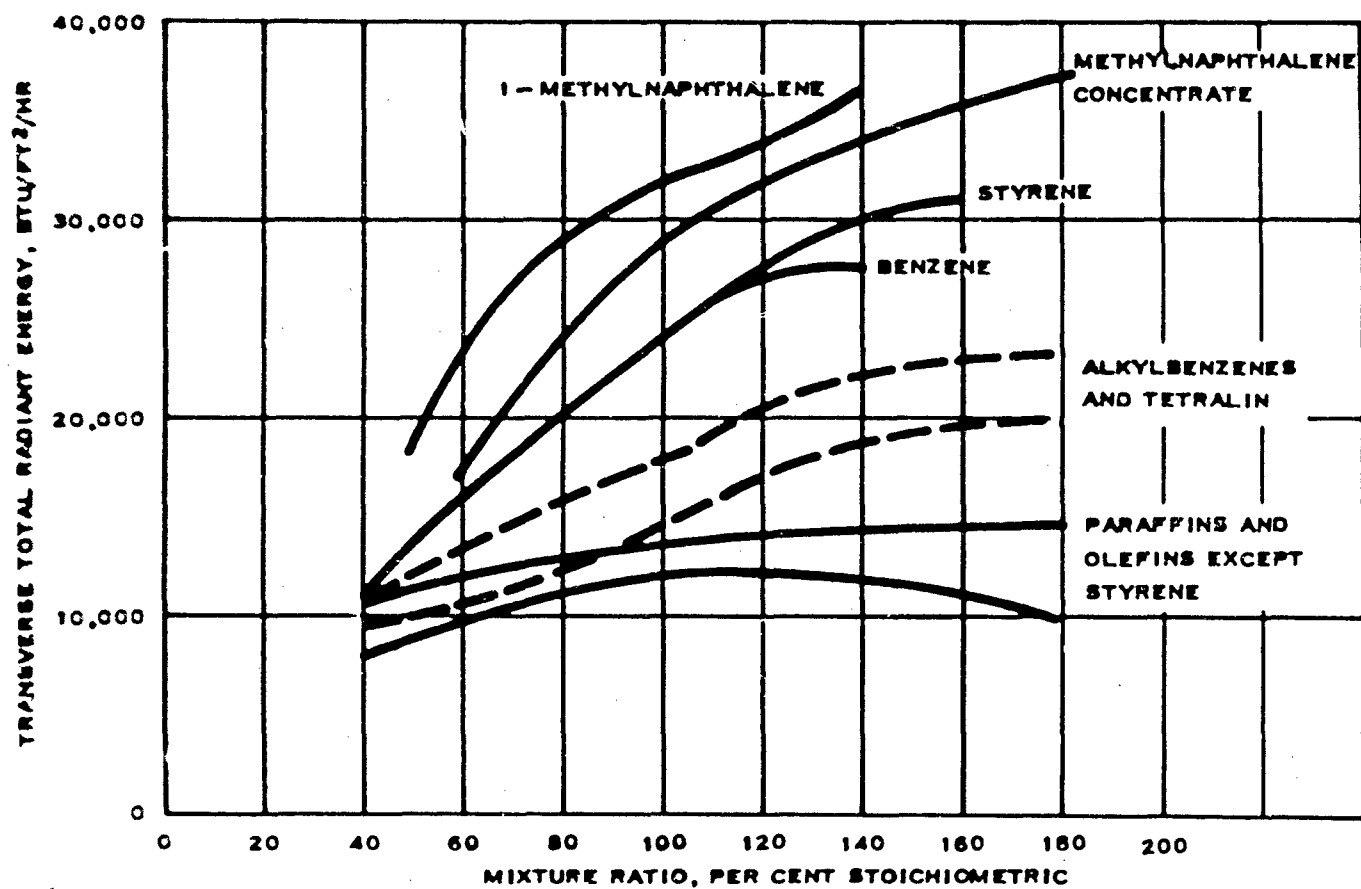


FIGURE 37
EFFECT OF HYDROCARBON TYPE ON TRANSVERSE
FLAME RADIATION IN PHILLIPS MICROBURNER

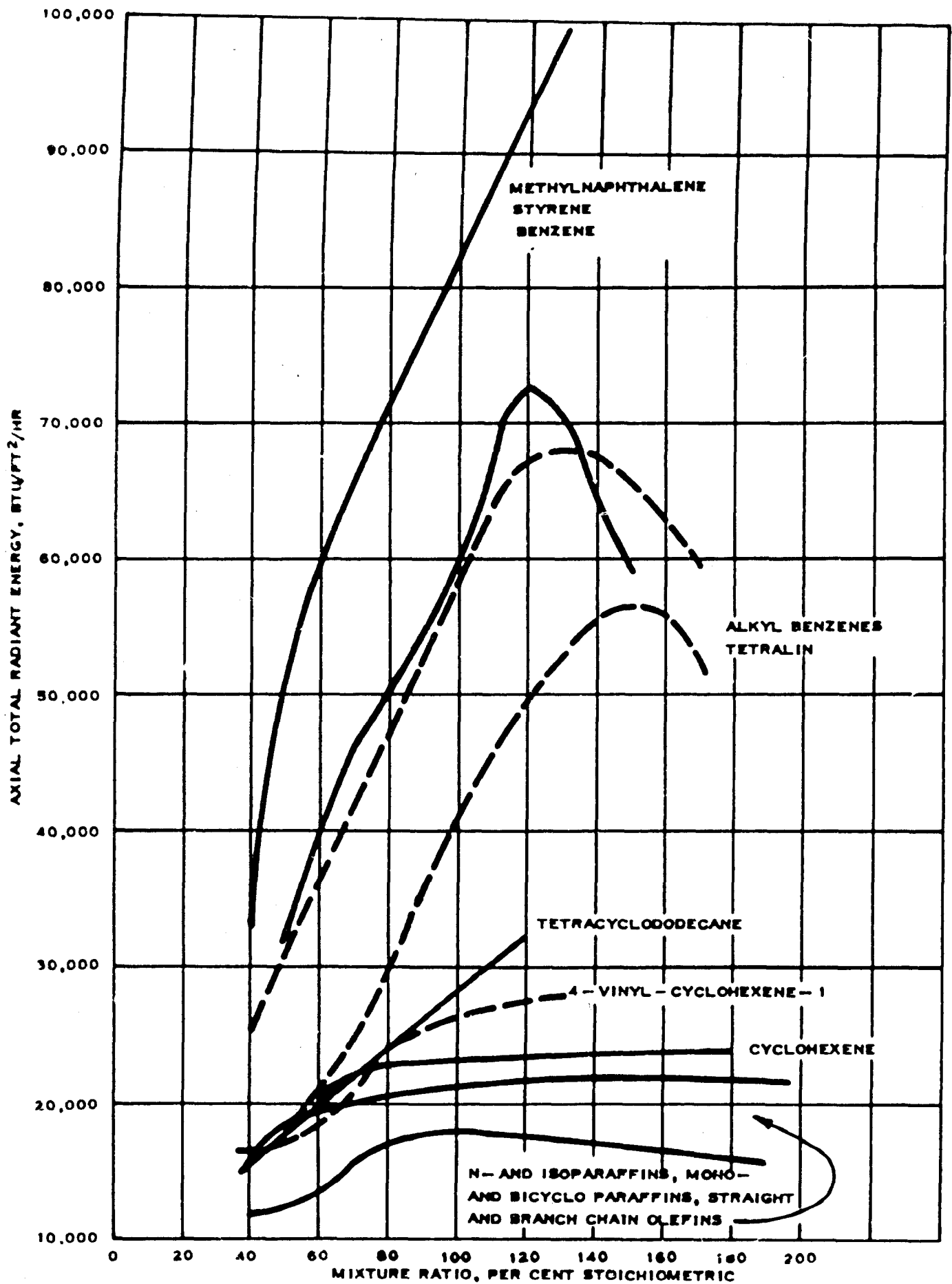


FIGURE 38
EFFECT OF HYDROCARBON TYPE ON AXIAL FLAME
RADIATION IN PHILLIPS MICROBURNER

This is illustrated for stoichiometric mixtures in Figures 39, 40, 41, and 42 representing the effect of hydrogen content, heat of combustion, Luminometer Number, and Smoke Point, respectively. Over a wide range of the higher values of each fuel property, the total radiant energy is nearly constant at a low level. In this range all of the normal- and iso-paraffins and most of the cycloparaffins and olefins are included. After the upward break in the curves, there is in each case a rapid increase in total radiant energy with decrease in hydrogen content, heat of combustion, Luminometer Number, and Smoke Point. In the region beyond the break, fall all of the aromatics and the aromatic olefin, styrene. For axial flame radiation the tetracycloparaffin, tetracyclododecane, and the cycloolefin, 4-vinyl-cyclohexene-1 are also found after the curves break but at a lower level than the aromatics. The other cycloolefin, cyclohexene, exhibits somewhat high axial total radiant energy relative to the other hydrocarbons having about the same heat of combustion, Luminometer Number and Smoke Point.

The curves for hydrogen content and heat of combustion differ from those for Luminometer Number and Smoke Point mainly in the extent of the range of constancy of flame radiation and in the steepness after the upward break. These effects are summarized in Table XX where the magnitude of the region of constancy is expressed for comparability as percentage of the total range of the particular property as well as in values of the property. Similarly the slopes are expressed as total radiant energy per per cent of the range.

TABLE XX
COMPARISON OF CURVES OF FLAME RADIATION
AGAINST HYDROCARBON PROPERTIES

	<u>Hydrogen Content</u>	<u>Heat of Combustion x 10⁻³</u>	<u>Luminometer Number</u>	<u>Smoke Point</u>
1. Region of Constant Radiant Energy				
Approx. Range of Property				
Axial	13.1-16.4	18.2-19.2	47-226	21.4 to over 50
Transverse	11.2-16.4	17.9-19.2	37-226	10.9 to over 50
% of Total Range				
Axial	35	40	75	64 ^a
Transverse	56	55	79	87 ^a
2. Approx. Slope after Break in Curve, Btu/ft ² /hr per % of Range				
Axial	1.0	1.0	2.5	2.3 ^a
Transverse	0.5	0.5	1.1	1.4 ^a

^a Based on a maximum Smoke Point of 50 although some of the hydrocarbons had Smoke Points above this limit of the method.

The region of constancy is narrower and the slope after the break is lower for hydrogen content and heat of combustion than for Luminometer Number and Smoke Point. Therefore, hydrogen content and heat of combustion have advantages over the other two properties for correlation purposes. However, so far as flame radiation under the conditions in the Microburner is concerned, increase in hydrogen content above about 13 weight per cent,

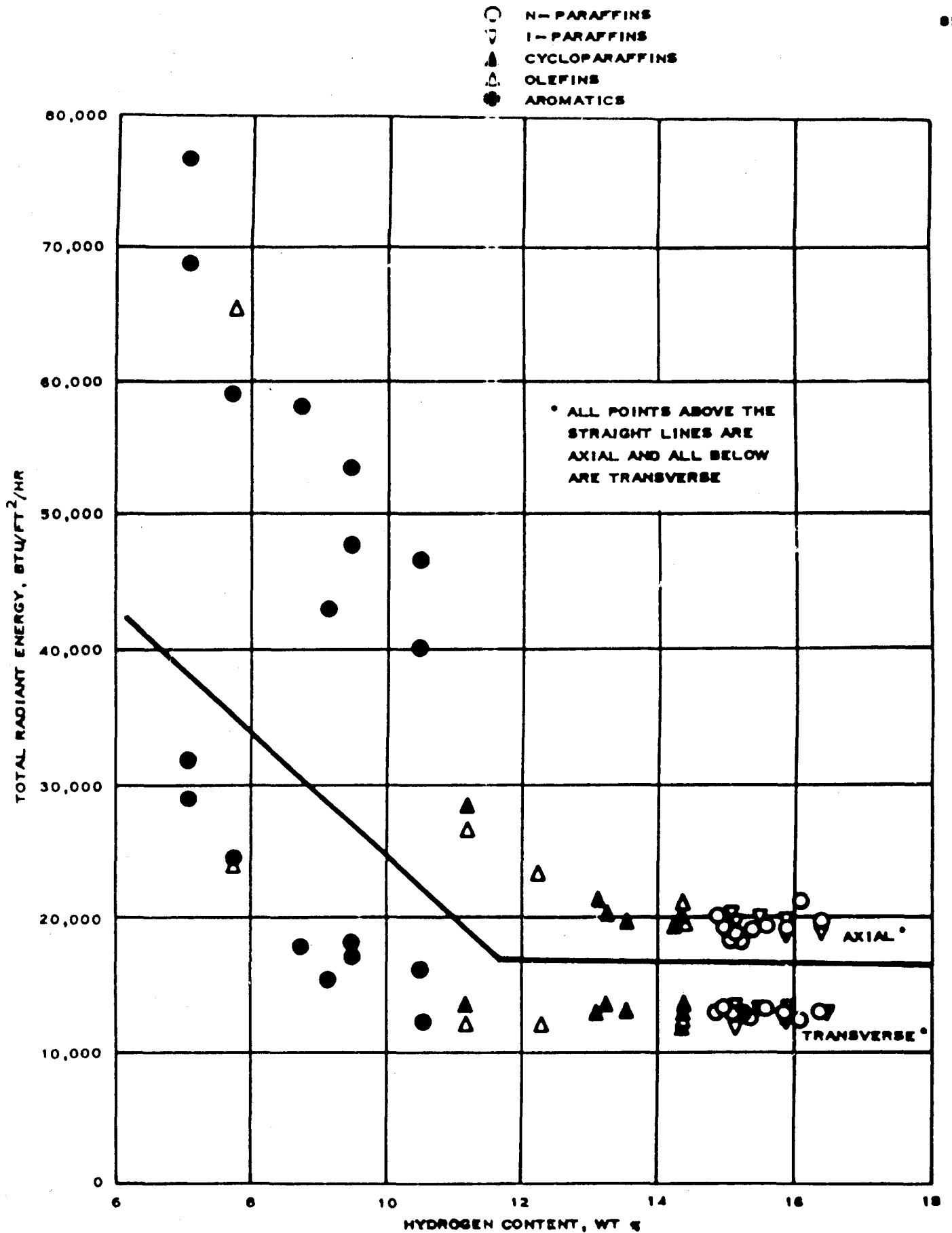


FIGURE 39
EFFECT OF HYDROGEN CONTENT ON FLAME RADIATION OF
STOICHIOMETRIC MIXTURES IN THE PHILLIPS MICROBURNER

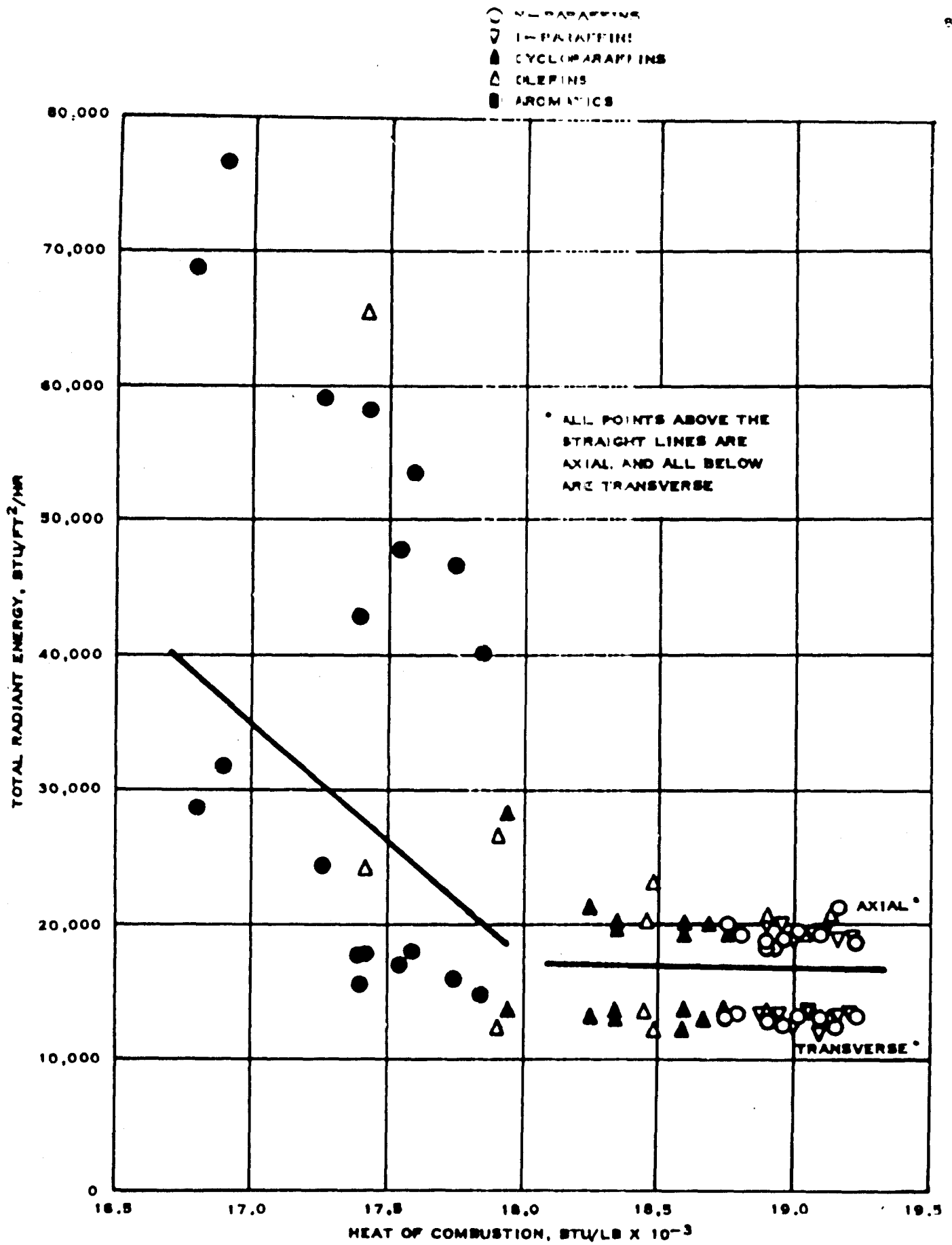


FIGURE 40
EFFECT OF HEAT OF COMBUSTION ON FLAME RADIATION OF
STOICHIOMETRIC MIXTURES IN THE PHILLIPS MICROBURNER

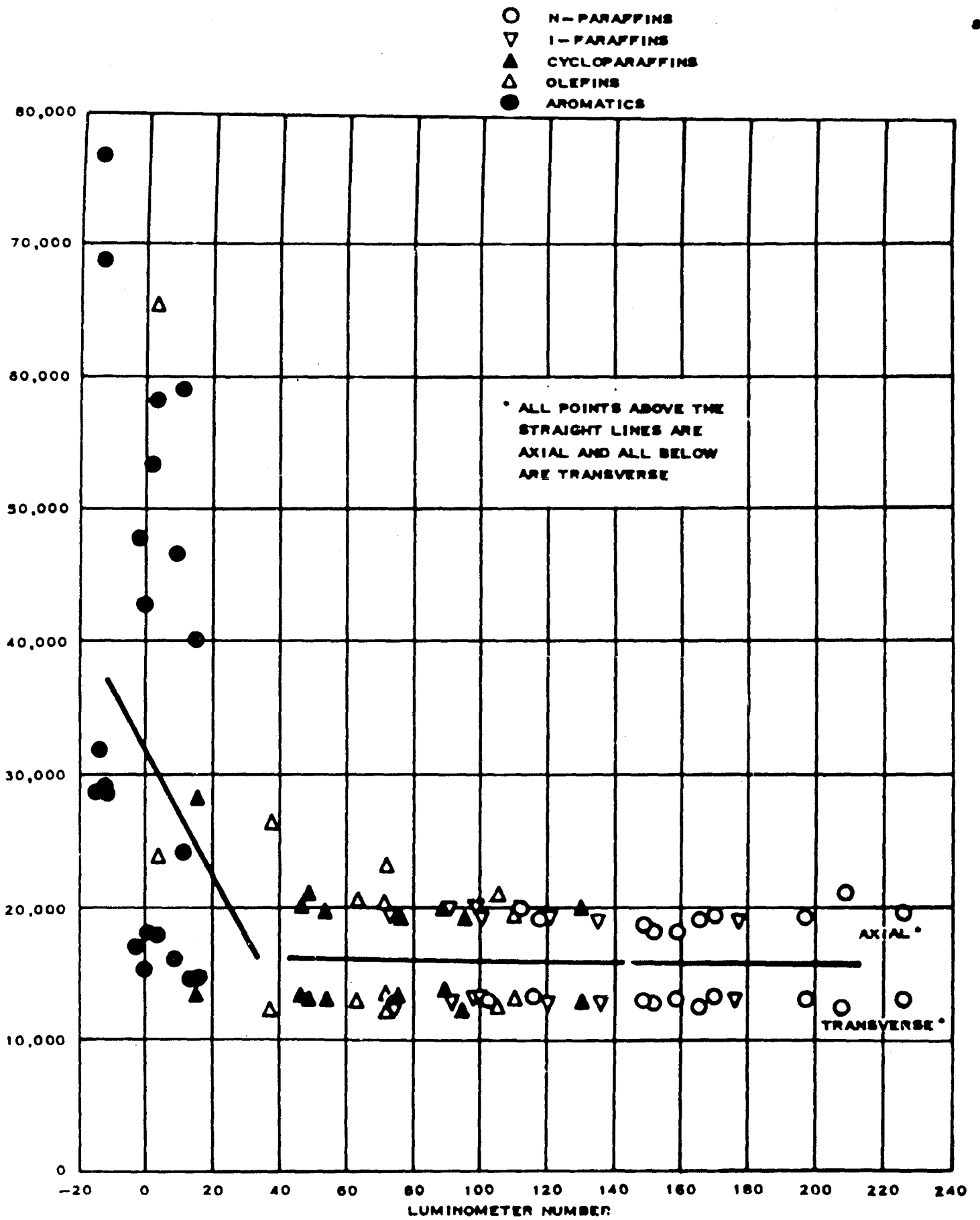


FIGURE 41
 EFFECT OF LUMINOMETER NUMBER ON FLAME RADIATION OF
 STOICHIOMETRIC MIXTURES IN THE PHILLIPS MICROBURNER

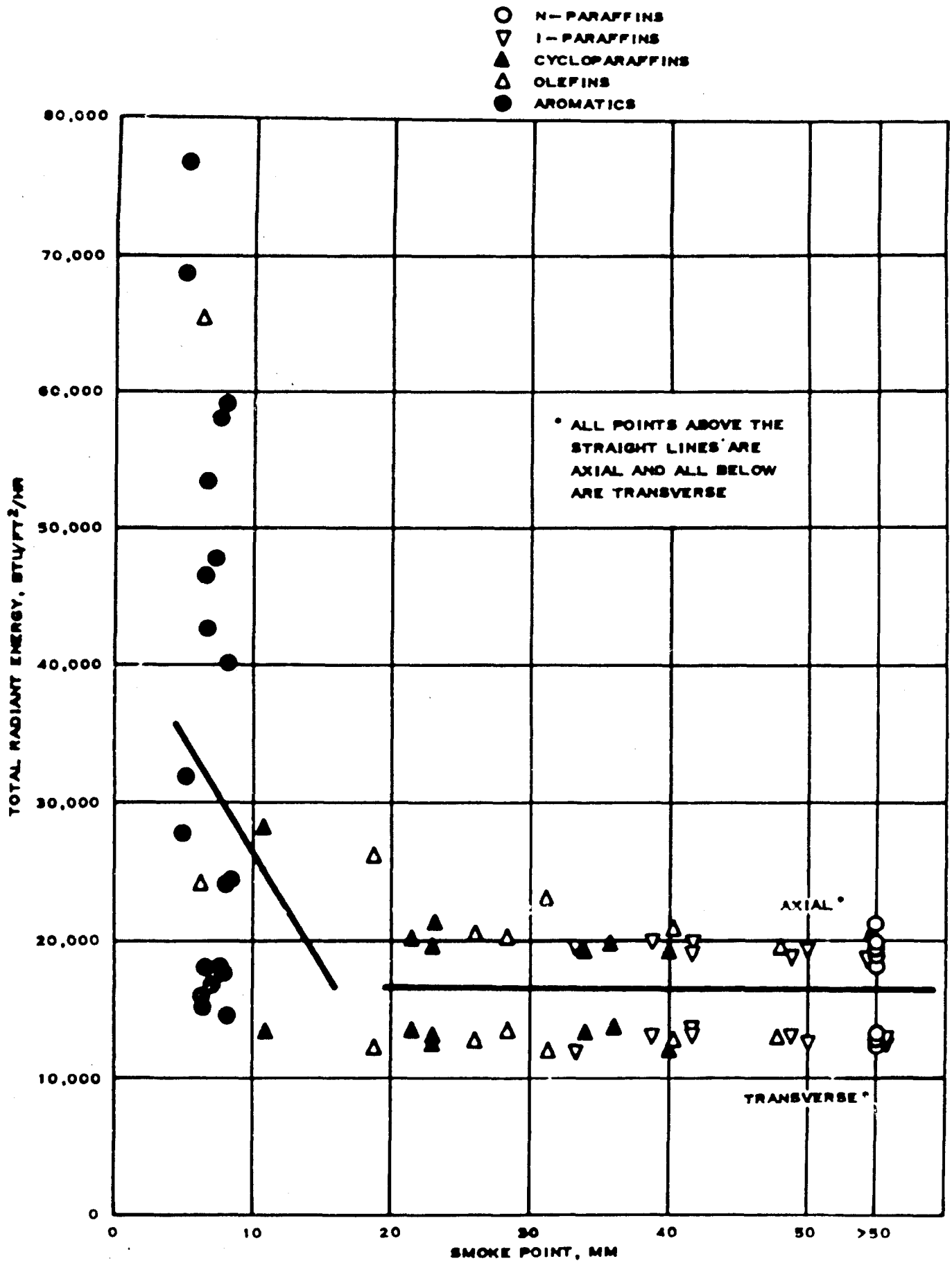


FIGURE 42
EFFECT OF ASTM SMOKE POINT ON FLAME RADIATION OF
STOICHIOMETRIC MIXTURES IN THE PHILLIPS MICROBURNER

in heat of combustion above about 18,200 Btu/lb., in Luminometer Number above about 40, and in Smoke Point above about 20 has no significant effect.

The above discussion of the relationships between fuel properties and flame radiation in the Microburner has been confined to 100 per cent stoichiometric mixtures. At other percentages of stoichiometric, the conclusions are generally similar because there is a reasonably good correlation between flame radiation of the 100 per cent stoichiometric mixtures and flame radiation at other percentages stoichiometric. As has been shown in Figures 37 and 38, the magnitude of the total radiant energy varies with mixture ratio and the spread in total radiant energies among the hydrocarbons is less at low than at high percentages stoichiometric.

In Figures 43 and 44, total radiant energy of stoichiometric mixtures is plotted against boiling point and it is seen that volatility is not a significant factor under the test conditions. For example, although the boiling points of the normal paraffins range from 156 to 548 F, the radiation from their flames was nearly the same.

3. Correlation with Full-Scale Combustors

Although no flame radiation measurements were made in the present series of tests in the Phillips 2-inch combustor (29) or in aircraft turbine engine combustors, there is reported information (21, 26, 41, and 42) which permits some estimate of the probable degree of correlation of the Microburner results with total radiant energies in these combustors.

Correlations of the fuel properties, hydrogen content and Luminometer Number have been made (21) with total radiant energy in the Phillips 2-inch combustor (41) and in the J-57 combustor (26). Similar correlations for the J-79 combustor have been made in Reference 42. Figures 45 and 46 indicate these relationships. The operating conditions for the three combustors are shown in Table XXI, the pressure being approximately 5 atmospheres in each case and the inlet air temperatures varying from 400 to 540 F.

The relationships shown in Figures 45 and 46 are markedly different from those between total radiant energy in the Microburner and hydrogen content and Luminometer Number (Figures 39 and 41).

In the 2-inch combustor and the J-57 and J-79 combustors, the measured total radiant energy is a straight line function of hydrogen content. In contrast, in the Microburner total radiant energy was essentially constant for hydrogen contents above about 13 weight per cent and then increased sharply with decrease in hydrogen content.

The plots of total radiant energy as a function of Luminometer Number exhibit curvature in all four combustion systems. However, the curve representing the Microburner is quite different from those representing the 2-inch combustor and the J-57 and J-79 combustors. In the Microburner, flame radiation was nearly constant for Luminometer Numbers above 40 and then increased rapidly with decrease in Luminometer Number. In the 2-inch and J-57 and J-79 combustors, the increase in flame radiation with decrease in Luminometer Number is more gradual over the entire range.

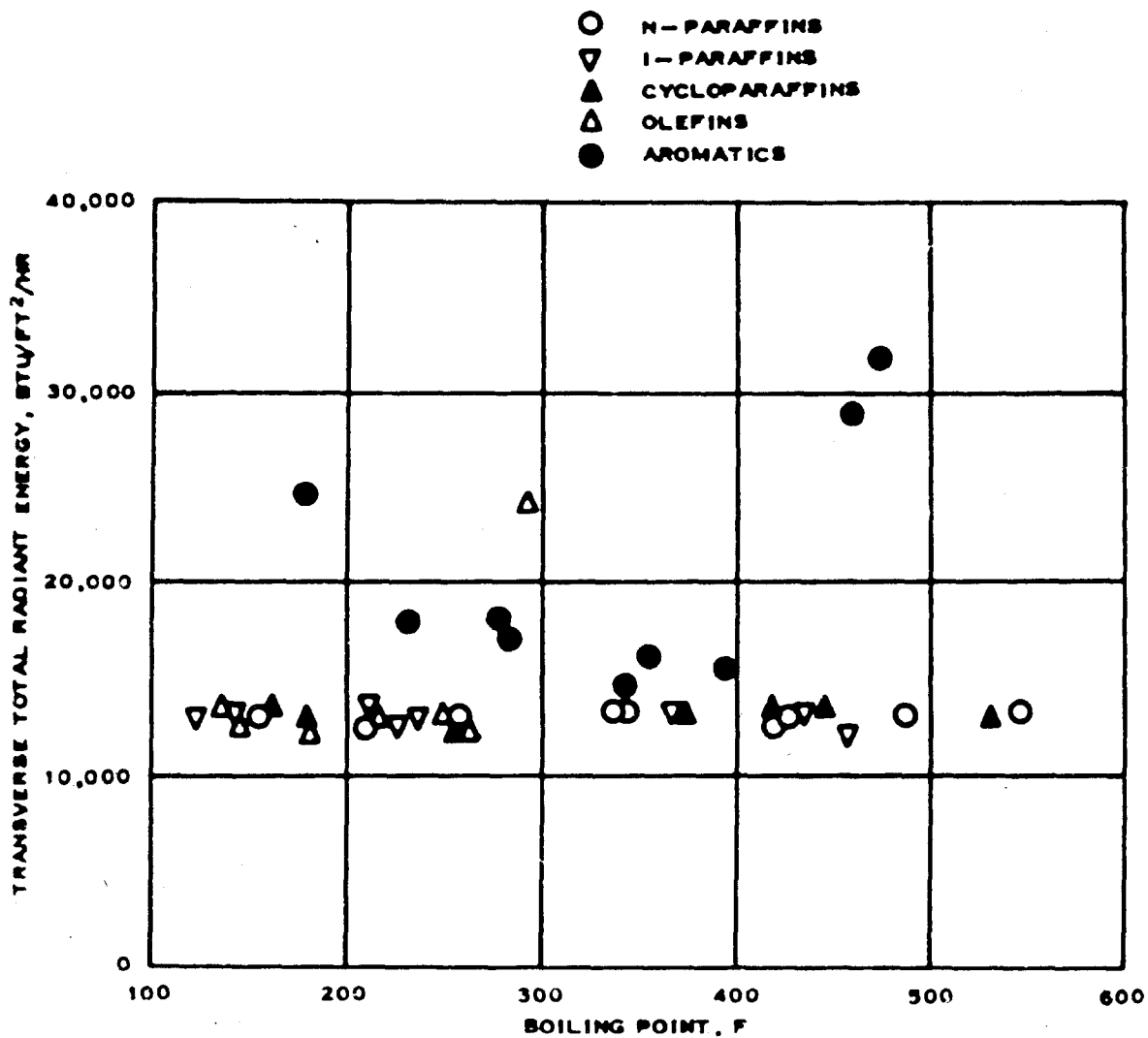


FIGURE 43
 ILLUSTRATION OF THE LACK OF EFFECT OF VOLATILITY ON
 TRANSVERSE RADIANT ENERGY OF STOICHIOMETRIC
 MIXTURES IN THE PHILLIPS MICROBURNER

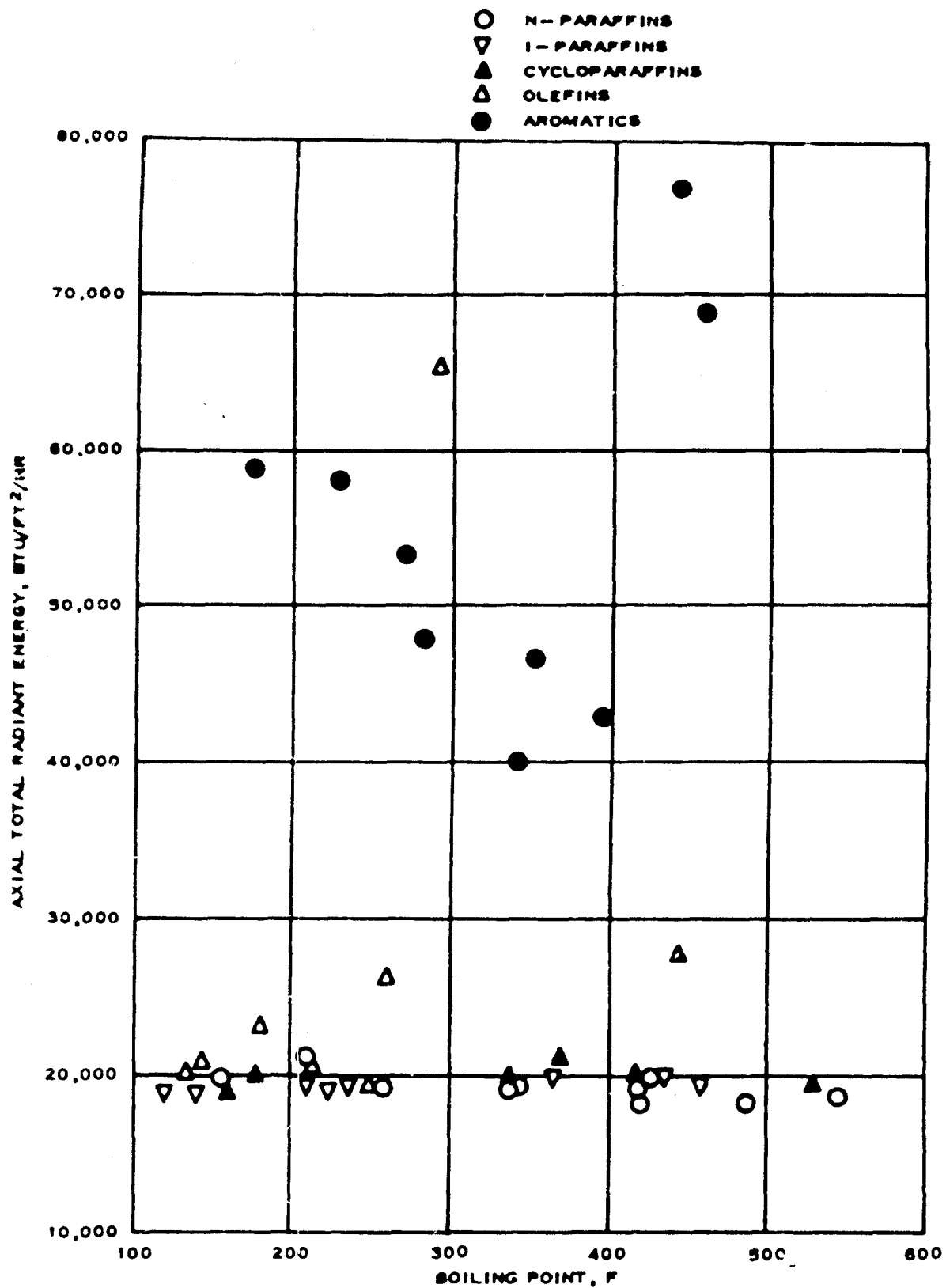


FIGURE 44
 ILLUSTRATION OF THE LACK OF EFFECT OF VOLATILITY ON
 AXIAL RADIANT ENERGY OF STOICHIOMETRIC
 MIXTURES IN THE PHILLIPS MICROBURNER

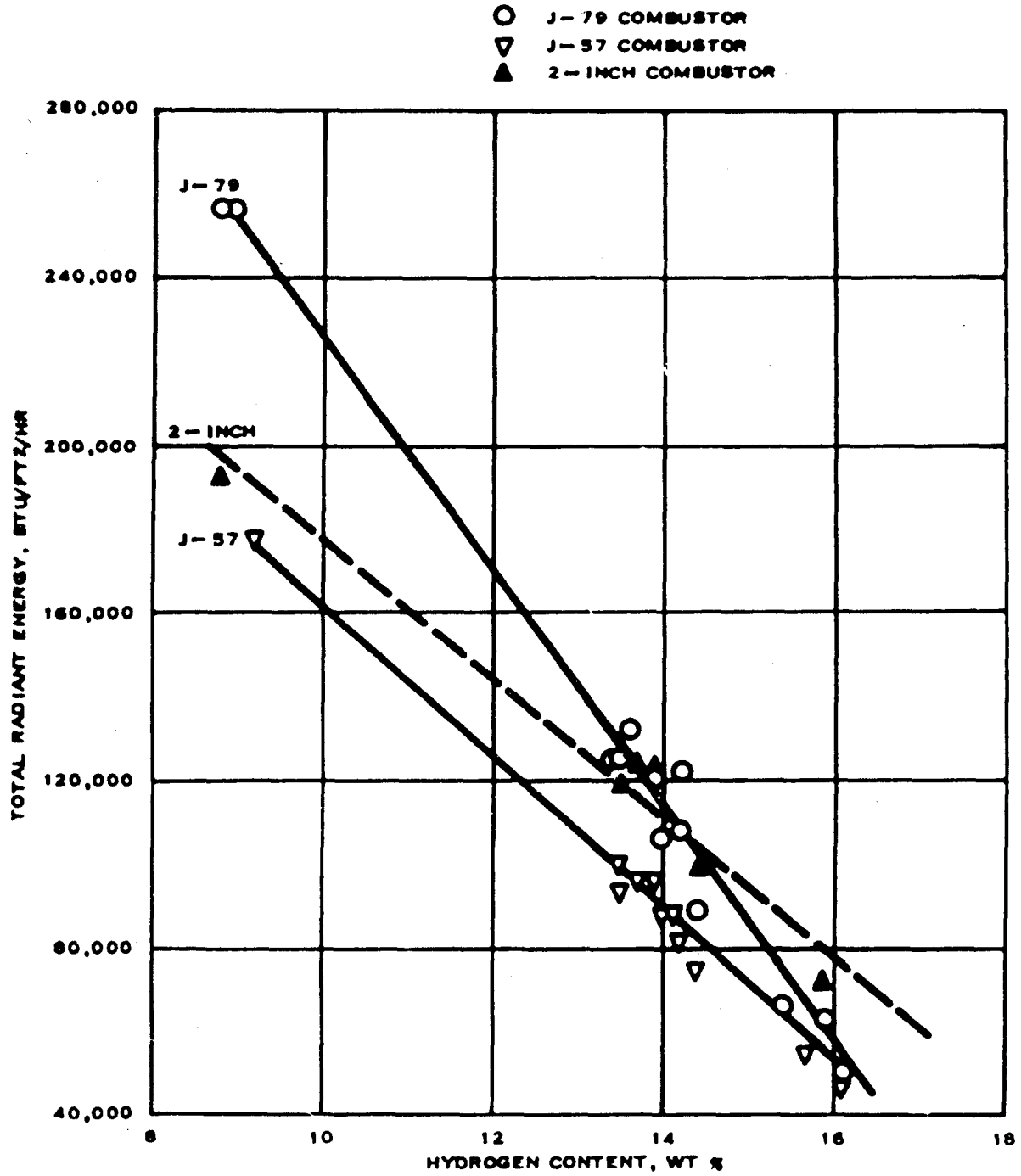


FIGURE 45
CORRELATION OF HYDROGEN CONTENT WITH FLAME RADIATION
IN THE PHILLIPS 2-INCH COMBUSTOR AND THE J-57 AND J-79
COMBUSTORS AT 5 ATMOSPHERES PRESSURE

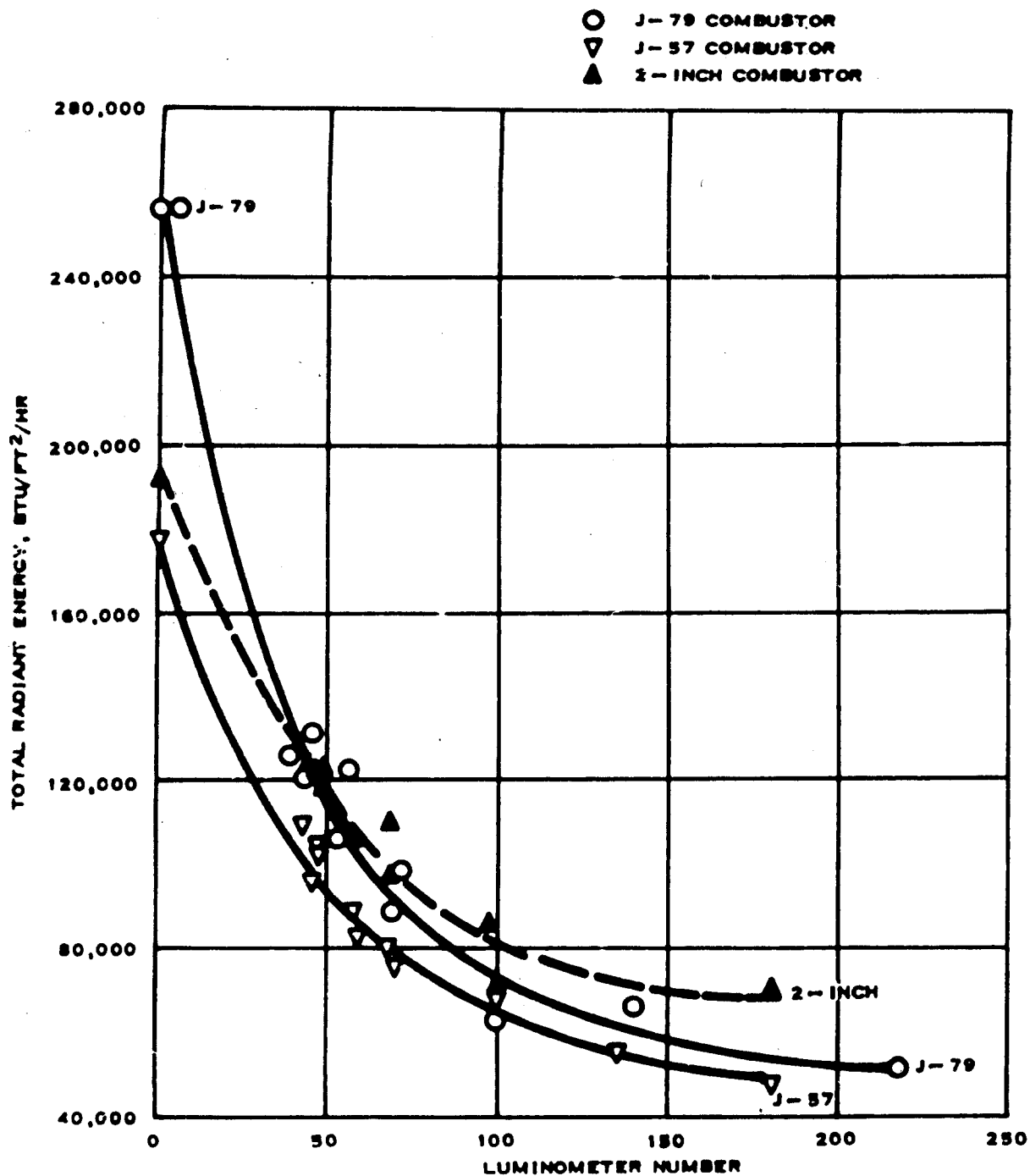


FIGURE 46
CORRELATION OF LUMINOMETER NUMBER WITH FLAME RADIATION
IN THE PHILLIPS 2-INCH COMBUSTOR AND THE J-57 AND J-79
COMBUSTORS AT 5 ATMOSPHERES PRESSURE

Reference 42 also includes data on flame radiation at 5 atmospheres pressure and an inlet air temperature of 850 F measured in the J-79 combustor. At this temperature level the radiation was greater than at 540 F but the relationships with hydrogen content and Luminometer Number were of the same general form.

It has been amply demonstrated that increased operating pressure favors the formation of soot in flames as evidenced by the heavier smoke occurring during takeoff of turbine powered aircraft. More important, radiant heating by soot laden flames of high emissivity during such operation presents a critical hot section component durability limitation, as well as specific power limitation. However, recent studies by NGTE (23) indicated a high order of overall pressure dependence of soot forming reactions which varies with hydrocarbon structure. Generally, aromatics showed a low pressure dependence, as compared to naphthenes and paraffins. Thus, flame radiation from naphthene and paraffin hydrocarbons can be expected to exhibit a relationship to aromatics at atmospheric pressure which is quite different from that encountered by aviation turbine fuels under severe operating conditions. Therefore, it is concluded that the study of aviation turbine fuel burning quality, as it relates to flame radiation in aviation turbine engines, should not be conducted in atmospheric pressure devices—such as the Phillips Microburner or the ASTM-CRC Luminometer.

TABLE XXI

CONDITIONS OF OPERATION OF THE PHILLIPS 2-INCH

COMBUSTOR AND THE J-57 AND J-79 AIRCRAFT TURBINE ENGINE COMBUSTORS

<u>Conditions of Operation</u>	<u>Combustor</u>		
	<u>Phillips 2-Inch^a</u>	<u>J-57^b</u>	<u>J-79^c</u>
Pressure, Atm.	5.0	4.7	4.7
Inlet Air Temperature, F	400	540	530
Ref. Velocity, ft/sec	100	-	93
Mass Air Flow, lb/sec	0.5	9.6	7.5
Heat Input Btu/lb of Air	200	195	190
	250	240	240
Position of Transverse Flame Radiation Measurements, Per Cent of Burner Length		285	280
	30	18	26
	45	33	40
	60	48	65

- (a) Points plotted in Figures 45 and 46 for the 2-inch combustor represent averages of transverse radiant energy measured at the three stations and under the two heat input rates.
- (b) Points plotted in Figures 45 and 46 for the J-57 combustor represent averages of transverse radiant energy measured at the three stations and under the three heat input rates.
- (c) Points plotted in Figures 45 and 46 for the J-79 combustor represent averages of transverse radiant energy measured at 40 per cent of the burner length and under the three heat input rates. The 40 per cent position

was used because one fuel (toluene) showed abnormally low flame radiation at the 26 per cent position and one value was not specifically evaluated at the 65 per cent position.

F. CONCLUSIONS

1. The Microburner did not differentiate among the hydrocarbons having (a) hydrogen contents above about 13 weight per cent, (b) heats of combustion above about 18,200 Btu/lb., (c) Luminometer Numbers above about 40 and (d) ASTM Smoke Points above about 20 mm. Below these values, there was a rapid increase in flame radiation with decrease in each of these properties, the rate of increase being less with decrease in hydrogen content and heat of combustion than with decrease in Luminometer Number and Smoke Point.

2. The Microburner rated the hydrocarbons in the following general order of increasing flame radiation:

(a) The ten normal paraffins, the eight isoparaffins, the seven mono- and bi-cycloparaffins and the four straight and branch chain olefins.

(b) The two cycloolefins (cyclohexene and 4-vinyl-cyclohexene-1).

(c) The one tetracycloparaffin (tetracyclododecane).

(d) The five alkylbenzenes and the bicyclic aromatic with one saturated and one unsaturated ring (tetralin).

(e) Benzene and the olefinic aromatic (styrene).

(f) The two bicyclic aromatics with both rings unsaturated (1-methylnaphthalene and methylnaphthalene concentrate).

3. The relationships between the fuel properties, hydrogen content, or Luminometer Number, and total radiant energy in the Phillips Microburner are different from the relationships between these properties and total radiant energy in the Phillips 2-inch combustor and in the J-57 and J-79 combustors.

4. Since the soot forming tendency of various hydrocarbon classes do not have the same pressure dependence, the effect of hydrocarbon structure on flame radiation should be studied at the pressure levels of interest in realistic combustors rather than in atmospheric pressure devices.

G. RECOMMENDATIONS

Further studies of flame radiation as related to hydrocarbon structure should be made using the Phillips 2-inch combustor. This is based upon (a) variations shown in the pressure dependence of soot forming reactions with hydrocarbon structure (38), (b) need for evaluation at high pressure, 10 to 15 atmospheres, where the contribution by flame radiation can be a significant factor in determining the operating temperature of hot section components (43), and (c) demonstrated capability of the Phillips 2-inch combustor to simulate the performance characteristics of aircraft turbine engine combustors satisfactorily for research studies of the burning quality of aircraft turbine fuels (27).

A program for this purpose has been proposed (28). A statistically designed procedure would be used to study flame radiation in the 2-inch combustor operated at 10 and 15 atmospheres pressure with exhaust gas temperatures of 1400, 1600, 1800 and 2000 F. A series of 20 hydrocarbons including normal-, iso-, and cyclo-paraffins, olefins and aromatics would be studied and these fuels would be supplemented by JP-5 blends, aromatic-free and containing mono- and bi-cyclic aromatics.

A Barnes Engineering Company, Model R-8D2 Research Radiometer would be used to improve the precision of flame radiation measurements. It is a dual-channel thermister bolometer, with the incoming radiation to both channels chopped and continuously compared with that from an internally controlled black body. One channel would be used to measure total radiant energy and the other to measure radiant energy at the 4.4 micron CO₂ peak. The latter was shown (43) to have an emissivity of one in the Phillips 2-inch combustor. Hence, it can serve as a direct measure of flame temperature, from which overall flame emissivity can be calculated by comparison with the total radiant energy measurement.

Flame radiation would be measured from a transverse position; i.e. across the combustor. The effect of variations in flame radiation on the temperature of exposed metal parts would be measured at the axial position; i.e. downstream of the combustor. Metal strips mounted in the exhaust gas stream, six inches downstream of the combustor, would simulate nozzle guide vanes or turbine blades. Their temperature would be measured through suitable sighting ports by use of a Leeds and Northrup optical pyrometer.

IV. ACKNOWLEDGMENTS

This work was administered under the direction of C. C. Singleterry, Head, Fuels and Lubricants Branch, Power Plant Division, Bureau of Naval Weapons, Department of the Navy, with S. M. Collegeman as project engineer.

The authors wish to express their appreciation for guidance and assistance in the areas of:

- (a) Test Equipment and Design and Operation by E. H. Fromm, R. A. Mengelkamp, and W. L. Streets.
- (b) Metallographic Analysis by H. W. Schutz.
- (c) Scale Analysis by L. V. Wilson
- (d) Statistical Analysis by H. T. Quigg, M. R. Goss, and D. L. Weeks
- (e) Hydrocarbon Selection by M. R. Flinn
- (f) Hydrocarbon Analysis by J. W. Miller

14. "Effects of Fuel Sulfur Contamination and Sea Water Ingestion on the Durability of Jet Engine Hot Section Components," by W. L. Streets. Journal of the Institute of Petroleum, Vol. 48, No. 466, pp. 314-324, October 1962.
15. "Gas Turbine and Jet Engine Fuels," by W. L. Streets and R. M. Schirmer. Summary Report for U. S. Navy Contract N600(19)-58219. Phillips Petroleum Company Research Division Report 3529-63R.
16. "Gas Turbine and Jet Engine Fuels," by W. L. Streets. Progress Report No. 1 for U. S. Navy Contract Now 63-0406-d. Phillips Petroleum Company Research Division Report 3559-63R.
17. "Gas Turbine and Jet Engine Fuels," by W. L. Streets. Progress Report No. 2 for U. S. Navy Contract NOW 63-0406-d. Phillips Petroleum Company Research Division Report 3615-63R.
18. "Effect of JP-5 Sulfur Content and Sea Water Ingestion on Hot Gas Corrosion," by R. M. Schirmer, H. T. Quigg and R. A. Mengelkamp. Progress Report No. 3 for Navy BuWeps Contract NOW 63-0406-d. Phillips Petroleum Company Research Division Report 3686-64R.
19. "General Considerations in the Design of Combustion Chambers for Aircraft and Industrial Gas Turbines," by J. S. Clarke and S. R. Jackson. Paper No. 444A presented at SAE International Congress, Detroit, January 1962.
20. "Measurement of Total Radiant Energy from Jet Combustor Flames," by R. M. Schirmer. Paper 379E presented at SAE Summer Meeting, St. Louis, June 1961.
21. "Specification of Jet Fuel Hydrogen Content for Control of Combustion Cleanliness," by R. M. Schirmer. Progress Report No. 1 for Navy BuWeps Contract N600(19)-58219. Phillips Petroleum Company Research Division Report No. 3195-62R.
22. "Characteristics of Flame Radiation of High Temperature Hydrocarbon Fuels," by W. L. Streets. Summary Report for USAF Contract AF 33(616)-5543. Phillips Petroleum Company Research Division Report No. 2307-59R.
23. "Soot Formation in Hydrocarbon/Air Flames. Premixed Flames of C₅ and C₆ Hydrocarbons at Pressures up to 20 Atmospheres," by J. J. Macfarlane and F. H. Holderness. National Gas Turbine Establishment Report No. R. 253.
24. "Radiation from Laboratory Scale Jet Combustor Flames," by E. C. Miller, A. E. Blake, R. M. Schirmer, G. D. Kittredge, and E. H. Fromm. Special Report for Navy BuAer Contract NOas 52-132-c. Phillips Petroleum Research Division Report 1526-56R. Condensation of this report was presented at the Symposium on Characteristics of Flames and of Gaseous and Liquid Fuels, Sponsored by Division of Gas and Fuel Chemistry of the American Chemical Society, Urbana, May 1958: "Radiation from Jet Combustor Flames," by R. M. Schirmer and E. C. Miller.

25. "Effects of Flame Radiant Heating on Temperature and Durability of Laboratory Scale Jet Combustor Flame Tubes," by G. D. Kittredge. Special Report for Navy BuAer Contract NOas 58-310-d. Phillips Petroleum Company Research Division Report 2033-58R.
26. "Radiation from Flames in Gas Turbine Combustors," by R. M. Schirmer, L. A. McReynolds and J. A. Daley. SAE Transactions, Vol. 68, 1960, pp. 554-561.
27. "Gas Turbine and Jet Engine Fuels," by R. M. Schirmer. Progress Report No. 4 for Navy BuWeps Contract NOw 61-0590-d. Phillips Petroleum Company Research Division Report 2977-61R.
28. "Microburner Studies of Flame Radiation as Related to Hydrocarbon Structure," by R. M. Schirmer and E. W. Aldrich. Progress Report No. 4 for Navy BuWeps Contract NOw 62-0406-d. Phillips Petroleum Company Research Division Report 3752-64R.
29. "Design and Calibration of the Improved Phillips Jet Fuel Testing Facility," by E. H. Fromm. Phillips Petroleum Company Research Division Report 3527-63R.
30. "Chemical Technology of Petroleum," by W. A. Gruse and D. R. Stevens. Third Edition. Published by McGraw-Hill Book Company, Inc., New York, 1960.
31. "Aviation Fuel," by O. C. Blade. Petroleum Products Survey Nos. 4, 9, 14, 19, 24, 29 and 34, Bartlesville, Oklahoma, Petroleum Research Center, Bureau of Mines, U. S. Department of the Interior, 1958, 1959, 1960, 1961, 1962, 1963 and 1964.
32. "The Oceans as a Chemical System," by E. D. Goldberg, p. 4. "The Sea," by M. N. Hill, Volume 2, "The Composition of Sea-Water." Interscience Publishers, John Wiley & Sons, Inc., 1963, New York.
33. "Sampling Atmospheric Sea-Salt Nuclei Over the Ocean," by A. H. Woodstock and M. M. Gifford. Journal of Marine Research, Vol. 8, 1949, p. 194.
34. "Ultrafine Particles in the Atmosphere and Space," by R. D. Cadle, pp. 20-40. "Ultrafine Particles" by W. E. Kuhn, H. Lamprey and C. Sheer. John Wiley & Sons, Inc., 1963, New York.
35. "Gas Turbine for Unconventional Craft," by G. L. Graves and R. S. Carleton. Paper 685A presented at SAE-ASNE National Aero-Nautical Meeting, Washington, April 1963.
36. "Statistical Methods," by G. W. Snedecor. Fifth Edition. The Iowa State University Press, Ames, Iowa, 1956.
37. "Principles and Procedure of Statistics," by R. G. D. Steel and J. H. Torril. Chapter 5. McGraw-Hill Book Company, Inc., New York, 1960.

38. "Phillips Microburner--A Tool for Evaluating the Burning Quality of Jet Fuels," by W. L. Streets. Phillips Petroleum Company Research Division Report 1793-57R.
39. "Temperature Measurements in Engineering," Vol. II, pp. 77-78, by H. D. Baker, E. A. Ryder and N. H. Baker. John Wiley & Sons, Inc., New York, 1961.
40. "Effects of Fuel Properties on Liner Temperature and Carbon Deposition in the CJ8C5 Combustor for Long-Life Applications," by R. W. Macaulay and M. W. Shayeson. Paper No. 61-WA-304 presented at ASME Winter Annual Meeting, New York, November 1961.
41. "Gas Turbine and Jet Engine Fuels," by G. D. Kittredge. Progress Report No. 5 for U. S. Navy Contract NOas-58-310-d. Phillips Petroleum Company Research Division Report 2100-58R.
42. "Effects of Jet Fuel Constituents on Combustor Durability," by C. C. McClelland. Phase C Report on WEPTASK P.A. NAE-RAPP-41017, Naval Air Material Center (Aeronautical Engine Laboratory) report NAEC-AEI-1736, 15 May 1963.
43. "Gas Turbine and Jet Engine Fuels," by G. D. Kittredge. Summary Report for U. S. Navy Contract NOas-58-310-d. Phillips Petroleum Division Report 2182-58R.